

**Identification of a new eukaryotic phylum '*Picozoa*'
in the oceanic environment**

Inaugural-Dissertation

Zur Erlangung des Doktorgrades

der Mathematisch-Naturwissenschaftlichen Fakultät

der Universität zu Köln

vorgelegt von

Ramkumar Seenivasan

aus Thirumangalam, Indien

Köln 2012

Berichterstatter:

Prof. Dr. Michael Melkonian

Prof. Dr. Hartmut Arndt

Tag der mündlichen Prüfung:

23rd January 2012

Dedication

This thesis dedicated to my parents, Seenivasan and Ranjitham

Thank you for your encouragement, constant support and sowing confidence in me
that I am capable of doing anything I put in mind to.

Thank you!

To discern the truth in every thing, by whomsoever spoken, is wisdom

Thiruvalluvar, Tirukural 423

Take up one idea. Make that one idea your life - think of it, dream of it, live on that idea. Let the brain, muscles, nerves, every part of your body, be full of that idea, and just leave every other idea alone. This is the way to success, that is way great spiritual giants are produced

Swami Vivekananda

Abstract

Recent molecular phylogenetic analyses of picoeukaryotic (< 3 μm) 18S rDNA environmental sequences revealed a deep branching lineage formally described as ‘picobiliphytes’ with unknown affinity to other eukaryotes. Until now, no cultured representatives existed to enable further investigation regarding the biodiversity and morphology of this newly erected clade. This work, reports on a newly-discovered, free-living eukaryotic protist *Picomonas judraskeda* gen. et sp. nov., from European marine coastal habitats which has a ‘picobiliphyte’ 18S rDNA signature. Its morphological and ultra-structural characters clearly show that it contains, neither chlorophyll nor phycobilin autofluorescence, both of which are main attributes of ‘picobiliphytes’. The phycobilin was assumed to have been derived from a secondary endosymbiont; and the host of the ‘picobiliphytes’ was postulated to be a sister to cryptophytes/ katablepharids. The isolate *Picomonas* is slightly elongated and 2.5-5 μm in length with two unequal flagella. It exhibits unique cell movements (jump, drag, and skedaddle mode of locomotion). Light and electron microscopic studies reveal that the cells are naked, the flagella not covered by hairs or scales and that a plastid is lacking. The cells thus are heterotrophic, although their food source could not be determined and food vacuoles containing bacteria are never observed. The cells harbor several unique compartments that do not match those of any other known eukaryotes. This uniqueness is corroborated by phylogenetic analyses of the complete nuclear ribosomal operon placed them into a new phylum ‘Picozoa’.

Keywords

‘Picobiliphytes’, ‘biliphytes’, *Picomonas judraskeda*, *PicoPCR*, cell PCR, 18S rDNA, electron microscopy, Picozoa, TSA-FISH

Deutsche Kurzzusammenfassung

Molekulare phylogenetische Analysen von 18S rDNA Umwelt-Sequenzen wiesen auf eine neue Gruppe von Picoplanktern unbekannter Affinität zu anderen Eukaryoten. Vor einigen Jahren wurde diese Organismengruppe formal als „Picobiliphyta“ beschrieben. Eine Kultur dieser Organismen war bisher jedoch nicht möglich, sodass keine weitergehenden Untersuchungen in Bezug auf die Biodiversität und Morphologie dieser Organismengruppe möglich waren. In der hier vorgelegten Arbeit wurde nun erstmals eine Kultur etabliert angelegt und die Morphologie einer Gattung detailliert untersucht. Die Gattung hat den Namen, *Picomonas judraskeda* Gen. et sp. nov. Erhalten. Sie kommt an den europäischen Atlantikküste vor und besitzt eine typische ‘picobiliphyte’ 18S rDNA Signatur . Licht- und elektronenmikroskopische Untersuchungen zeigen deutlich, sowie Untersuchungen der zellulären Autofluoreszenz zeigen eindeutig, dass sie weder Chlorophyll, Phycobiline oder einen Plastiden besitzt. Damit konnten wichtige frühere Befunde zu den "Picobiliphyta 'nicht bestätigt werden und *Picomonoas judraskeda* ist daher keine Alge mit sekundären Endosymbionten (Schwestergruppe zu den Cryptophyten und Katablephariden) sondern ein heterotropher Organismus.

Zellen von *Picomonas* sind etwas länglich, ca. 2-5 µm lang und besitzen zwei ungleiche Geißeln. Die Zellen zeigen einzigartige Fortbewegungen. Licht- und elektronenmikroskopische Untersuchungen zeigen, dass die Zellen nackt sind, und die Geißeln nicht durch Haare oder Schuppen bedeckt sind. Ein Plastid fehlt. Die Zellen sind somit heterotroph, obwohl leider ihre Nahrungsquelle bisher nicht bestimmt werden konnte. Nahrungsvakuolen mit Bakterien wurden bisher nicht beobachtet. Die Zellen besitzen mehrere einzigartige Membran-umhüllte Kompartimente, die nicht mit von anderen Eukaryoten bekannt sind. Diese Einzigartigkeit wird durch phylogenetische Analysen des vollständigen nuklearen ribosomalen Operons bestätigt. Daher wurden die Gattung *Picomonas* in einen neuen Stamm Picozoa eingeordnet.

3.2	Abundance of ‘picobiliphyte’ sequences from Helgoland roads (Reede) ...	28
3.3	‘Picobiliphytes’ from enriched cultures	30
3.4	Subsequent sample collection for ‘picobiliphyte’ culturing	31
3.5	Enrichment but no growth of ‘picobiliphytes’	33
3.5.1	Use of PicoBI01F and ITS1R for identifying ‘picobiliphytes’	34
3.5.2	Microscopy	35
3.5.3	Isolation of Picoeukaryotic cells	36
3.6	Microscopic results	42
3.6.1	Light microscopy	42
3.6.2	Cell division	44
3.6.3	Chemically fixed cells	44
3.6.4	Fluorescence images	45
3.6.5	Scanning electron microscopy	46
3.6.6	Transmission electron microscopy	48
3.7	Phylogenetic analyses	69
3.7.1	Phylogenetic analyses of <i>Picomonas</i> complete nuclear DNA operon ..	69
3.7.2	Diversity of ‘picobiliphytes’ in marine environment	71
4	Discussion	75
4.1	‘Picobiliphyta’: A cell with enormous mystery	75
4.2	Abundance and diversity of ‘picobiliphytes’	77
4.3	Molecular approach: an advantage or disadvantage?	77
4.4	Flow cytometry: as an approach for protists	78
4.5	The elusive clonal culture	79
4.5.1	Heterotrophic cell culture	79
4.5.2	Fluorescence markers	80
4.6	Microscopic studies	81
4.6.1	Light microscopy	81
4.6.2	Electron Microscopy	81
4.6.3	Ultra-structural character of <i>Picomonas</i>	82
4.7	Novel features of the cell	84
4.8	Feeding behavior and Food Sources	84
4.9	Evidence for the new phylum	87
4.9.1	Justification for a new phylum –Picozoa	87
4.10	Conclusion	89

5	References	91
6	Appendix	99
6.1	Sample collection in Helgoland time series station (Helgoland reede)	99
6.2	'Picobiliphytes' from enriched cultures	101
6.3	Specificity of 'picobiliphytes'	103
6.4	Sequence comparison of Picomonas clonal culture	105
6.5	FACS cell sorting using Mitotracker GreenFM	106
6.6	Picomonas cell view from ventral to dorsal.....	108
6.7	Golgi apparatus	109
6.8	The Cross section of basal apparatus.....	109
6.9	Three dimensional reconstruction of Picomonas	111
6.10	Full length nuclear operon of Picomonas sp	112
6.11	Ultrastructure of Goniomonas flagellar transition region.....	114
7	Abbreviations.....	116
7.1	A1: General	116
7.2	A2: Cellular organelle abbreviations.....	117
8	Acknowledgements	119
	Erklärung.....	120
	Lebenslauf.....	121

1 Introduction

Phytoplankton (marine and fresh water) plays a pivotal role in many biogeochemical processes and provides amenities and services that are essential to mankind's existence, including food production, remediation of waste and regulation of aspects of the climate in the biosphere (W. K. W. Li 1994; Pace 1997). All major oceans and seas are dominated numerically by microscopic protists and phototrophic prokaryotes and contribute to biomass, primary production and respiration in the ecosystem (Li 1994; Stockner & Antia 1986; Biegala et al. 2003). Recent studies revealed that relatively-small, ecologically important but less-known, heterotrophic protists also contributed to the ecosystem, by sustaining the carbon cycle through respiration, grazing on phytoplankton, and being preyed on by larger zooplankton (Fuhrman & McManus 1984; Jeong et al. 2008).

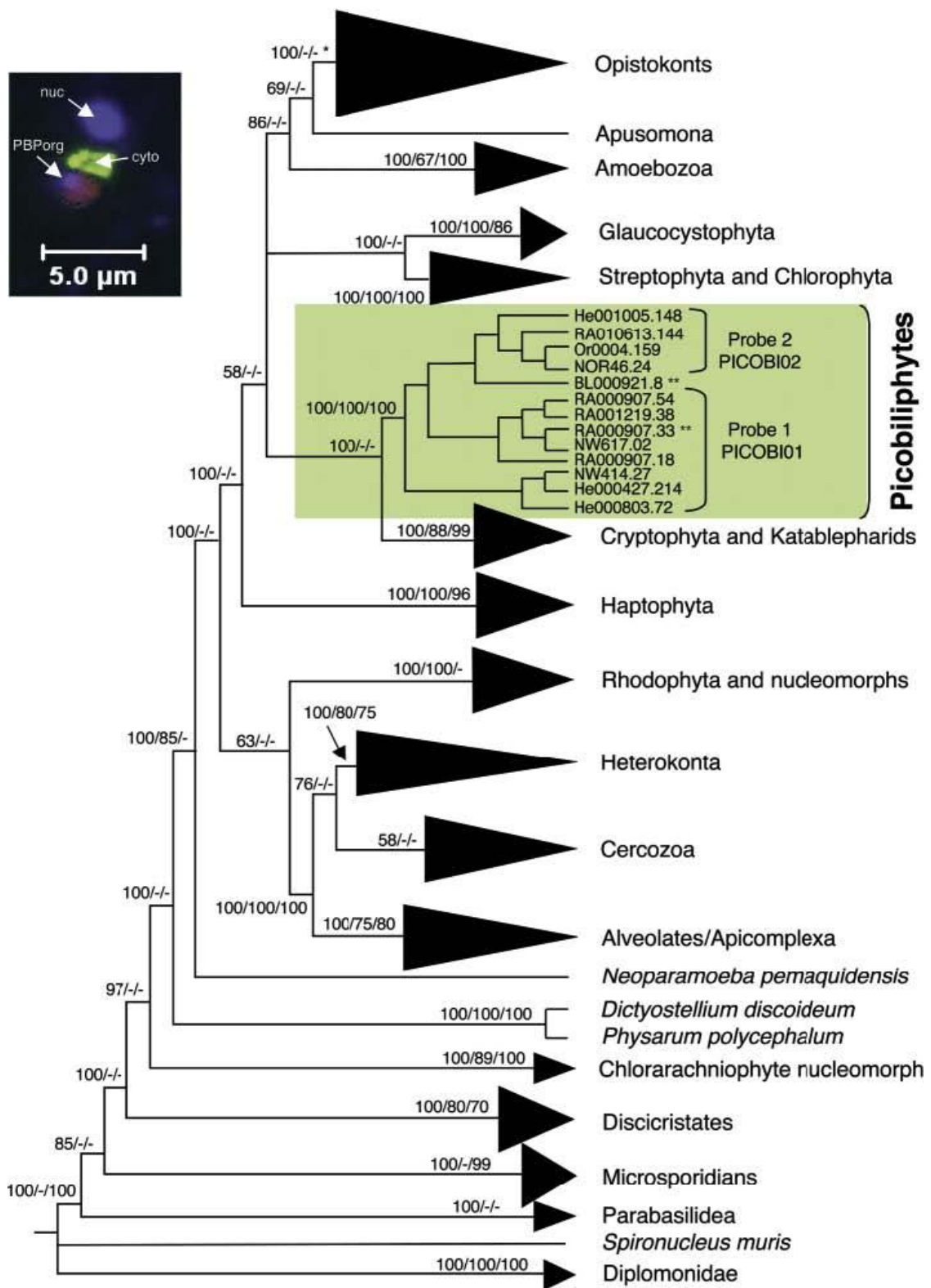
Major groups of nano- and micro-plankton often can be identified microscopically and very little is known about pico-sized plankton ($< 3 \mu\text{m}$), and their morphological features are largely uncharacterized. These, however, equally dominate the biomass and are distributed widely in many coastal and fresh water ecosystems, in the oligotrophic and mesotrophic regions (Biegala et al. 2003; Not et al. 2007b; Medlin et al. 2006; Massana et al. 2004). Because of the poor morphological characterization of picoplankton, molecular analysis is warranted to highlight any biodiversity of this component in aquatic environments. The biodiversity of picoeukaryotes at the species level has only ever been demonstrated by molecular techniques such as polymerase chain reaction (PCR), single strand confirmation polymorphism (SSCP), environmental 18S rDNA clonal libraries and flow cytometry of the unculturable cells (Medlin et al. 2006). Analyses of clonal libraries in phylogenetic trees often highlights many novel diversity among the species level and many new higher-order taxa exist (Giovannoni et al., 1988; Amann et al., 1990; Díez et al., 2001; Moon-Van Der Staay et al., 2001; Not et al., 2002; Not et al., 2007b; Biegala et al., 2003; Massana et al., 2004; Medlin et al., 2006). Taxon-specific (phylum, division, class, or genus) rDNA oligonucleotide probes coupled with flow cytometry have also proven as a useful methods in recent estimates of the abundance of nano- or picoeukaryotes in the ecosystem (Simon et al., 1995, 2000; Not et al., 2002; Biegala et al., 2003; Sekar et al., 2004; Not et al., 2007a).

Up on, investigating the diversity of picoplankton from coastlines of Europe the North Atlantic and Arctic Oceans, several novel groups are discovered (Romari et al. 2004; Medlin et al. 2006). One of them is putatively algal; termed Rosko Group II, which has shown an incredible diversity from environmental 18S rDNA phylogenetic analyses (Romari & Vaultot 2004; Medlin et al. 2006). This new group of 'algae' formed three distinct clades and two oligonucleotide probes (picobili-probes -PicoBI01/PicoBI02) are obtained for FISH analysis. These probes are applied to $3 \mu\text{m}$ filtered field samples and positive signals are thought to be unicellular, slightly oblong (approximately 2-6 μm) and to contain one plastid (the pigments of which are not removed by the alcohol dehydration during FISH,

therefore signalling the presence of phycobilins). The DAPI stained body in the plastid is also suggested the presence of a nucleomorph, retained from a secondary endocytobiosis, as in cryptophytes (Fig. 1.1, Not et al. 2007a). Molecular phylogenetic analyses of these cells have revealed that the organism previously termed ‘picobiliphyte’ was sister to cryptophytes and katablepharids thus apparently supporting the data from FISH (Not et al., 2007a). The authors also examined 3 μm filtered field samples by using molecular probes coupled to Fluorescent Activated Cell Sorting (FACS) against their orange fluorescence (phycoerythrin), 48 to 61% of the sorted cells were positive to Picobili-probes, suggesting that the cell exhibited phycobilin-like pigments.

In addition to Not et al. 2007, the ‘trophic’ nature of ‘picobiliphytes’ are confirmed by Cuvelier et al. 2008, by applying ‘biliphyte-specific probes’ on samples, obtained from Atlantic subtropical regions (Sargasso Sea and the Florida Current, (Cuvelier et al. 2008)). However, unlike results from the initial publication on these organisms, they could not detect a nucleomorph, either visually, or by targeted primers. Furthermore, the results of cell size indicated that ‘picobiliphytes’ are nanoplanktonic.

Figure 1.1: Phylogenetic tree illustrating the position of the novel ‘picobiliphytes’ relative to other major eukaryotes (Not et al., 2007a). Although the tree topology has shown that ‘picobiliphytes’ are a sister group to Cryptophyta and katablepharids, no bootstrap support from maximum parsimony/neighbor-joining are observed. The methods used in this study are Mr Bayes /maximum parsimony/neighbor-joining. PICOBI01 and PICOBI02 are ‘picobiliphyte’ probes used for FISH. (Insert) ‘Picobiliphytes’ targeted by the probe PICOBI02 in FISH (specific for picobiliphyte clade 2). The DAPI-stained nucleus (nuc) in blue; green fluorescence for probe-specific labelling of the small subunit rRNA in the cytoplasm (cyto), and the red autofluorescence indicates the phycobilin protein-containing organelle (PBPorg). →



1.1 Are 'picobiliphytes' heterotrophic?

The presence of phycobilin-like autofluorescence is strongly questioned by Kim et al. 2011, and the orange fluorescence is not detected on 'Picobiliphytes' by FISH. This in turn led to the speculation that 'picobiliphytes'/ 'biliphytes' are most likely not obligate photoautotrophs but rather facultative mixotrophs or phagotrophs, and that the occasional, transient detection of orange fluorescence merely represents ingested prey (Kim et al. 2011). In addition, a recent study by Single-cell Amplified Genome (SAG) analysis (using *Lysotracker* on marine heterotrophic protists) on three individual cells of 'picobiliphytes' has not shown any plastidal genes in their genome database (Heywood et al. 2011; Yoon et al. 2011).

1.2 Quantitative assessment of picoeukaryotes by different approaches

Molecular techniques can result in data that overstate the true degree of biodiversity; current understanding of marine eukaryotic biodiversity may be significantly skewed by PCR biases, by the occurrence of multiple copies of rDNA genes within a single cell, and by the persistence of DNA in extracellular material (Jürgens & Massana 2008). Investigation of biodiversity by targeting 18S rRNA rather than by 18S rDNA library construction, promises to minimize DNA biases and thereby offer new perspectives of understanding the diversity and function of picoeukaryotes (Not et al. 2009). Alternative approaches has focused on constructing clone libraries of individual cells, by flow cytometry by virtue of autofluorescence (chlorophyll/plastids) and using taxon-specific oligonucleotide probes in FISH (Veldhuis & Kraay 2000; Not et al. 2002; Biegala et al. 2003; Fuller et al. 2006; Lepère et al. 2009) has increased the diversity quantitatively. Metagenomics, environmental PCR-based fingerprinting (Vigil et al. 2009) and Quantitative real time PCR (qPCR; Zhu et al. 2005) are other methods used to determine the diversity among the picoeukaryotic community.

The genome sequencing of an individual cell (SAG) by flow cytometry allows the better possibility of analysing microbial communities, populations and biodiversity (Stepanauskas & M. E. Sieracki 2007; Woyke et al. 2009). However, this approach has its limitations for it could not be used for targeting heterotrophic cells in flow cytometry with respect to their optical properties. Thus, applying fluorescent markers like *Lysotracker* (which stains food vacuoles) or *Mitotracker* (for mitochondrial staining) are proved to work efficiently for sorting heterotrophic protists (Bassøe et al. 2003; Pendergrass et al. 2004; Heywood et al. 2011) and enhanced the resolution of heterotrophy diversity, significantly from the library of single amplified genomes (SAGs) over that from environmental libraries of the 18S rRNA gene, from the same coastal region (Heywood et al. 2011). Such libraries of SAGs, but not clonal libraries, also contained several recently-discovered, uncultured groups, including 'picobiliphytes'. The genome analysis of three individual 'picobiliphyte' has now been highlighted the true trophic interaction of picobiliphytes (Yoon et al. 2011).

Thus, not only the diversity and abundance of 'picobiliphytes'/'biliphytes' cannot be inferred based on clone libraries but also the morphological or functional attributes (FISH) that the cell possesses comes under scrutiny (Not et al., 2007a; Cuvelier et al., 2008; Heywood et al., 2011; Kim et al., 2011; Yoon et al., 2011). However, the identification, distribution and abundance of novel eukaryotic groups, from environmental sequences are informative to insight for sampling at appropriate sites and/or times and also enhance the prospect of establishing clonal culture.

1.3 Abundance and Diversity of 'picobiliphytes'

'Picobiliphytes' are eurytopic organisms, widely distributed in the biosphere. The abundance of these sequences varies depending on the ecophysiological nature, and methods applied. Temporal and spatial distribution of 'picobiliphyte' sequence data reveal that 'biliphytes' / 'picobiliphytes' are distributed from the Arctic Ocean to the Sargasso Sea and the Mediterranean coast. These sequences are also found in other oceanic environments such as the South-East Pacific Ocean (F. Le Gall et al. 2008), South China Sea (L. Li et al. 2008) and the Indian Ocean (Ramon Massana et al. 2011) indicating the widespread distribution of these organisms in the world's oceans. The diversity of 'picobiliphytes' varies from 4 to 89 m in depth vertically and from 5 to 30 °C, which is about 1.6 to 28 % of the total picoeukaryotic community (observed from environmental clone libraries) in all oceanic locations (Not et al., 2007a; Cuvelier et al., 2008; Li et al., 2008; Not et al., 2009; Heywood et al., 2011). The diversity at species level may be altered by using taxon-specific primers for clonal libraries; it shows apparently higher than analyses of 18S rDNA libraries (Liu et al. 2009). Culture independent studies also indicated that 'picobiliphyte' sequences are not obtained / detected in fresh water until now (Kim et al. 2011). Although, the diversity and abundance of 'picobiliphytes' are well known now the biggest constraint remains to date; that no cultural representative for this group exists, nor have any idea of the structural identity (ultrastructure) of such an organism available.

1.4 Culturing picoplankton

Picoplankton often grows very slowly and little is known of their nutrient requirements (D Vaultot et al. 2004). Most of the oligotrophic regions on earth have a better chance of providing cultures of picoplankton relative to other trophic state environments. Live cells can be sorted against autofluorescence into various culture media, including preconditioned media (Surek & Melkonian 2004; D Vaultot et al. 2004; F. Le Gall et al. 2008). The isolation of clonal cultures by micro-pipetting can be impractical because of the extremely small dimensions of the cell and its optical properties, but also most of the time the growth requirements are unknown. An alternative approach can be possible to use fluorescent probe-aided cell sorting to isolate relatively small, under-studied heterotrophic protists and bring them into culture in the presence of filtered (unautoclaved) natural sea water.

1.5 Phylogenetic analyses

By combining phylogenetic trees with ultra-structural and biochemical analyses, at least six super groups of distinct eukaryotes i.e., Opisthokonta, Amoebozoa, Plantae, Rhizaria, Chromalveolata and Excavata are proposed (Cavalier-Smith 2004; Adl et al. 2005). However, the increasing number of biodiversity studies using different environmental samples cast doubt on the monophyly of current eukaryotic super groups (Parfrey et al. 2006). The newly-erected taxon, Hacrobia, which includes haptophytes, cryptophytes, telonemids, katablepharids, centrohelids, *Palpitomonas* and possibly 'biliphytes' ('picobiliphytes'), has not yet been clearly assigned to any of the super groups (Okamoto et al. 2009; Yabuki et al. 2010). The hacrobian taxa, however, are morphologically distinguished and phylogenetically long-branched; sharing a common second transitional region at the distal basal plate in one of the flagella, thus, placing them into a likely monophylum (Yabuki et al. 2012).

1.6 Aims of this study

In this study, the morphology of a new eukaryotic class, previously only reported (albeit speculatively) by environmental sequences, is characterized. A clonal culture is established by using fluorescent probes (*Mitotracker*) coupled with fluorescence-activated cell sorting. The established culture is used to characterize the 'picobiliphytes' at light and electron microscopic levels. Environmental clone libraries are made with taxon-specific primers in order to obtain better diversity in Helgoland Time Series Site. The complete nuclear ribosomal operon of 'picobiliphytes' is used for finding the significance and phylogenetic occurrence of its initial discovery.

2 Materials and Methods

2.1 Materials

2.1.1 Chemicals

Chemicals were obtained from the following companies:

Biomol (Hamburg, D), Difco (Hamburg, D), Duchefa (Haarlem, NL), Eurobio (Les Ulis Cedex, F), Fluka AG (Buchs, CH), Merck (Darmstadt, D), Roche (Mannheim, D), Roth (Karlsruhe, D), Fisher Scientific GmbH (Schwerte, D), Chromatographie Service GmbH (Langerwehe, D) and Sigma-Aldrich (Deisenhofen, D). Research grade purity was used for all purposes.

2.1.2 Membrane filters

Isopore membrane filters (10, 5, 3, 2, 0.2 μm)	Millipore
Glass microfibre Filter	Whatman
Nucleopore Tracketch (0.2 μm)	
VaccuCap60	PALL corporation
Mixed cellulose ester membrane filter (0.8, 0.4, 0.2, 0.1 μm)	Schleicher&schuell

2.1.3 Enzymes

Enzymes for molecular biology were obtained from the companies:

Invitrogen (Karlsruhe, D), MBI Fermentas (St. Leon-Rot, D), Promega (Mannheim, D), Qiagen (Hilden, D), Roche (Mannheim, D) and Sigma (Deisenhofen, D).

2.1.4 Kits

The following Kits were used according to the manufacturer's protocols:

DNeasy Plant Mini Kit (Qiagen)

Big Dye® Terminator Cycle Sequencing Kit v3.1 (Applied Biosystems, Foster City, USA)

CompactPrep Plasmid Midi (Qiagen GmbH, Hilden, D)

QIAquick Gel Extraction Kit (Qiagen GmbH, Hilden, D)

2.1.5 Antibiotics

The following antibiotics are used in this experiment. Stock solutions are prepared according to the manufacturer instructions. The final concentration been used as low as possible in enriched 'picobiliphyte' flasks to inhibit only the bacterial growth.

Antibiotic	stock solution		Final conc. for 10ml of samples
Ampicillin	50 mg/mL	in water	50 $\mu\text{g}/\text{ml}$
Carbenicillin	50 mg/mL	in water	50 $\mu\text{g}/\text{ml}$

Kanamycin	50 mg/mL	in water	50 µg/ml
Tetracyclin	25mg/mL	In water	25 µg/ml
Chloramphenicol	15 mg/mL	in ethanol	15 µg/ml

2.1.6 Bacterial strain

Genotype of JM109

F⁺ (traD36, *proAB*⁺ *lacI*^q, Δ (*lacZ*)M15) *endA1* *recA1* *hsdR17*(rk-, mk+) *mcrA* *supE44* λ -*yrA96* *relA1* Δ (*lacproAB*)*thi-1*

2.1.7 Software

Acrobat Reader Version 9.0

Photoshop Version CS4

Adobe Illustrator CS4

Adobe

SeqMan II

Edit Seq

DNA-Star Inc

Sequence Detection Software v1.4

Applied Biosystems

AlignIR V2.0

Licor

Blender V. 2.63

<http://www.blender.org/>

2.2 Methods

2.2.1 Sample collection, culturing and Isolation

2.2.1.1 *Sample collection in Helgoland*

The Helgoland time series station (Helgoland roads) is located at 54° 11.3'N, 7°54.0'E in the central German bight of the North Sea. North Sea surface water (depth, 5 –to 8-m) was collected early morning (6-7 am) from Helgoland roads (Helgoland reede) from July 2007 to October 2007. The samples were immediately fractionated with different filters and final fractionation was done with 3 µm membrane filter which is ideal for Picoeukaryotes (L K Medlin et al. 2006).

Helgoland sea water was serially filtered with 10, 5 and 3 µm isopore membrane filters (Millipore). The 3 µm filtered sea water was used for three different purposes: Firstly, 50 ml of sea water was directly transferred into 50 ml culture flask (Falcon) allowing the growth of 'picobiliphytes', secondly, 200 ml of sea water further filtered on 25 mmΦ polycarbonate membrane (Millipore), washed with modified saline ethanol (22 ml of 100% ethanol, 5 ml of deionized water, 3 ml of 25X SET (3.75 M NaCl, 25 mM EDTA, 0.5 M Tris–HCl and pH 7.8) for one hour to fix the cells before storing at -80°C for FISH analysis and finally, 500 ml of sea water was filtered on 0.2 µm filter and further used for genomic DNA extraction by 3% CTAB method (J. J. Doyle & J. L. Doyle 1990). However, the 3%CTAB method for DNA isolation did not yield enough DNA; a modified protocol from DNAeasy method (Qiagen) was necessary for DNA isolations from the environmental samples (see below 2.2.2.1.2). DNA was quantified by Nanodrop (ND1000 spectrophotometer, NanoDrop) and 100ng of DNA was used to check the presence of 'picobiliphytes' with taxon specific forward primers (PICOBI01F and PICOBI02F) with 18S eukaryotic reverse primer.

2.2.1.2 *Enrichment and clonal culturing of Pico cells*

Fractionated sea water (3 µm) was enriched with various culture media (see below 2.2.7) with minimal nutrients (diluted to 1:50) for photosynthetic eukaryotes (Surek & Melkonian 2004; D Vaultot et al. 2004; F. Le Gall et al. 2008). For Heterotrophic protists, the sea water was fractionated with 10 µm membrane filter and passed through a second 2 µm membrane filter. 100 ml of fractionated sea water was split into two 50ml falcon tubes and centrifuged at 4000g for 10 min; the supernatant was filtered using a 0.2µm filter. Both the pellet and membrane filter remnants were transferred into culture flask with 0.2µm Filter Sterilised Sea Water (FSSW).

2.2.1.3 *Primary culture - a methodical approach*

In this study, two different strategies were applied to obtain an enrichment of 'picobiliphyte' cell. The first approach was a direct enrichment of 3 µm filtered sea water with addition of minimal nutrients including; Keller (Keller et al. 1987),

Drebes (Drebes & Schulz 1989), GP5% (Loeblich & Smith 1968) and IMR (Eppley et al. 1970) media (1:50 dilution) and allowed the cells to grow in a 50 ml tissue-culture flasks. The second approach was based on cell sorting, and targeted specific populations (orange fluorescence (FL2), also chlorophyll fluorescence (FL3)) by its optical properties. Cells were sorted into 96 well/24 well plates (Surek & Melkonian 2004; D Vaultot et al. 2004; F. Le Gall et al. 2008) and were incubated at 15°C. Enriched cultures were examined several times by utilizing FACS and microscopy observations followed by molecular methods such as using taxon specific PCR primers and FISH probes (Veldhuis and Kraay, 2000; Not et al., 2002; Biegala et al., 2003; Fuller et al., 2006; Not et al., 2007a).

2.2.1.4 Heterotrophic cell culture

Samples from 2 µm filtered sea water, from the Helgoland Time Series Site were initially maintained in FSSW and tested by PCR with specific primers (*PicoPCR*) for the presence of ‘picobiliphytes’. Such PCR positive flasks were duplicated in FSSW and were maintained by regular transfer into fresh FSSW for every 2 weeks with periodic check for PCR positive cells. These were later transferred into minimal nutrient media and were checked only by *PicoPCR* and not by light microscopy, since the overgrowth of contaminants (eukaryotic and bacterial) was hindering the identification of ‘picobiliphytes’.

2.2.2 Molecular approach

2.2.2.1 Isolation of genomic DNA

2.2.2.1.1 gDNA extraction from membrane filters – 3%CTAB method

Picoplanktons were retained on 0.2 µm filter from 500 ml of 3 µm pre-filtered Sea water. The filter was dried at room temperature and folded before inserting into a 15 ml screw cap tube. 700 µl of 3%CTAB solution was added incubated at 60°C for 2 min with intermediate vortexing. 300 µl of TE or 1XSET was added to the tube and vortexed it again. The aqueous solution was transferred to 1.5 ml tube. The sample was centrifuged at 12000 rpm for 1min (to remove cell debris). The liquid was transferred into new 1.5ml tube and 0.6 volume of isopropanol was added and incubated at RT for 10 min. The sample was centrifuged at 12000 rpm for 15 mins. The pellet was washed with 600 µl of 80% ethanol by centrifuging it at 12000 rpm for 2 min. The supernatant was decanted and the pellet was air dried. Pellet was re-suspended with 20 µl of TE buffer.

2.2.2.1.2 gDNA extraction from membrane filters –DNAeasy method

Genomic DNA was isolated from 0.2 µm filter (also for cultures) by using Qiagen- DNAeasy Plant Mini kit protocol according to the manufacturer’s instructions with few modifications. For each filter, 700 µl of AP1 buffer was added and incubated at 65°C for 5min. 200 µl of AP2 was added and incubated on ice for 5min. Samples were centrifuged at 10000 rpm for 15min. The supernatant was transferred into the column followed manufacturer’s instructions. Alternatively, (when the cells were few) after centrifugation, the supernatant was transferred into 1.5 ml tube and 0.6 % of Isopropanol was added followed CTAB method.

2.2.2.2 Polymerase chain reaction-PCR

For environmental samples, 100ng of genomic DNA, 200 μ M dNTPS, 2-5 picomoles of forward and reverse primers and 1U of DreamTaq DNA polymerase (Fermentas) were used in a 20 μ l PCR reaction volume. The PCR run was carried out in two different thermocyclers a *Primus 96plus* (MWG Biotech, Ebersberg, Germany) and a *T personal* (Biometra) under following conditions.

PCR condition:

Initial denaturation - 95 °C for 5 min.
 Denaturation - 95 °C for 30 sec
 Annealing - 50-58 °C ** for 30sec
 Extension - 72 °C for 1min 30sec

The cycle was repeated for 35times*

Final extension 72 °C for 5min
 Store 10 °C forever

*a) in case for re-amplification, both primary and secondary amplification 30cycles were carried out and b) for *PicoPCR* specific primers were used from both end (PicoBi01F & ITS1R), and 37cycles were performed.

** All PCR experiments were carried out with 55°C, except for environmental PCR with rDNA primers at 50°C

PCR products were checked by running on a 1% Biozym LE agarose gel containing ethidium bromide (1 μ l of 1% EtBr solution for 50ml of 1% agarose gel). For direct cell PCR (**cell PCR**) from cultures, 100 μ l of enriched cultures were added to PCR tubes and centrifuged to pellet down cells at 8000 rpm for 10 min. PCR mixture with enzyme (20 μ l) was added directly to the PCR tube and amplified with mentioned above conditions. 1 μ l of primary amplicons were used for reamplification as shown in Fig. 2.1 & 2.2 *PicoPCR* is same as **cell PCR**, differ from two **a)** 'picobiliphytes'-specific primers (PicoBI01F/ITS1R) were used as primers **b)** amplification cycles were increased to 37.

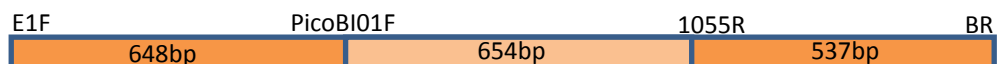


Figure 2.1: PicoBI01F and Eukaryotic 18S reverse (BR) are used for primary amplification and internal eukaryotic reverse (1055R) used for reamplification.



Figure 2.2: ITS region was identified for Picobiliphytes and ITS1R (Specific for Picobiliphytes-*Clade I&II*) was used as reverse primer for primary amplification

For colony PCR, the individual colonies were picked by toothpick and patched on LB agar+ ampicillin plate and remaining cells were directly dipped into PCR mixers in PCR tubes with an increased initial denaturation step (95°C for 7min) to lyse the cells.

2.2.2.3 Cloning and plasmid preparation

PCR products were purified by microspin G-25 columns (Amersham Biosciences) and checked on the gel. The purified PCR products were ligated into pGEMTeasy vector (Promega) at 12 °C overnight. 2 µl of ligated product was added into 40 µl of *Escherichia coli* strain JM109 (Promega) chemical competent cells and kept on ice for 5mins. A heat shock was given at 42 °C for 45 seconds and 500 µl of SOC was added immediately after the heat shock. The cells were allowed to grow for 45 min at 37 °C and 100 µl of cells were spread on LBagar+ ampicillin (100 µg/ml) and 70 µg/ml X-GAL and 80 mM of IPTG for Blue/White screening. The plates were incubated at 37 °C overnight. White colonies were picked for inoculation and/or colony PCR.

A PCR positive from the colony PCR were inoculated into LB medium and supplemented with 50 µg/ml ampicillin and incubated for overnight. Plasmids were isolated using QIAprep spin miniprep kit (Qiagen). The plasmids were quantified on agarose gel and further taken forward for sequencing.

2.2.2.4 DNA sequencing

For confirming PCR products, 10 to 25 ng amplicons of DNA (For Plasmid DNA, 100 to 200 ng) were taken directly for sequencing with BigDye Terminator v3.1. The products were sequenced by the sequencing service facility at the University of Cologne (Cologne centre for Genomics) and at the Alfred Wegener Institute for Polar and Marine Research (AWI, Bremerhaven).

2.2.2.5 Sequencing reaction

The DNA samples were added into 8 well PCR strip and dried at 50 °C. The following reaction was setup -

5Xsequencing buffer	1.6 µl
Primers	1.6 pm
BDT v3.1	1 µl
ddH ₂ O up to	10 µl

Cycle sequencing reactions were performed in *Primus96 plus thermocycler* with following conditions

Initial denaturation	94 °C for 2mins
35cycles:	
Denaturation	94 °C for 20secs
Annealing	50 °C for 30secs
Extension	60 °C for 2mins
Final extension	60 °C for 6mins

2.2.3 Fluorescence Activated Cell Sorting (FACS)

Filtered sea water (3 µm) was taken for cell sorting. The cells were sorted using autofluorescence phycoerythrin (PE) in FL2 (orange fluorescence) against chlorophylls in FL3 (red fluorescence). The sorted cells (single cells or more cells at

times) were collected in 96 well plate for identifying ‘picobiliphytes’ (Not et al., 2007a). Heterotrophic protists were sorted by using *Mitotracker* Green FM (M7514 Invitrogen); a green fluorescent dye that stains mitochondria in live cells. A stock solution was prepared in DMSO as per manufacturer’s instruction. 20 nM of working concentration was added to 10 ml of sample and incubated at 15°C in dark for 15-20 min. The stained samples were immediately sorted under blue laser at 488nm in FACSvantage^{SE} (University of Cologne). The cells which emitted high green fluorescence (FL1) were sorted against side scatters (SSC). Second window was also used to monitor the Green fluorescence (FL1) against orange fluorescence (FL2). Two types of cell sorting were performed: target cells sorted directly into PCR tubes for PCR amplification, single cell sorting was performed and collected into 96 well and 24 well plates and incubated at 15 °C. Samples from 96/24 well were checked for ‘picobiliphytes’ by PCR with specific primers.

2.2.3.1 Tyramide signal amplification – Fluorescence In-Situ Hybridisation (TSA-FISH)

2.2.3.1.1 Probe labelling and design

Picobiliphyte probes PICOBI01, PICOBI02, Picoclade2D and Picoclade1G were designed for TSA-FISH Chemscan analysis earlier by (Not et al. 2007a). CHLO02 probe which was used for chlorophyta (Simon et al. 2000) also used in this study as a positive control. All the probes were labelled with horseradish peroxidase (HRP) at the 5’ end and were obtained from Linda Medlin Lab (AWI, Bremerhaven).

TSA-FISH experiment was carried out for cells which were sorted by FACS with red (chlorophyll) and orange (PE) fluorescence. FISH was also carried out for field samples collected from Helgoland; pre-processed membranes were placed on the manifold. Both experiments were conducted as per methods mentioned by Kerstin Toebe (Tobe et al. 2006) where 20% formamide was added in the hybridization buffer. Hybridisation was carried with 50 µl of hybridisation buffer containing 1ng/µl of probe at 37 °C for both experiments. For TSA reaction 100µl (1:50) of fluorescein tyramide (TSA-direct Kit, Perkin Elmer, USA) was added.

Hybridization Buffer

5X SET

0.1 % (v/v) Nonidet P40 (Sigma)

20 % formamide

2 % blocking reagent

Probe preparation

50 ng of each probe (PICOBI01, PICOBI02, Picoclade2D and Picoclade1G) was mixed with 46 µl of HB.

Substrate solution

Mix 1volume of 40% dextran sulphate (in water) with volume of amplification diluents and 1/50 volume of tyramide solution (Fluorescein labelled).

2.2.3.1.2 TSA-FISH on glass slide

1ml of cells was fixed with 100 µl of 16% PFA for 4hrs at 4 °C in a 1.5ml centrifuge tube which was previously treated with Dichlorodimethylsilan (Fluka). Cells were centrifuged at 8000g for 5min at RT. Pellet was re-suspended with 2X PBS buffer and transferred on to a glass slide which was treated with Poly-L-lysine (Sigma) and allowed to settle on the slide for 30min to 1hour. Dehydration step was followed by adding modified saline ethanol and washed again with 1xSET. Probes (5 ng/µl final conc.) were then added to hybridization buffer and incubated at 37 °C for 2 hrs. TSA-reaction was followed as mentioned by Tobe et al., 2006.

2.2.3.1.3 Solid phase cytometry analyses

A ChemScan RDI (chemunx) was used for solid phase cytometric (SPC) analyses. A blue green laser at a 488nm wavelength from argon lamp was used to do an overlapping scan on the TSA-FISH filter membrane to detect the FITC fluorescence. Methods were followed as mentioned by Tobe et al., 2006. The software generated a comparison output before and after discrimination step was applied (called as scan map). These scan map results were validated by epifluorescence microscope (Nikon, Eclipse E800) by placing on the motorized stage. The images were captured with CCD-1300CB camera Vosskuehler, Germany.

2.2.4 Microscopy

2.2.4.1 Light microscopy

Cells were regularly sub-cultured into 50 ml tissue culture flask (Falcon) and observed on Inverted light microscope (Olympus CK40) and images were taken by Olympus U-CMAD3 camera. A video to capture the motility of cell by was recorded using a Panasonic SDR-H80.

2.2.4.2 Fluorescence microscopy

Samples from FACS cell sorting (autofluorescence, *Mitotracker*® Red CMXRos and *Mitotracker*® Green fluorescence) were fixed with 1.25 % glutaraldehyde (GA) and observed under Nikon, Eclipse E800 microscope. For excitation maxima the CMXRos is 579 and emission was at 599nm which were visualised with TRITC filter, and Green FM (excited at 490 and emitted at 516 nm) was visualised with GFP filter under the microscope. A DAPI stained nuclear body was observed under DAPI filter (Excitation at 340-380 and emission at 435-485 nm).

Fluorescein fluoropore was used for TSA- FISH reaction and cells were observed under same FITC filter (Fluorescein has absorption maximum at 494 nm and emission maximum at 521 nm). Images were captured by CCD camera and images were analysed using Metamorph software tool Version 6.3r4. The colourless fluorescence images were later superimposed in Adobe Photoshop and artificial fluorescence were induced by following stepwise protocol.

i) All the required images were imported into Adobe, and image mode was set to RGB colour. (Set foreground and back ground in Black by adjusting R=0;B=0;G=0)

ii) Image was selected by using 'ctrl+A' option, and the unwanted two channels were removed by delete option in the channel windows. Example for DAPI image, Green and Red channels were deleted and Blue channel was retained. Images were superimposed with another image and transparency set to screen mode. Note (a. all images were adjusted with bright/contrast before applying RGB mode, b. Background was set to layer 0 by double clicking the image in adjustment panel)

2.2.4.3 Scanning Electron microscopy

Cells were fixed with 1% Para-formaldehyde (PFA) and 1.25% of Glutaraldehyde (GA) in enriched media for 30 min. on ice. Fixed cells were directly placed on glass slide coated with Poly L-lysine and allowed to settle for 30 min at RT. To avoid the damage and contraction of the cell, they were slowly replaced with firstly; 0.1 μm sterile sea water, and subsequently 100%, 50% and 25% SSW with water then dehydration step was followed as in Martin-Cereceda et al., 2009. In the last step a critical point to be noted was that the drying was done with liquid CO₂. Scanning images were taken in QuantaTM 250FEG imager.

2.2.4.4 Transmission Electron microscopy

2.2.4.4.1 Fixation and Embedding

The fixation and embedding was slightly modified for the heterotrophic cells from Geimer and Melkonian, 2004; Buchmann and Becker, 2009. 10ml of healthy grown cells (approx. 10days old cells) were fixed with mixture of 200 μl of 16%PFA, 50 μl of 25%GA and 50 μl of OSO₄ and kept on ice for 30 min. The cells were transferred into 1.5 ml centrifuge tubes which was pre-coated with Dichlorodimethylsilan then pelleted at 4000g for 10 min. The supernatant was carefully decanted and step was repeated until a visible pellet was seen. The cell pellet was re-suspended and pelleted twice with 500 μl of 0.1 μm filtered SSW. 50 μl of 50% BSA added and carefully re-suspended and centrifuged at 4000g for 10 min. The supernatant of BSA was cautiously removed with pipette, without disturb the pellet. 50 μl of 1.25% GA in SSW was added to fix the pellet on ice for 30 min. The fixed pellet was carefully transferred to new 1.5ml centrifuge tube for dehydration (To remove pellet, the centrifuge tube was placed upside down and the tip was cut with razor vertically into two halves). Initially the flake was saturated with 100% SSW and 50% SSW in 15% ethanol, 25% SSW in 22.5% ethanol, followed by 30%, 50%, and 70% for 15mins each on ice. Subsequently, the flakes were dehydrated with 70%, 90% and 100% (twice) ethanol for 15mins each at -20 °C. Before resin embedding, the flakes were treated with EtOH: Propylenoxide (1:1), Propyleneoxide and Propylenoxide: Epon (1:1) for 30min at -20 °C. Propylenoxide was evaporated under the hood for O/N. The pellet was transferred into fresh epon and incubated for 8 hrs. The samples were place on rubber mold and baked overnight at 65 °C for hardening the epon block.

2.2.4.4.2 Microtome sectioning and staining of Ultra-thin sections

The epon block was trimmed with a razor blade to get closer to the pellet and the block was fixed with block holder which was then mounted on microtome arm (Leica EM UC7). A glass knife was used to trim and section to form a trapezoid with 90° angle and to make the bases at 75° and 105° angle to create heights to obtain isosceles trapezoid. 100 nm, 60 nm thin sections were made using diamond knife (DiATOME 45°, Leica). Sections were collected on pioloform of the slot grid; air dried and place on the rubber mat for further analyses.

For staining the sections, the grids were placed on a rubber grid holder, covered with a drop of uranyl acetate (UAC) and incubated for 10 min. in dark at RT. The grids were washed twice with ddH₂O. Grids were placed on a petridish with NaOH flakes. Drop of lead citrate (PbC) added to the grids and incubated for 3.5 min. Grids were then washed with NaOH (5 mN) solution and finally washed with ddH₂O. The grids were air dried and stored in grid holder until further analysis. Observation and documentation: Samples were observed under a transmission electron microscope (Philips CM10); images were taken by Gatan ORIUS TEM CCD camera. Images were analysed by Gatan Digital Micrograph software.

2.2.5 3D construction of *Picomonas*

3D reconstruction of EM serial sections was achieved by freely available software IMOD 4.1.10 (Kremer et al. 1996) programme from <http://bio3d.colorado.edu/imod/>. IMOD is supported by cygwin (Cygwin 1.7.1) (<http://www.cygwin.com/>), a collection of tools which look like a Linux environment on Windows. The serial sections from EM were initially aligned (all the sections were placed in one file) with Adobe Photoshop (CS4), with transform tool (ctrl+t) option. Once the alignment was completed the layers were exported as ‘tif’ files in </usr/local> directory in Windows. All the ‘*.tif’ files were then converted into newname.mrc file. MIDAS (alignment tool in IMOD) was run for the newname.mrc file to check the alignment once again. Once the alignment was established, the sections were visualised in 3dmod programme. Each contour was drawn manually for each section and all the contours were viewed in model view.

The Z-scale value was assigned by calculating the 200 nm scale bar in Photoshop (image magnification is 19000X and pixel value is 2400X2400) is equal to 3.25 cm. In Photoshop, 28.346 pixels is equal to 1cm. so, 2.17 nm of the scale bar gives 1pixel.

That is 1pixel = $(\{200/3.25\}28.346)$. If the thickness of the each section is 60 nm, it will be divided by 2.17 and gives a Z scale value as 27.65pixels.

Finally, the 3D construction was exported as ‘*.tif’ images, which can be used as image or can be used as movie. The final 3-D animation was constructed by Blender software version 2.63 (<http://www.blender.org/>).

2.2.6 Phylogenetic analyses

2.2.6.1 Full length sequences of *Picomonas*

The *Picomonas* full length rDNA operon was obtained by primer walking method, using different primer combinations, and re-amplification was carried out with picobiliphyte-specific primers. Overlapping primers were designed to identify the full length operon. The primers which were used in this study are listed in section 2.2.8. The detailed full length sequencing for this cell is given in appendix 6.10. The full length ribosomal sequence of *Picomonas* cell and other nine new environmental sequences have been deposited with the accession number (acc no JX988758 for culture isolate and acc no JX988759- JX988767 for the environmental sequences) in Genbank. Full length 18S and 28S rDNA sequences were used for search of other ‘picobiliphyte’ sequences by BLAST (<http://blast.ncbi.nlm.nih.gov/Blast.cgi>). New sequences (environmental) were downloaded from the Genbank Database. These sequences from ‘picobiliphytes’ were added to the existing aligned data set, which covers the most eukaryotic groups, consisted the complete nuclear SSU and LSU sequences (kindly provided by Dr. Birger Marin and Nicole Sausen). The ‘picobiliphytes’ sequences were pre-aligned with ‘muscle’ in Seaview 4.2 and manually aligned for secondary structures with existing aligned sequences (<http://pbil.univlyon1.fr/software/seaview.html>). Total three dataset was produced for the following analyses; 1. dataset1 contained all eukaryotic complete full length ribosomal sequences (104 taxa with 4,461 aligned character), 2. dataset2 all eukaryotic 18S SSU sequences along with ‘picobiliphyte’ sequences (185 taxa, 1598 characters) and 3. dataset3 with ‘picobiliphyte’ SSU sequences (85 taxa, 1775 characters).

1. Detection of the phylogenetic position of ‘picobiliphytes’ inside of eukaryotes
2. Checked the environmental ‘picobiliphyte’ sequences biased with others. (not shown)
3. Analysed the diversity of the ‘picobiliphytes’ using the 18S rDNA sequences.

2.2.6.2 Phylogenetic analysis methods

For each alignment a maximum likelihood (ML) tree topology was analysed using the programme RAxML v 7.0.3 (Stamatakis 2006), (chosen the best topology from 20 replicates). For each analysis, ML 1000 bootstrap replicates with RAxML were calculated. For dataset-1, which covered the whole eukaryotes rDNA operon also neighbor joining (NJ), and maximum parsimony (MP) bootstrap values were calculated by PAUP (4.0b10). The GTR + I + Γ evolution model was chosen for ML and NJ analysis. For NJ analysis the model parameters were calculated by Modeltest (v3.7). Also, Bayesian analyses were performed over 5,500,000 generations sampling from two runs with four Markov chain Monte Carlo (MCMC) chains (one cold, four heated chains), and 500,000 generations were removed as burn-in. Branches with bootstrap values below 50% and Bayesian posterior probabilities below 0.95% were considered not supported.

2.2.7 Media for culturing Picoplanktons

K Medium (Keller et al. 1987)

950ml filtered sea water add:

Quantity	Compound	Stock solution
1ml	NaNO ₃	75.0g/L
1ml	NH ₄ Cl	2.68g /L
1ml	NaH ₂ PO ₄	5g/L
1ml	Na ₂ SiO ₃ .9H ₂ O	30g/L
1ml	H ₂ Seo ₃	1.29mg/L
1ml	Tris base pH7.2	121.1g/L
1ml	K trace Metal soln	
0.5ml	f/2 Vitamin soln	

Make up to 1L

K trace Metal soln_ 1Liter

Quantity	Compound	Stock solution
41.6g	Na ₂ EDTA.2H ₂ O	
3.15g	FeCl ₃ .6H ₂ O	
1.0ml	Na ₂ MoO ₄ .2H ₂ O	6.3g/L
1.0ml	ZnSO ₄ .7H ₂ O	22.0g/L
1.0ml	CoCl ₂ .6H ₂ O	10.g/L
1.0ml	MnCl ₂ .4H ₂ O	180g/L
0.5ml	CuSO ₄ .5H ₂ O	9.8g/L

Heat to Dissolve

f/2 vitamin soln

Quantity	Compound	Stock solution
1.0ml	Vitamin B12	1g/L
10.0ml	Biotin	0.1g/L
200.0mg	Thiamine HCl	

Make up to 1Liter

Drebes (Drebes & Schulz 1989)

Substance	Final conc in micro Molar	stock solution	vol for 1L culture medium
MnCl ₂ X ₄ H ₂ O	10	0.999g/50ml	100µl
NaNO ₃	50	2.125g/50ml	100µl
Na ₂ HPO ₄ X ₁₂ H ₂ O	3	0.538g/50ml	100µl
Na ₂ O ₃ Si x 9H ₂ O	35	5.000g/500ml	1ml
Fe-EDTA(Na-salt)	35	2.500g/500ml	1ml
Vitamin	(Asp12vita- stock)		1ml

Add all the substances into 0.2µm sterile sea water and filter sterile with 0.1µm filter

G.P5 modified (Loeblich & Smith 1968)

Ingredients	conc	Volume/L
KNO ₃	10%	1ml
K ₂ HPO ₄ .3H ₂ O	0.51g/100ml	2ml
Trace metals	Asp12	1ml
PII metals	wess	1ml
Soil extract		1ml
Vitamins	Asp12	1ml

add into 0.2µm filter sterilized SW and filtered with 0.1µm filter

2.2.8 Primers and probes

The detailed list of primers and probes used for construction of nuclear rRNA operon, diversity studies and for in-situ hybridisation experiments were given below.

Primers	Sequence	Author
PICOBI01F*	CGG ATT TTG GCA TCA CGC	Not et.al 2007a
PICOBI02F*	ACG GTT TGA CGG GCA TAT	Not et.al 2007a
PICOBI01R	GCG TGA TGC CAA AAT CCG	Not et.al 2007a
PICOBI02R	ATA TGC CCG TCA AAC CGT	Not et.al 2007a
P01ITS1F	CCA CGT GAA CAT TGA GAT G	In this study
P01ITS2F	CAG CGT AGC GTG GTA GTA	In this study
P01ITS2FII	GTC GCT CCA AGA GCA GAG	In this study
P01ITS1R	CAT CTC AAT GTT CAC GTG G	In this study
P01ITS2R	TAC TAC CAC GCT ACG CTG	In this study
P01ITS2RII	CTC TGC TCT TGG AGC GAC	In this study
1055F*	AGT GGT GGT GGT GCA TGG CCG T	In this study
1055R	ACG GCC ATG CAC CAC CAC T	Elwood 1985; Karsten2006
1F	AAC CTG GTT GAT CCT GCC AGT A	Medlin 1988 without polylinker
BR	CCCGGGATCCAAGCTTGATCCTTCTGCAGGTTACCTAC	(Marin et al. 2003) with poly linker
28S_PicoB20R	ACA ACC TGA CTC GCC AAG ATG TC	In this study
28S_PicoG4For	TAC CAC TAC TCG TTG TCT CG	In this study
28S_Eu_G2rev	ACT AGA GTC AAG CTC AAC AGG	In this study
28S_PicoD15F	CTT CCT AAC CGA GCG TGG	In this study
28S_PicoD21F	CAT CAG GGC AAA TGC GAT G	In this study
L52R	TTT CTT TTC CTC CGC T	In this study
28S 2933 rev	CAC GAC GGT CTA AAC CCA GCT GCT CAC GTT CCC	Marin 2012
28S_1433 rev	AAT ATT TGC TAC TAC CAC CAA GAT C	Marin 2012 (Courtesy: Birger Marin)
28S 336 forw	GAG ACC GAT AGC GAA CAA GTA C	Marin 2012
28S 3356 rev	GGC T(GT)A ATC TCA G(CT)(AG) GAT CG	Marin 2012
Gamp627F	TGG TCA ACT CGG CTC TTT CT	In this study
Gpac586F	AAG CTC GTA TTG GAT CTC GG	In this study

Probes	Sequence	Author
PicoBI01_FITC	FITC-GCG TGA TGC CAA AAT CCG	Not et.al 2007a with modifier
Goni01_FITC	FITC-GAA CCG CAG TCC TAT TCC	In this study
PicoBI01_TexRed	RED-GCG TGA TGC CAA AAT CCG	Not et.al 2007a with modifier
PicoBI01_BioTEG	BITEG-GCG TGA ZGC CAA AAT CCG BDT	Not et.al 2007a with modifier
Goni01_BioTEG	BITEG-GAA CCG CAG ZCC TAT TCC BDT	In this study
EUK1209R_BioTEG	BITEG-GGG CAZ CAC AGA CCT G BDT	Giovannoni et al. 1988
EUB338_BioTEG	BITEG-GCT GCC ZCC CGT AGG AGT BDT	Amann et al. 1990

3 Results

3.1 Identification of a 'picobiliphyte' population on the Helgoland sampling site

To establish the clonal cultures of formally described a putative novel algal class ('picobiliphytes' by Not et al., 2007a), Sea water is collected from open surface (5 meter depth) during the months of July – October 2007. The field samples are subsequently fractionated after sample collection (see M & M sect. 2.2.1.1) and the genomic DNA has been extracted for PCR analysis. PCR is performed to amplify the 18S ribosomal DNA from the genomic DNA, by using common eukaryotic 18S forward primer (*Eu1AF3*) and with equimolar concentration of picobiliphyte-specific reverse primers (*PicoBi01R* is designed to amplify clade I and II, and *PicoBi02R* for clade III according to Not et al. 2007a). The PCR product is yielded two fragments with size range of 645 bp (*Eu1AF3*+ *PicoBi01R*) and 685 bp (*Eu1AF3*+*PicoBi02R*). A plasmid DNA (He000427.214) containing 'picobiliphyte' sequence for clade II is used as positive control (Not et al., 2007a).

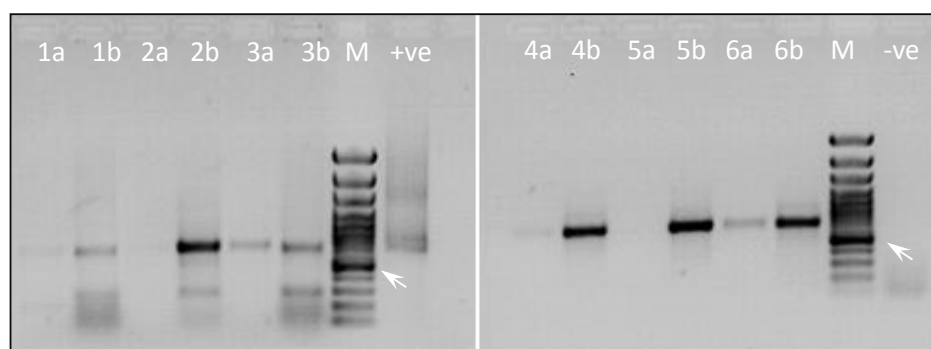


Figure 3.1: PCR product amplified from (a) Samples from 3 μm filter membrane and (b) Samples from 0.2 μm filter membrane. 1-6 corresponds to field samples from Pico070720 (Pico/yy/mm/dd), Pico070723, Pico070724, Pico070725, Pico070726, and Pico070727 respectively. M- 1Kb ladder-plus, +ve plasmid DNA He000427.214 (band is not bright), -ve negative control. (Arrow =500 bp).

Figure 3.1 shows predominantly, the existence of 'picobiliphytes' on samples that are from 0.2 μm filter membrane compared to samples from 3 μm filter membrane. The amplified product is further sequenced to confirm the presence of picobiliphyte-specific sequences. BlastN analysis is performed comparing the obtained sequence data against nr (NCBI) database thus, finding similar environmental sequences (Not et al., 2007a)

3.2 Abundance of 'picobiliphyte' sequences from Helgoland roads (Reede)

Genomic DNA extracted from $< 3 \mu\text{m}$ filtered sea water samples between July to October 2007 are shown the abundance of 'picobiliphytes' sequences throughout the period. They are detected in water ranging from 12 to 16 $^{\circ}\text{C}$ during the sample collection period in the Helgoland time series station. Among 55-day sample collection, pico-positive sequences are detected in 43 days, which is 78% of overall sampling in Helgoland (appendix 6.1). This indicates that cells are distributed during this period (except beginning and end of August and end of October). 'Picobiliphytes' are found in summer supporting with previous data shown (Not et al., 2007a), from samples collected in fall and winter (Fig. 3.2) thus indicating the possible existence throughout the year.

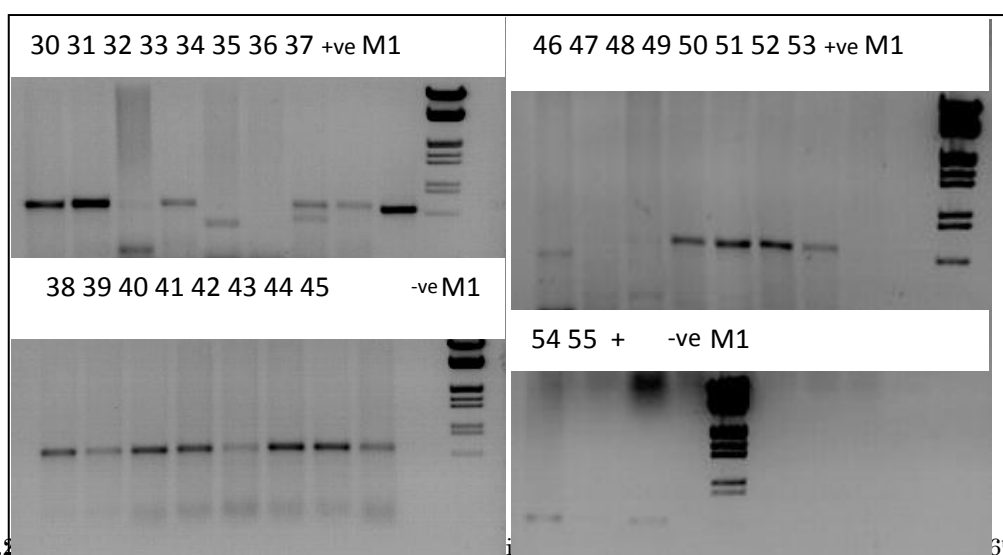
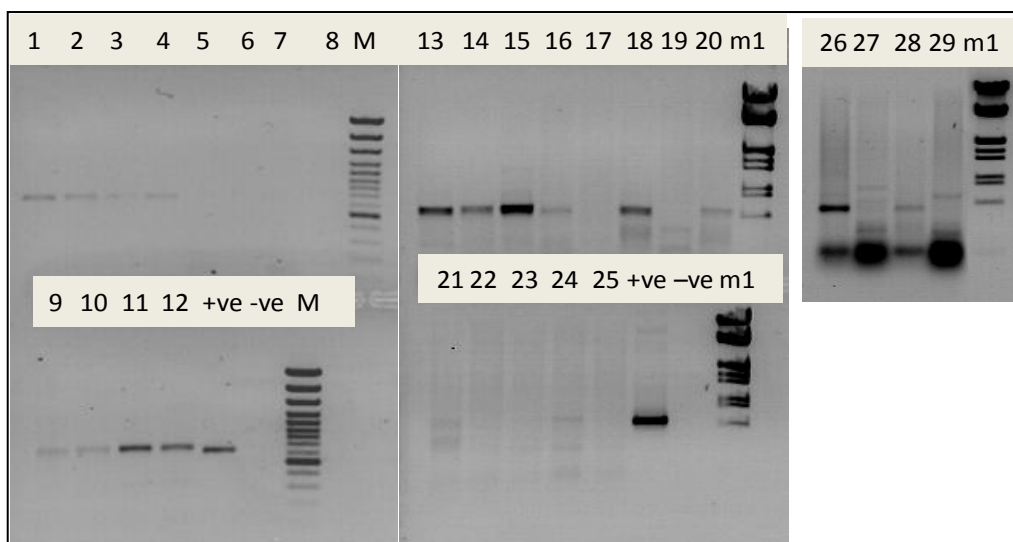


Figure 3.4 July to 31st October 2007 (Numbered 1-55, detailed sampling see appendix, 6.1) has shown that 'picobiliphytes' are abundant throughout summer to early winter in Helgoland. Markers for sample Lane 1-12 1kb ladder; rest λ digest with HindIII/EcoRI

3.3 'Picobiliphytes' from enriched cultures

The $< 3 \mu\text{m}$ fractionated environmental samples are grown in different marine media such as K (Keller), IMR, GP5, Drebes (1 ml of media and 50 ml of fractionated sea water) and incubated at $15 \text{ }^\circ\text{C}$ to enrich 'picobiliphytes'. 'Picobiliphytes' are identified by a PCR-based method (see appendix 6.2) and sorted against orange fluorescence (phycoerythrin) from the enriched flasks. Positive 'picobiliphyte' sample flasks are re-transferred into new flasks (20% inoculum), and the remaining are sorted and allowed to grow in 96 well plates (one, two and ten cells per individual wells).

TSA- FISH is carried out for sorted cells and enriched cells, with taxon-specific probes (*PicoBi01R* and *PicoBi02R*). *Micromonas pusilla* M0947 is used as a positive control for Chlorophyta probe (Chl02) in all experiments (data not shown). Results are indicated that green fluorescence for probe specificity and DAPI nuclear body, and without autofluorescence (phycobilin) as shown previously by Not et al. 2007a. A cell out of 50 cells (Fig. 3.3) is found with green fluorescence and DAPI nuclear staining, indicating that cells can be heterotrophic in nature.

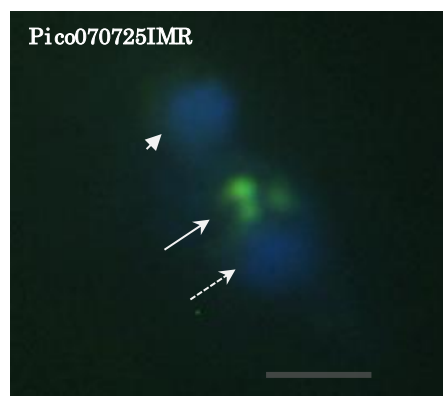


Figure 3.3: Cell with green fluorescence (probe specificity- arrow) and DAPI nuclear body (dotted arrow) is observed but no (orange) autofluorescence are detected. Arrow head- nuclear stained non-specific cell. Bar- $5 \mu\text{m}$.

3.4 Subsequent sample collection for 'picobiliphyte' culturing

Sample collection is repeated again from Helgoland roads (Reede) in the summer of 2008 and immediately filtered with 10 μm and 2 μm membrane filters respectively (thus, series of filtration is avoided from the previous approach). In order to confirm the presence of 'picobiliphytes' on the day of collection, gDNA is extracted and PCR is performed with picobiliphyte-specific primers. Subsequently 2 μm membrane filtered field samples are divided into three parts of 500 ml and two 50 ml. The 500 ml is used for genomic DNA extraction and followed by PCR confirmation. All the samples (Pico080825-29) are shown positive to pico-specific PCR. Simultaneously, the first part of 50 ml is used for cell enrichment. The second aliquot of 50 ml (2 μm fractionated field samples) is centrifuged at 4000g for 10 min. at 15 °C; the pellet is re-suspended with 10 ml of 0.1 μm filter sterilized sea water (FSSW, flask-F1). The supernatant is filtered on 0.2 μm filter membrane and this filter membrane as a whole is placed into a flask containing 10 ml of FSSW (flask-F2). Both flasks are incubated at 15 °C for a week. In order to confirm the presence of 'picobiliphytes' in these cultures, gDNA has been isolated and primer specific PCR is performed (Fig. 3.4). Three samples are shown positive to 'picobiliphytes' (Pico080827, Pico080828, Pico080829) in both pellet and membrane filtered samples.

	4000g pelte Flask-1 (F1)	0.2 μm Flask-2 (F2)
Pico080825	-	-
Pico080826	-	-
Pico080827	+	+
Pico080828	+	+
Pico080829	+	+

Figure 3.4: PCR results showed positive to field samples which are collected in August 2008. Samples (F1 & F2) are tested with pico-specific PCR after a week incubation at 15°C. Among 5 field samples three are shown positive to 'picobiliphytes'.

Enriched samples from Pico080827, Pico080828, and Pico080829 (membrane and pellet) are tested with *PicoBi01F/02F* and eukaryotic reverse primer **BR** and reamplification is done for individual clade-specific forward primer (*PicoBi01F/ PicoBi02F*) and **1055R** to check the diversity among the clades (I, II & III), as shown in fig. 3.5.

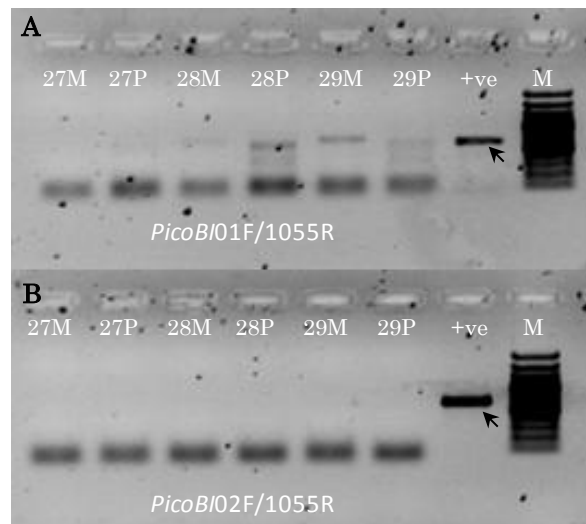


Figure 3.5: **A.** PCR confirmation for Pico080827, Pico080828, and Pico080829 with clade-specific primers showed amplification for clade I&II (*PicoBI01F*) and **B.** no amplification for Clade III (*PicoBI02F*) of 'picobiliphytes'. M. Flask **F1** P. Flask **F2**. (100bp marker M, arrow = 650bp).

The PCR product (Fig. 3.6) indicated that cells belonging to clade I & II are enriched in the flasks (1 & 2). However, no PCR amplification is observed for sample Pico080827 in both pellet and membrane. Subsequently, the positive cultures Pico080828 and Pico080829 are transferred to new FSSW (20% inoculum) and allowed to grow for a week at 15 °C. PCR is conducted for those samples; results are shown that the cells are actively growing in Pico080829, although no amplification is observed in Pico080828.

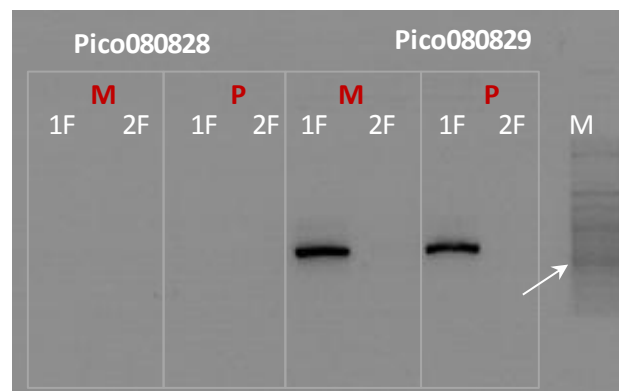


Figure 3.6 Diversity is checked for the positive samples with *PicoBi01F* and *PicoBi02F*. No PCR amplification has been observed from Pico080828; amplification from Pico080829 for *PicoBi01F* clearly indicates that the cells belong to Clade I & II (Not et al., 2007a). M. Flask **F1**, P. Flask **F2**, 100bp marker; arrow 500bp.

3.5 Enrichment but no growth of ‘picobiliphytes’

Cells (Pico080829) are regularly transferred in every two weeks into new FSSW, and the presence of ‘picobiliphytes’ all the time is checked by PCR regardless of its growth. The cells are easily amplified by *cellPCR* method (100 μ l of cells pelleted in PCR tubes, and PCR mix added to it), thus, the extraction of genomic DNA is excluded each time. The PCR products are sporadically sequenced to ensure the results concurred with ‘picobiliphytes’. Cells from the old flasks decreased numerically prolonged periods of incubation (more than four weeks), suggesting that these cells could be a heterotrophic in nature, contradictory to ‘picobiliphytes’ sensu (Not et al., 2007a).

Culturing of cells for prolonged growth is attempted by regular inoculations in different enrichment media (1:50 dilution of K and Drebes media) and incubated at 15 °C. Other marine media like, artificial sea water (ASW), *f/2*, ESM, L1 and PE; sterilized either by autoclave or filter sterilization are also tried in parallel. ‘Picobiliphytes’ are unable to grow in autoclaved media but they could grow in K and Drebes media which are prepared in FSSW. The presence of ‘picobiliphytes’ in these media are tested with pico-specific primers. Fig. 3.7 has clearly shown the specificity for picobiliphytes.

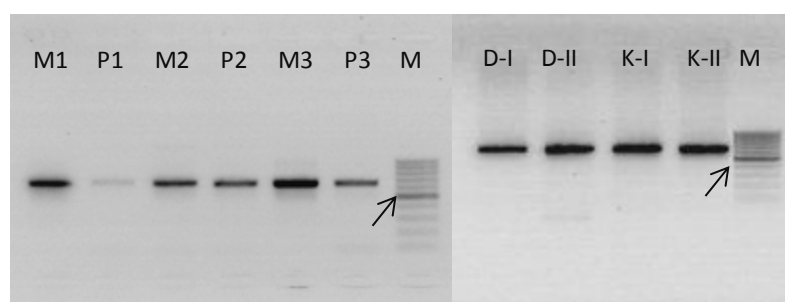


Figure 3.7: FSSW and enriched cells showed positive to Pico080829 consistently. M. Flask F1, P-Flask F2, 1, 2 and 3 are different cultures. D. Drebes K. Keller. Arrow indicates 500bp

The enriched samples could not be differentiated from other contaminants when observed under the microscope. These are sorted in FACS against autofluorescence (Fig. 3.8) and cells have not shown any fluorescence. Thus, neither culture, nor FACS data has shown the presence of any photosynthetic organelles. Hence, it is believed that the cells are truly heterotrophic in nature. Most of the contaminants in the flasks are heterotrophic as well and could not be differentiated from each other. Many other contaminants like *Pteridomonas* sp. and *Telonema* sp. are removed either by serial dilution or filtration (2 μ m membrane filter). However, the two prominent contaminants *Goniomonas* sp. are dominated in the media.

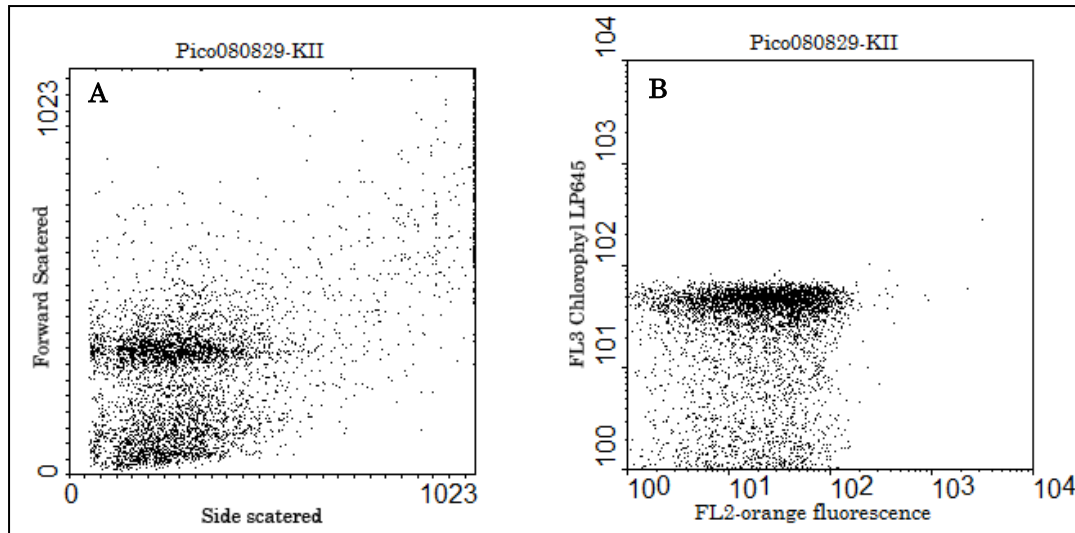


Figure 3.8: Cell sorting performed for Pico080829 positive samples from two different flasks, no autofluorescence is detected by FACS despite cells are showing PCR positive to ‘picobiliphytes’. KII, sample from keller medium. Cytogram A) with forward scatters (FSC) and side scatters (SSC); B) Chlorophyll filter (Red fluorescence) and phycoerythrin auto fluorescence

3.5.1 Use of PicoBI01F and ITS1R for identifying ‘picobiliphytes’

‘Picobiliphytes’ has shown difficulty to distinguish from other eukaryotic contaminants, since the morphology could not be differentiated, hence the PCR based approach (cell PCR) is applied for most of the identification procedures. However, two-step amplifications (amplify with PicoBI01F and Euk BR, followed by PicoBI01F and 1055R) are required to enhance the PCR product specificity by this approach. Hence, to improve the specificity of PCR identification the Pico ITS primers are newly designed (appendix 6.3). Using Pico ITS primers are become more reliable than the two-step amplification performed. Henceforth, two picobiliphyte specific primers (*PicoBi01F/ PicoITS1R*) are used for amplification (*PicoPCR*) at an annealing temperature of 50 °C for 37 cycles. The amplified 1.2kb is further confirmed by sequencing.

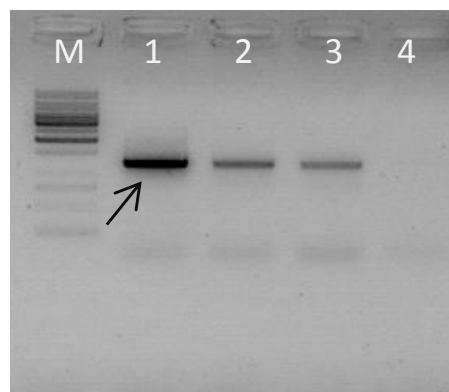


Figure 3.9: Positive cells from flasks (1-4) are checked with two specific primers *PicoBi01F/ PicoITS1R* with 37cycles. Arrow indicates 1.2kb from ‘picobiliphytes’. M- 1kb ladder

3.5.2 Microscopy

Though, the 'picobiliphyte' cells are not able to observe by both light and fluorescence microscope; the positive signals are observed in the mixed culture, indicated the higher magnification for closer examination is warranted. To overcome the problem, scanning electron microscopic (SEM) study has performed for the whole-cell population, which has revealed a unique protist (arrow head, Fig. 3.10), with two unequal long flagellum. This could not be detected earlier by light microscope.

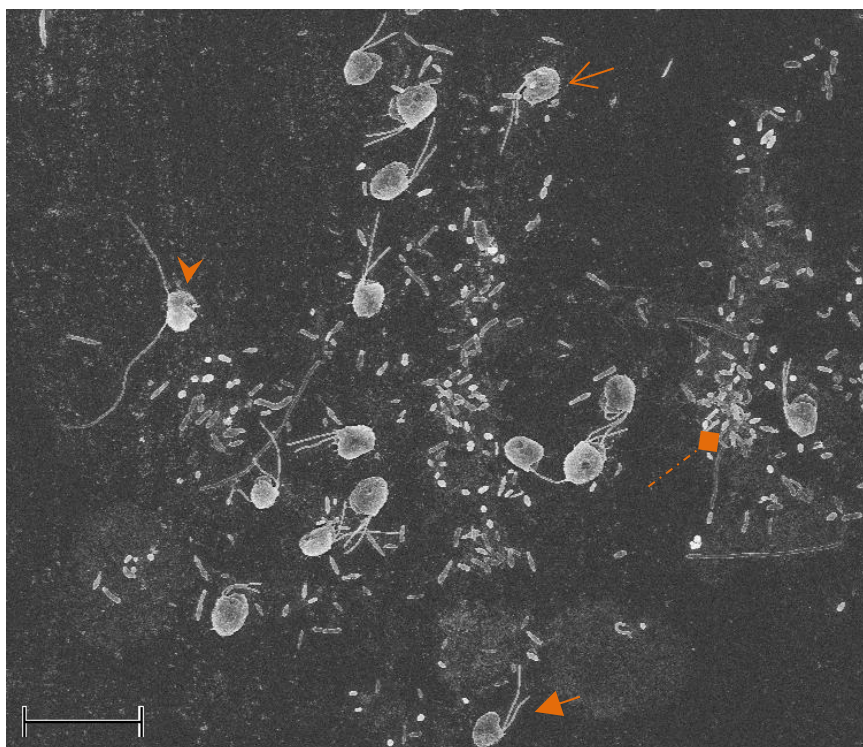


Figure 3.10: SEM image showed 'picobiliphyte' with contaminants. Arrow head - 'picobiliphyte'; Closed arrow-*Goniomonas* sp1; Open arrow - *Goniomonas* sp2 and Diamond arrow - bacteria. Scale bar 10 μ m

3.5.3 Isolation of Picoeukaryotic cells

3.5.3.1 Targeting Heterotrophic fractions in FACS

The enriched non-photosynthetic cells are targeted at the heterotrophic region in FACS by applying only forward scatter (FSC) and side scatter (SSC) window. Region R1 (Fig. 3.11) is set to target all possible heterotrophic cells for sorting in 96 well plates (one cell per well). The result is shown that only four wells have had *Goniomonas* cultures; however, ‘picobiliphyte’ cells are not detected either visually or by *PicoPCR*.

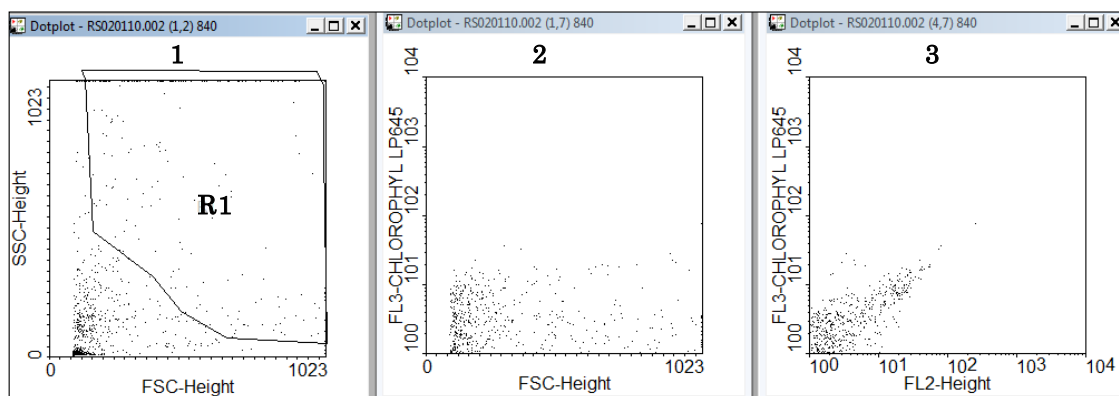


Figure 3.11: Cytograms show FACS cell sorting for ‘picobiliphyte’ enriched samples. Region R1 is set for sorting as shown in 1. Cytograms 2 & 3 clearly shown that the cells are non-pigmented (FL3- for chlorophyll fraction and FL2 for phycoerythrin fraction).

3.5.3.2 Percoll gradient separation

The *PicoPCR* positive enriched cultures are added into a Percoll gradient to separate the cells according to their buoyant density. After the centrifugation 100 μ l of cells from each fraction is used for *PicoPCR* for confirmation. With the results that are shown in fig. 3. 12a indicates that ‘picobiliphytes’ are able to separate at 20% and 40% Percoll fraction. The *PicoPCR* results to the corresponding gradients (20% and 40%) are further confirmed by sequencing. The remaining samples are transferred into 24-well plate and observed a unique type of cell (not seen in cultures before) exhibited a characteristic movement (jump and drag, see 3. 18b). However, the cells could not grow any further (24 well plate) due to the increasing bacterial contamination and/or sensitivity to Percoll itself (endotoxins). Nevertheless, the enrichments are also contaminated with a few *Goniomonas* sp. possibly by cross contamination from one gradient into another.

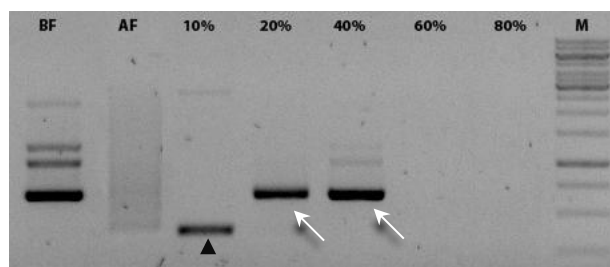


Figure 3.12a: Reamplification of cells obtained from all the fractions from Percoll gradients and positive bands are observed in 20 and 40% fractions (white arrow). BF: Before centrifugation, AF: after centrifugation of the sample. Note that non-specific amplification from 10 % percoll fraction (mostly because of bacteria). M 1kb ladder

3.5.3.3 Antibiotic treatments

Previous studies suggest that bacterial growth inhibit the ‘picobiliphytes’ cell growth, irrespective of the growth of *Goniomonas* sp. Hence, cell growth has been maintained under low nutrient media. A set of experiments are carried out as an alternative to inhibit the prokaryotic population (thus, reducing the *Goniomonas* population) by applying wide spectrum of antibiotics. Many different types of bacterial metabolic inhibitors, e.g. peptidoglycan inhibitors (ampicillin and carbenicillin), ribosomal 30S small subunit inhibitors (kanamycin and tetracycline), and 50S large subunit inhibitors (chloramphenicol) are used into the enriched sample flasks. PCR has been performed (Fig. 3. 12b) for all samples and resulted that the cell wall inhibitor (ampicillin) has reduced the bacterial growth drastically and thus *Goniomonas* populations to an extent. However, the growth of ‘picobiliphytes’ is not affected by the presence of ampicillin (25 µg/ml final conc.), that proved their growth was independent to bacterial population.

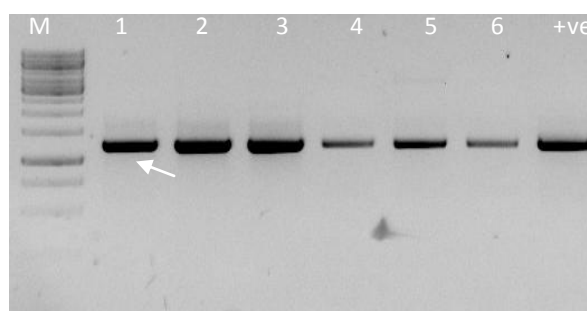


Figure 3.12b: PCR amplification of ‘picobiliphytes’ treated with different bacterial antibiotics. Lane 1-5 are samples treated antibiotics ampicillin (25 µg/ml), carbenicillin (50 µg/ml), Chloramphenicol (15 µg/ml), Kanamycin (50 µg/ml) and Tetracycline (25 µg/ml). Lane 6. Cells treated with mixture of carbenicillin, kanamycin and Tetracyclin. M. 1Kb ladder; arrow. 1kb ladder.

3.5.3.4 *Mitotracker* as a fluorescent marker

Many attempts such as serial dilution, filtration, Percoll gradient and cell sorting are made to isolate 'picobiliphytes' and become unsuccessful. In FACS sorting for heterotrophic fractions failed to isolate 'picobiliphytes,' though, *Goniomonas* sp. are successfully achieved. To increase the possibility of isolating only 'picobiliphytes,' fluorescent markers (mitochondrial staining markers) are added to the cultures and *Goniomonas* sp is used as positive control (for methods, see 1.2.4.2). *Mitotracker* stained *Goniomonas* cells are retained the fluorescence very well (*Mitotracker*® Red CMXRos, Invitrogen) even after aldehyde fixation and detergent washing steps (Fig. 3.13).

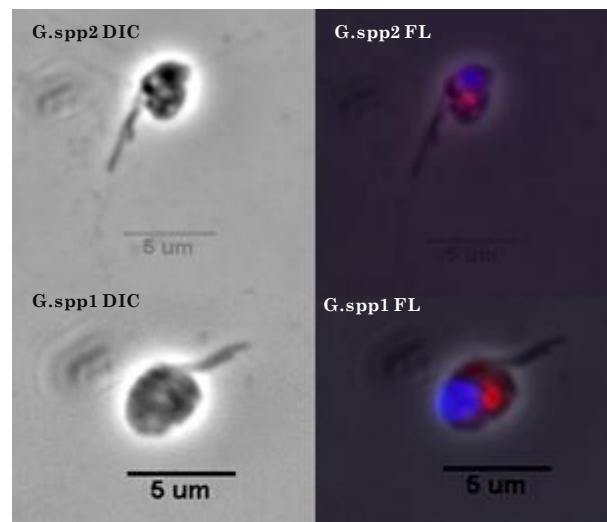


Figure 3.13: *Mitotracker* Red stained cell for *Goniomonas* sp1 and G.sp2, showing the retained dye after the fixation and detergent wash. Red fluorescence- Mitochondrion stained with *Mitotracker* Red. Blue – DAPI stained nuclear body.

3.5.3.5 Isolation of *Goniomonas* sp - using *Mitotracker* GreenFM

Mitotracker Green FM is used for cell sorting for two reasons. Firstly, the GreenFM has the excitation at 490 nm and emission at 516 nm, suits for FACS sorting (Argon laser- 488 nm). Secondly, the GreenFM fluorescence dye is not well retained in the mitochondria and diffuses quickly thus not affecting the viability of the sorted cells. The cell viability test is conducted for such stained *Goniomonas* sp. and observed under the fluorescence microscope (Nikon EclipseE8000). Later, cells are sorted in the FACS against the green fluorescence (FL1) together with forward scatter (FSC); single cells are collected in 96 well plates and kept at 15 °C. Two kinds of G. species are sorted successfully (Fig. 3. 14A) by this approach and cell growth has not been affected, indicates that *Mitotracker* GreenFM does not inhibit growth of the cell. Thus, mitochondrial staining could be the ideal method for isolating heterotrophic protists from the mixed population. The same procedure is applied to isolate 'picobiliphytes' from the enriched cultures.

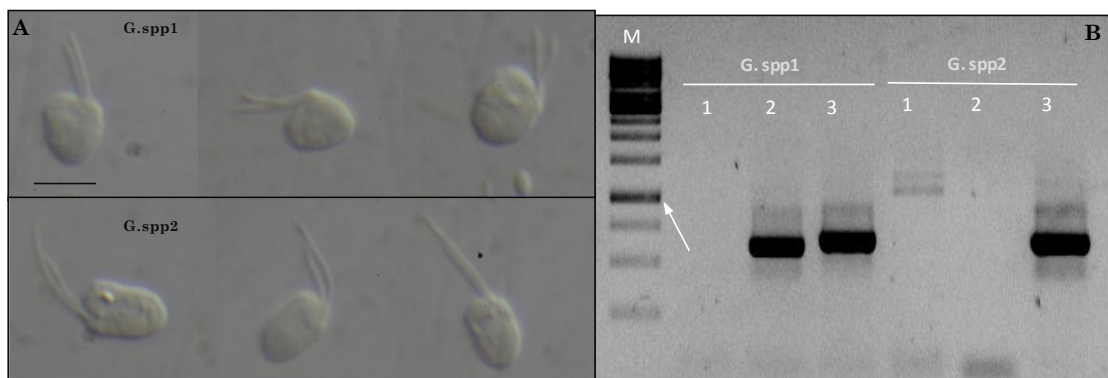


Figure 3.14: Cell sorting using *Mitotracker* GreenFM. A. Heterotrophic cells (*Goniomonas sp1* and *Goniomonas sp2*) are isolated on micro-titre plate. Pictures are taken from cells which are grown in the well. *Mitotracker* did not inhibit the cell growth. Scale bar 5 μ m. B. PCR product from *G. sp1* and *G. sp2*. Lane 1- negative control with picobiliphyte-specific primers (*PicoPCR*), lane 2 - *Goniomonas* specific primers (*G.amphinema* primers) and lane 3 - *Goniomonas* specific primers (*G.pacifica* primers). *Goniomonas sp1*, showed PCR amplification for both primers. M- 1Kb ladder, arrow- 1kb.

The two types of isolates are PCR amplified and sequenced (Fig. 3. 14B); *Goniomonas sp1* (two sub equal flagellates) is shown the affinity to *Goniomonas* aff. *amphinema*, and *Goniomonas sp2* (two unequal flagella) to *Goniomonas* sp. SH1.

3.5.3.6 Isolation of ‘picobiliphytes’ using *Mitotracker* GreenFM

‘Picobiliphytes’ enriched cultures (*PicoPCR* positives) are used for cell sorting as mentioned in 3.5.3.5 with *Mitotracker* GreenFM (50 nM) and sorted against Green fluorescence (FL1) and forward scatter (FSC) window, and also with FL1 and orange fluorescence (FL2). Cells are initially sorted at different regions in cytogram and confirmed that region-R1 is positive to ‘picobiliphytes’ (Fig. 3. 15a, see appendix 6.5). Although, *Mitotracker* Green FM has emission maxima at 516 nm (FL1), its emission spectrum is widely distributed up to 560 nm. Hence, the fluorescence is also detected by orange filter (FL2, 545 nm) in 488 argon ion laser. The PCR results have shown (Fig. 3. 15b) that ‘picobiliphytes’ are predominantly grouped under region R1. For isolation of ‘picobiliphytes,’ the cells are sorted from ‘Region R1’ and individual cells are collected into 96 and 24 well plates (one cell at a time) containing 500 μ l of K1:10 with 0.1 μ m filter sterilized sea water. Plates are then incubated at 15 $^{\circ}$ C for two weeks and monitored at regular intervals.

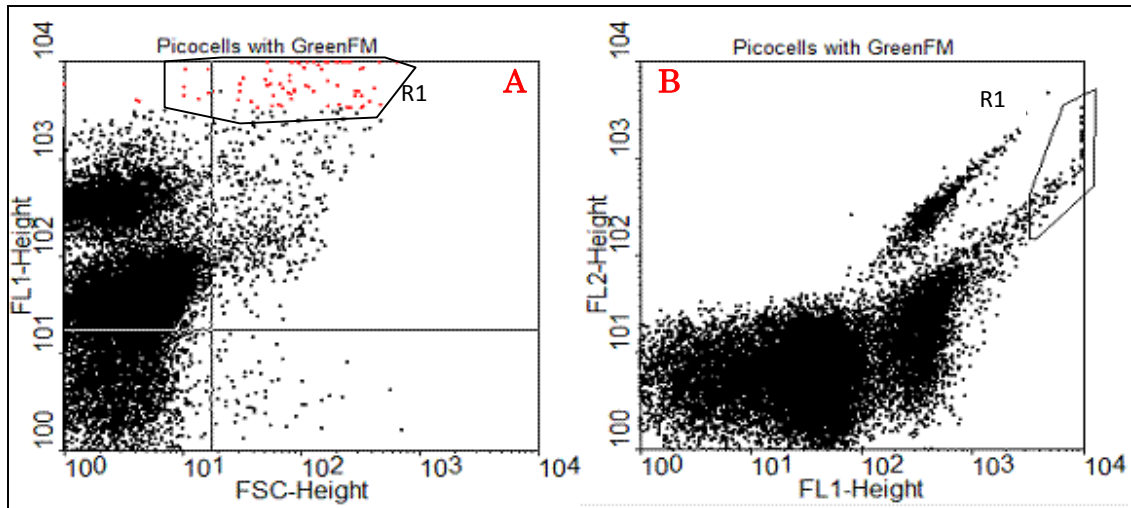


Figure 3.15a: Cytograms of *Mitotracker* GreenFM treated 'picobiliphytes' enriched cultures; *Region R1* is set for sorting the 'picobiliphytes' into 24 well plate containing 500 μ l of K1:10 in 0.1 μ m filter sterilized sea water. A) High green fluorescence cells (shown in red) sorted against FL1 and forward scatter. B) Depicts the *Mitotracker* GreenFM has long emission wavelength detected in orange fluorescence filter (FL2) in FACS.

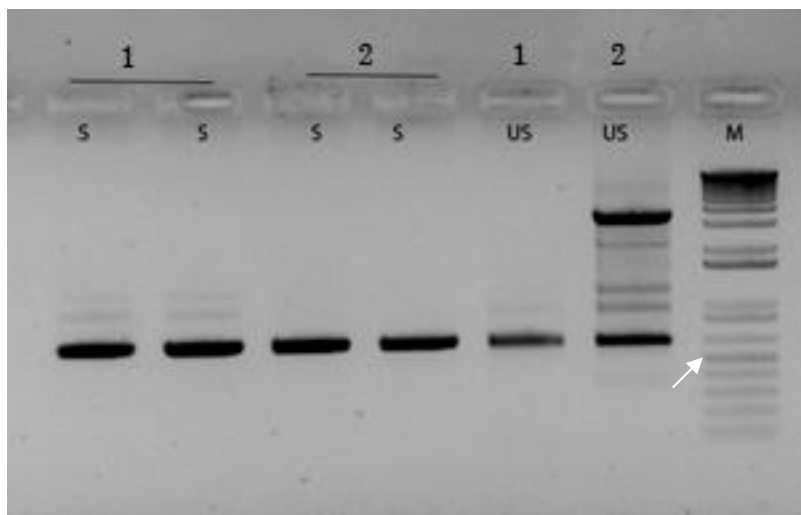


Figure 3.15b: PCR products from cell sorted on *Region R1*. S. 500cell sorted from R1 region, US. Unsorted cells used as a positive control. Sample 1- Cell from K1:10 medium and Sample 2 Cells from K1/4 medium. M- 1kb ladder plus, Arrow 500bp. Note: Sample 2 unsorted lane showed a non-specific amplification; it appears when the cultures are highly contaminated with bacteria.

The four wells out of 24 wells has shown a unique flagellates without contaminations (for eg. *Goniomonas* sp.), other few samples are contaminated with both 'picobiliphytes' and *Goniomonas* sp2. Samples from these wells are taken for *PicoPCR* (PicoBi01F & ITS1R) at 37 cycles. Amplicons from these samples are shown in fig. 3.16. The clonal culture of 'picobiliphytes' has grown slowly compared to the mixed population; hence, the PCR product obtained is also low in concentration in those particular samples.

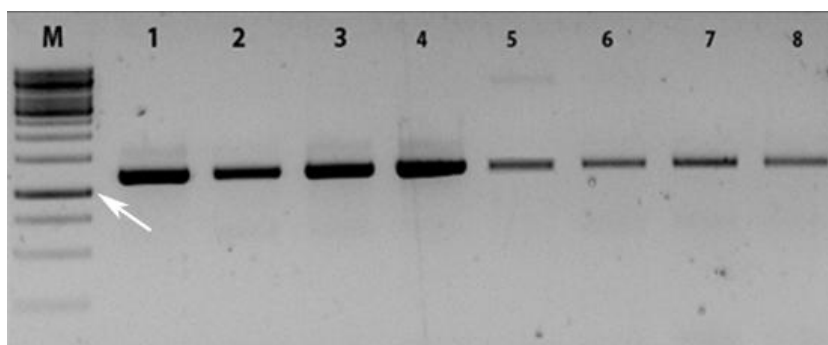


Figure 3.16: PCR confirmation for sorted cells by using *Mitotracker* GreenFM cell sorting. Lane 1-4 samples with both *Goniomonas* sp2 and 'picobiliphytes'. Lane 5-8 show positive to 'picobiliphytes' clonal culture. The PCR product is 1.2kb. M- 1 kb ladder; Arrow- 1kb

3.5.3.7 Enrichment of 'picobiliphytes'

Clonal cells are initially inoculated in K 1:10 medium with FSSW in a tissue culture flask. To test the axenic nature of the cells, samples are tested by PCR with 18S universal primers, *Goniomonas*-specific primers and 'picobiliphyte'-specific primers (Fig. 3. 17a). These cultures are often retransferred into fresh media and monitored at regular intervals.

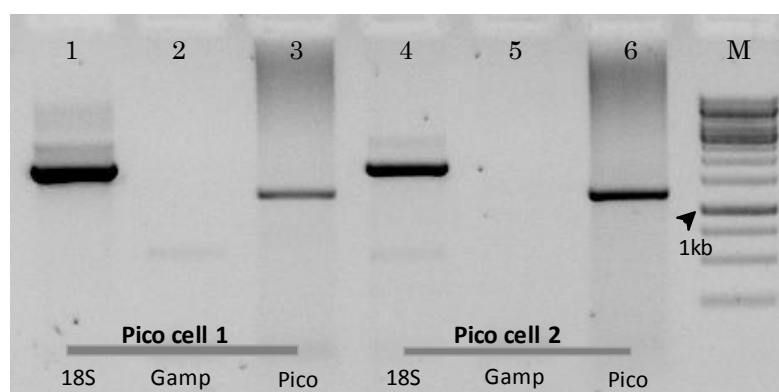


Figure 3.17a: PCR product from two 'picobiliphyte' clonal cultures (Pico cell 1&2). Lane 1&4 are amplified with Universal 18S primers (1F/BR), 2&5 with *Goniomonas* specific primers (Gamp627F/BR) and 3&6 with picobiliphyte specific primers (PicoBI01F/ITS1R). M-1kb ladder.

The clonal culture of 'picobiliphytes' resorted in FACS to test for its autofluorescence if any, but the results has shown neither FL2 nor FL3 filters could detect any autofluorescence, which suggested that these cells are non photosynthetic (Fig. 3. 17b). On the other hand, the rDNA 18S sequence of these culture has clearly revealed high sequence similarity to photosynthetic 'picobiliphytes' as in Not et al. 2007a (appendix 6.4). To avoid the confusion further to call the non-photosynthetic 'picobiliphytes', these cells are renamed as '*Picomonas* sp.'

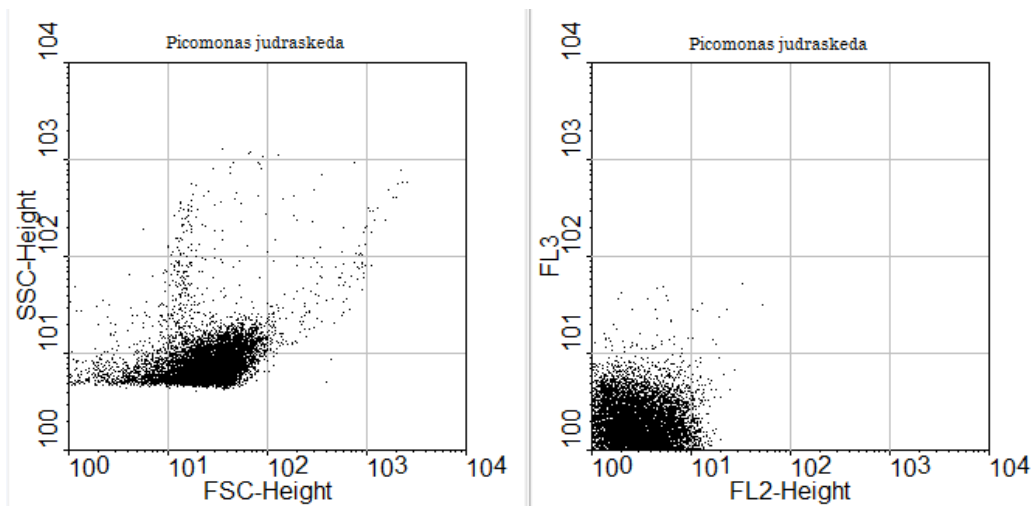


Figure 3.17b: Cytogram of clonal culture of *Picomonas* sp. A) *Picomonas* cells are scattered in FSC and SSC window (cells are lower in concentration). B) No autofluorescence are observed in FL2 (phycoerythrin) and FL3 (chlorophyll) filters for the same cells.

3.6 Microscopic results

3.6.1 Light microscopy

The growth rate of *Picomonas* is unstable, unpredictable and their nutrient requirement is unknown, hence the cells are maintained under low nutrient composition. Presence of bacteria, in sterile filtered natural sea water (0.1 μm filter sterilized) and low nutrient composition (Soil extracts, K 1:10) are found to be an optimal condition for maintaining these cells. Live cell images (Fig.3.18a) has shown that live cells are very fragile and sensitive to any kind of protuberance, so they could collapse easily. In clonal culture, the swimming behavior of the cells is unique: the cells generally are found to be immobile or stagnant most of the time, floating in the water column. During movement, they ‘jumped’ a short distance (approximately 3-5 μm) into the anterior direction, immediately followed by a slower drag movement to the opposite (posterior) direction. Movement of such cells lasted for about 2 s, in which the cells traveled a distance approximately four times its cell length. This jump/drag-cycle is observed for two to five times after which the cells suddenly ‘shot’ away (a behavior termed skedaddle here) with rapid speed in the posterior direction covering a distance of approximately 50 μm before they became immotile again, until the next jump/drag cycle is observed (Fig. 3.18b). During resting periods of the cell, the posterior flagellum (PF) was held closely adjacent to the ventral cell surface curving around the posterior end of the cell, often visible under the microscope and mostly immotile, while the anterior flagellum extended from the cell surface revealing an undulatory wave pattern. The behavior of the flagella during the jump/drag/skedaddle cycle was not studied in detail but apparently involved flagellar re-orientation and rapid undulatory movements of one or both flagella. The ‘jump/drag and skedaddle’ like movement are considered as novel feature of this heterotrophic cell, hence the species been provi-

sionally named as *Picomonas judraskeda* (derived from 'ju' (jump), 'dra' (drag) and 'skeda' (skedaddle)).

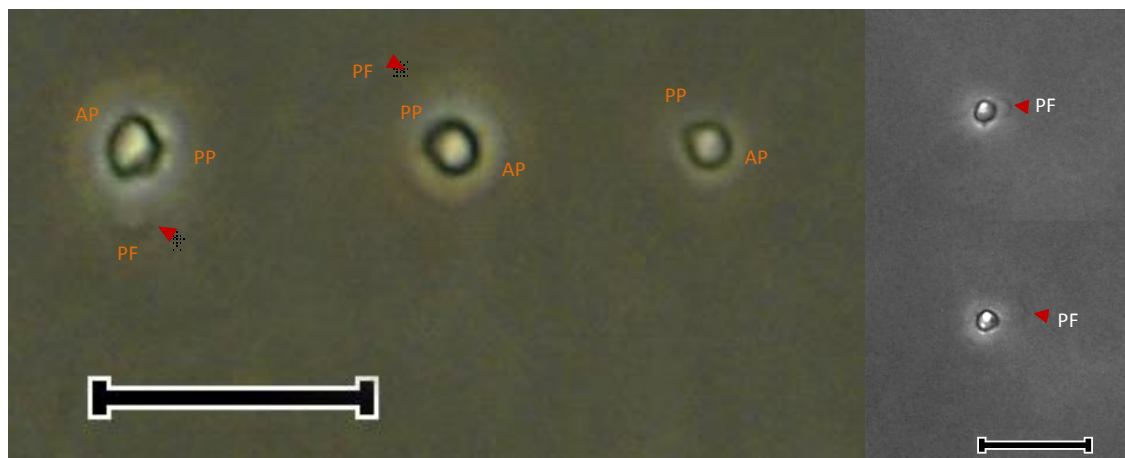


Figure 3.18a: Microscopic observation (phase contrast) of three different *Picomonas* cells. Images are taken from live cells, the anterior flagellum (AF) is not seen visibly whereas the posterior flagellum (PF) is often forms crooked-finger like appearance around the cell during stagnation. The *Picomonas* cell size is $< 5 \mu\text{m}$. AP, Anterior part; PP, Posterior part. Scale bar $20 \mu\text{m}$.

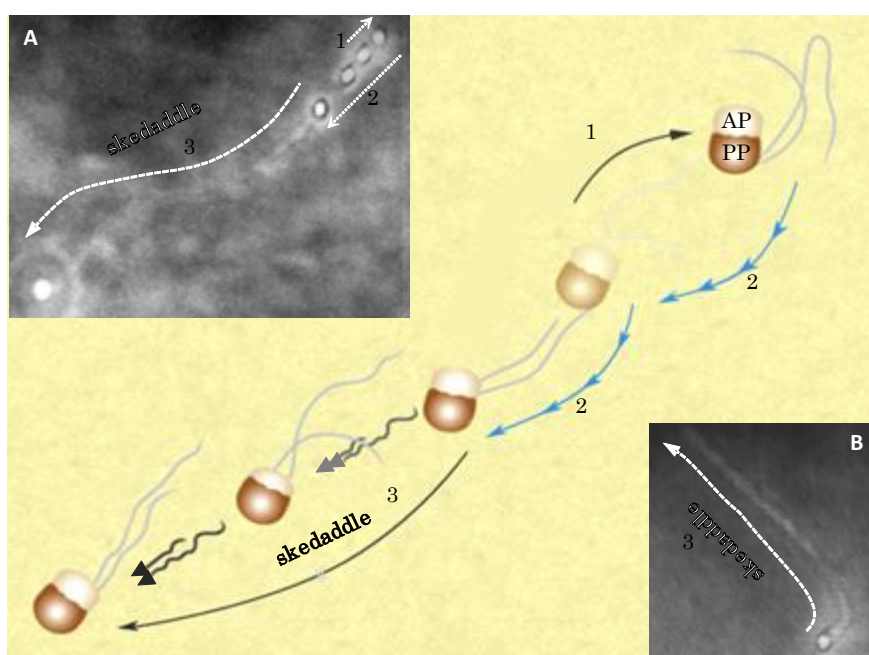


Figure 3.18b: Cellular movement of *Picomonas* cell. 1- The first movement of the cell, jump to a short distance; followed by a drag to the opposite direction for a short distance (2) and run (skedaddle) vigorously before reaching to next destination (3). A & B: Direction of skedaddle movement of the cell showed in white dotted arrow. (A & B are cell movement of two individual cells captured in a video graph and frames are superimposed)

3.6.2 Cell division

Cells divide by simple division; however, notably, at the final stage of cell division, two daughter cells detached by a force, which likely is the fast movement (skedaddling) of cell. Both daughter cells repel each other into opposite direction, move away from one location to other and continue their growth as described in 3.6.1 (Fig. 3.18C).

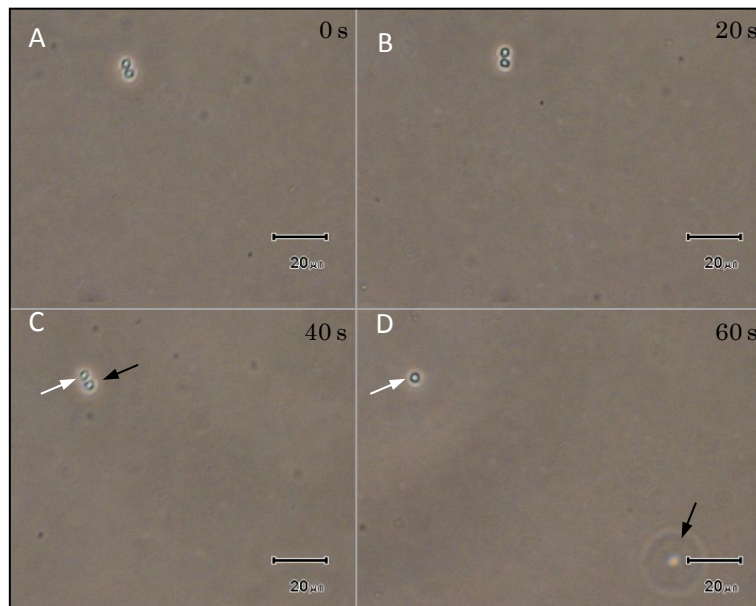


Figure 3.18c: Cell division of *Picomonas*- two daughter cells are detached from each other by a force and skedaddled from the location, A-C preparation for cell division, D- zero time point where two daughter cells detached from each other

3.6.3 Chemically fixed cells

Picomonas cells are fixed with 1.25 % glutaraldehyde for 30 min and 100 μ l aliquot are placed on a poly L lysine coated glass-slide. Cells at higher magnification are shown that they are slightly elongated and comprising with two hemispherical parts, namely anterior part (AP) and posterior part (PP) (see Fig. 3.19). Cell sizes 2.5-5 μ m in long. Each cell displayed two heterodynamic flagella of unequal length. Both flagella are inserted laterally at the anterior part defining the ventral surface of the cell. The anterior flagellum (AF) is longer (\sim 12-14 μ m) and orients parallel to cell axis and runs towards to cell's anterior end. The posterior flagellum (PF) is shorter (\sim 8-9 μ m) and orients towards the posterior part (often curves at around the posterior end and extends to the dorsal surface of the cell [Fig. 3.18a]).

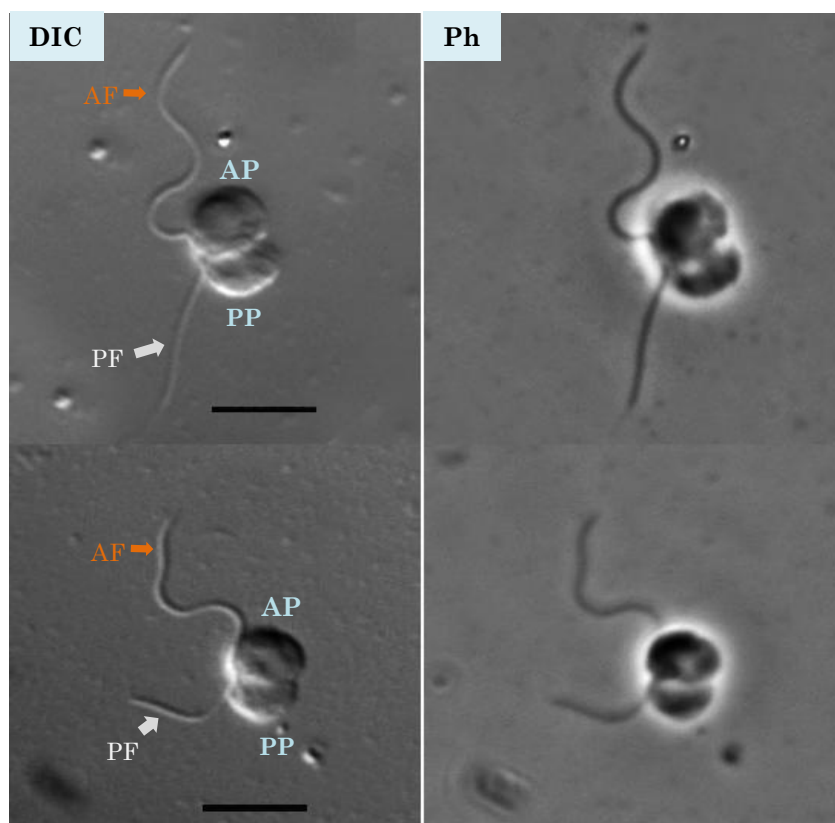


Figure 3.19: Light microscopy of *Picomonas* at higher magnification (100X). Cells are separated into two parts; the anterior part (AP) and posterior part (PP). Each cell contains two flagella with unequal length; the long flagellum is anterior flagellum (AF); the short flagellum is posterior flagellum (PF) Scale bar-5 μm .

3.6.4 Fluorescence images

Mitotracker[®] Red CMXRos (50 nM/ml final conc.) is added to *Picomonas* as described in section 1.2.4.2 and incubated at 15 °C for 20mins in dark chamber and fixed with 1.25% glutaraldehyde. These fixed cells are placed on a glass slide (Poly-L-lysine coated). DAPI is used as a counter stain. The fluorescence images (Fig. 3.20) are superimposed with light microscopic images. A discrete red fluorescence is observed for mitochondrion at the centre of the cell body, and DAPI stained nuclear body is in the anterior part. No autofluorescence is detected from any of these cells, confirming the absence of plastids. Both Red *Mitotracker* and DAPI fluorescence are always observed at the anterior part of the cell (no single cell observed with fluorescence at the posterior end), demonstrating that these organelles accommodate together at the anterior part.

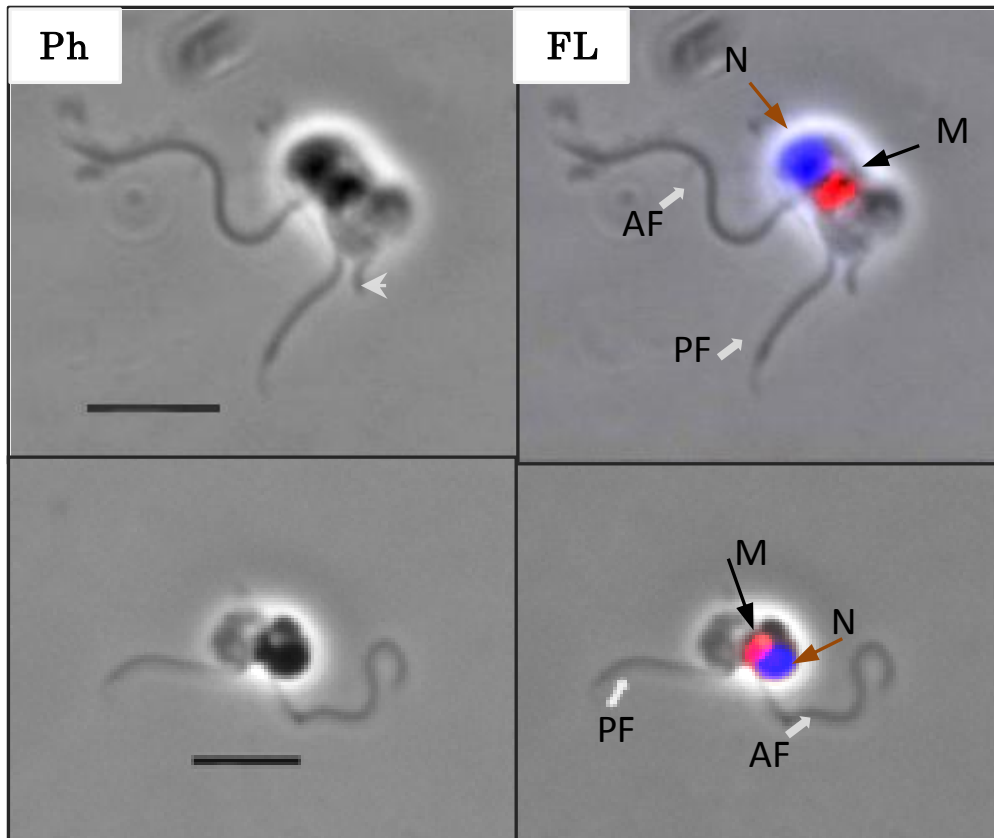


Figure 3.20: Fluorescence microscopy of *Picomonas*; cells are stained with mitochondrial (*Mito-tracker* Red CMXRos) and nuclear (DAPI) staining. The cells with red fluorescence show Mitochondrion (M) and blue fluorescence for nucleus (N). Both Mitochondrion and Nucleus are found in the anterior part of the cell. No other autofluorescence is observed from the cell. AF, anterior flagellum; PF, posterior flagellum. Arrow head, bacterium. Scale bar 5 μm .

3.6.5 Scanning electron microscopy

Two flagella are inserted without any invagination on the ventral surface (Fig. 3.21). No flagellar appendages (mastigoneme or non-tubular hairs) are observed at the surface of both flagella. The flagella may shed at the transitional region; when they shed, a conspicuous flagellar stub (transitional region-tr2 from AF and PF, see below) remain attached to the flagellar base of the flagellum (tr2 in PF shown in Fig. 3.22 A&B). Flagellar bases are displaced anti clockwise if the cells are viewed from ventral (refer to Fig. 3.30). The flagellar bases form an angle of $120\text{-}140^\circ$ ($n=5$). When viewed from the ventral side, the anterior flagellum projects towards the cell's left, its base forming an angle of about 40° to the antero-posterior cell axis. The posterior flagellum deviates only slightly ($\sim 10\text{-}20^\circ$) from this axis projecting towards the cell's right and extending to the cell's posterior. A lobe that extends from the base of the posterior flagellum towards posterior part is observed in SEM indicated the possible feeding apparatus (arrow heads, Fig. 3.22 A&B).

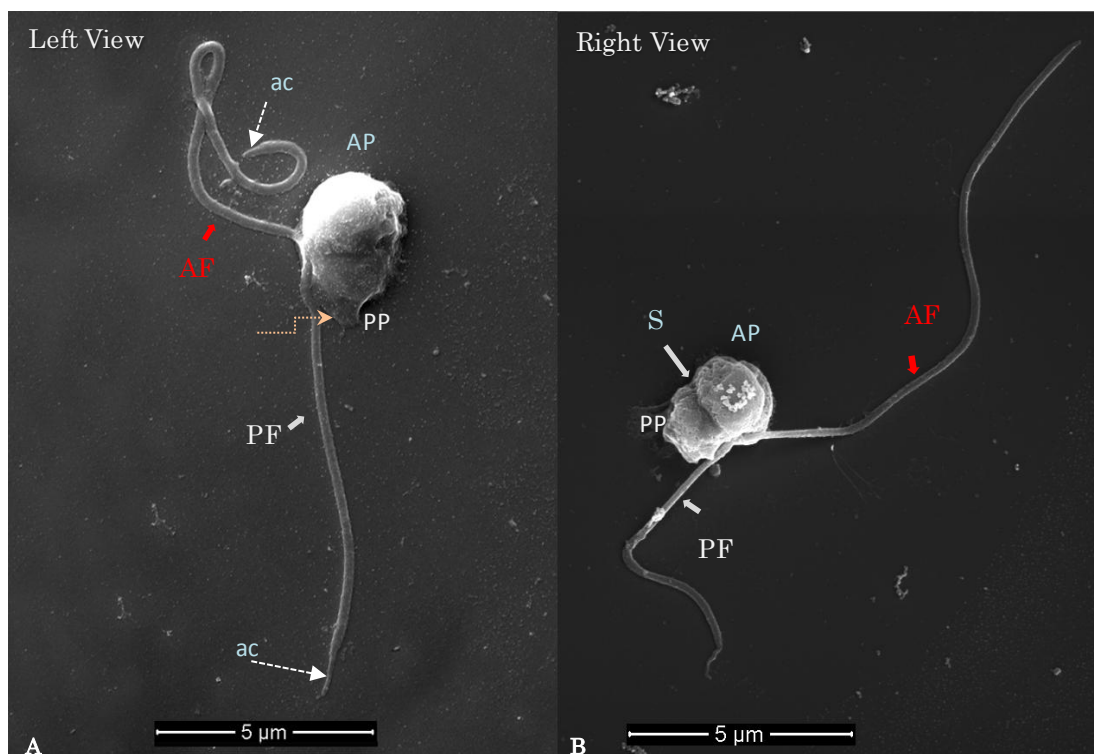


Figure 3.21: SEM images show the flagella insertion at the ventral surface on the anterior part without mastigonemes. AF, anterior flagellum; PF, posterior flagellum; ac, acronema; AP, anterior part; PP, posterior part; Cl, cleft. Scale bar 5 µm.

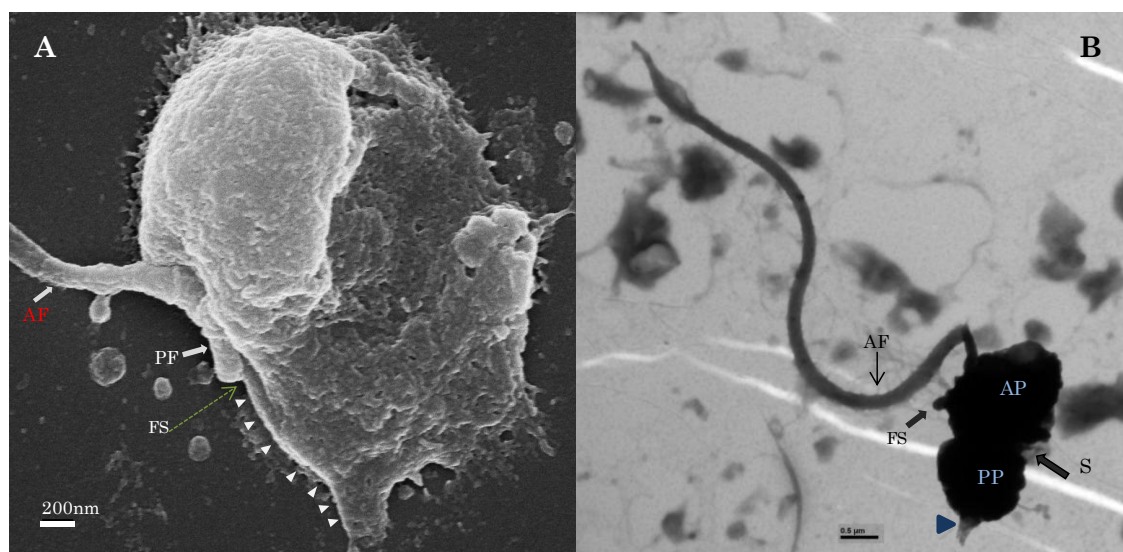


Figure 3.22: A) SEM images - *Picomonas* with flagellar stub (FS) in the posterior flagellum (PF) after shed. The length of the stub is about 300 nm from the flat ventral surface. A lobe-like structure from ventral posterior surface (arrow heads) is a cytostome extends from the base of the proximal flagellum to posterior end. B) Whole cell mount image - *Picomonas* shows two distinct cell bodies (AP, anterior part and PP, posterior part) distinguished by a deep cleft (Cl). The arrow head shows the membranous protrusion at posterior end.

3.6.6 Transmission electron microscopy

An overview of a longitudinal median section from a series of a *Picomonas* cell (section in the flagellar plane) is shown in fig. 3.23. [Left and right defined as if seen from the cell's interior. Ventral side is where flagella inserted, dorsal opposite side. Anterior side is that facing forward when the cell swims, posterior is the opposite side to this. In a dorsal view, the left side is on the left, and the right is on the right (opposite in ventral view)]. The ultrastructure of *Picomonas* cells reveal many unique structural components, and not observed in any other eukaryotes. In general, all cell constituents, as expected for flagellates, occupied defined positions in the cell. Major metabolic active components are observed at the anterior part (AP) of the cell, a hemisphere nucleus; flagellar apparatus; Golgi body; a single mitochondrion; rER; free ribosomes and peroxisome like micro bodies. The microbodies (perhaps peroxisomes) are single membrane-bound compartments present at the dorsal side in the anterior part. Each cell comprised more than one microbody, which are spherical (approximately 600 nm in diameter) in shape (Fig. 3.23, 3.24).

The volume inside the cell at the anterior part (AP) is constant. Contrastingly, a highly variable and functionally uncharacterized, single membranous substances (digestive sac, cytostome like structure and numerous single membrane bodies) are observed at the posterior part (PP) (Fig. 3.23-25).

Two longitudinal sections from a series of another *Picomonas* cell starting at the ventral side (view seen from, where flagella emerged) to the dorsal is shown in Fig. 3.24. Ventral view of the section depicted all organelles except flagellar apparatus and peroxisome. Two peroxisome-like micro bodies are visible near the dorsal end of the section (~660nm away from the ventral to dorsal).

In addition in order to understand the complete architectural arrangement of organelles in *Picomonas*, series of ultrathin sections (45, 60 and 100 nm respectively) are obtained from each cell. Overall, six cells are observed completely (observed minimum 25 to 65 sections according to the thickness) using TEM, of which complete structural characteristic of one single cell is shown fig. 3.25, depicting the non-sequential sections (60nm) of *Picomonas* from left to right; detailed view and description for each organelle are presented below (Second, non-sequential serial section of a cell from ventral to dorsal has also shown in appendix 6.6).

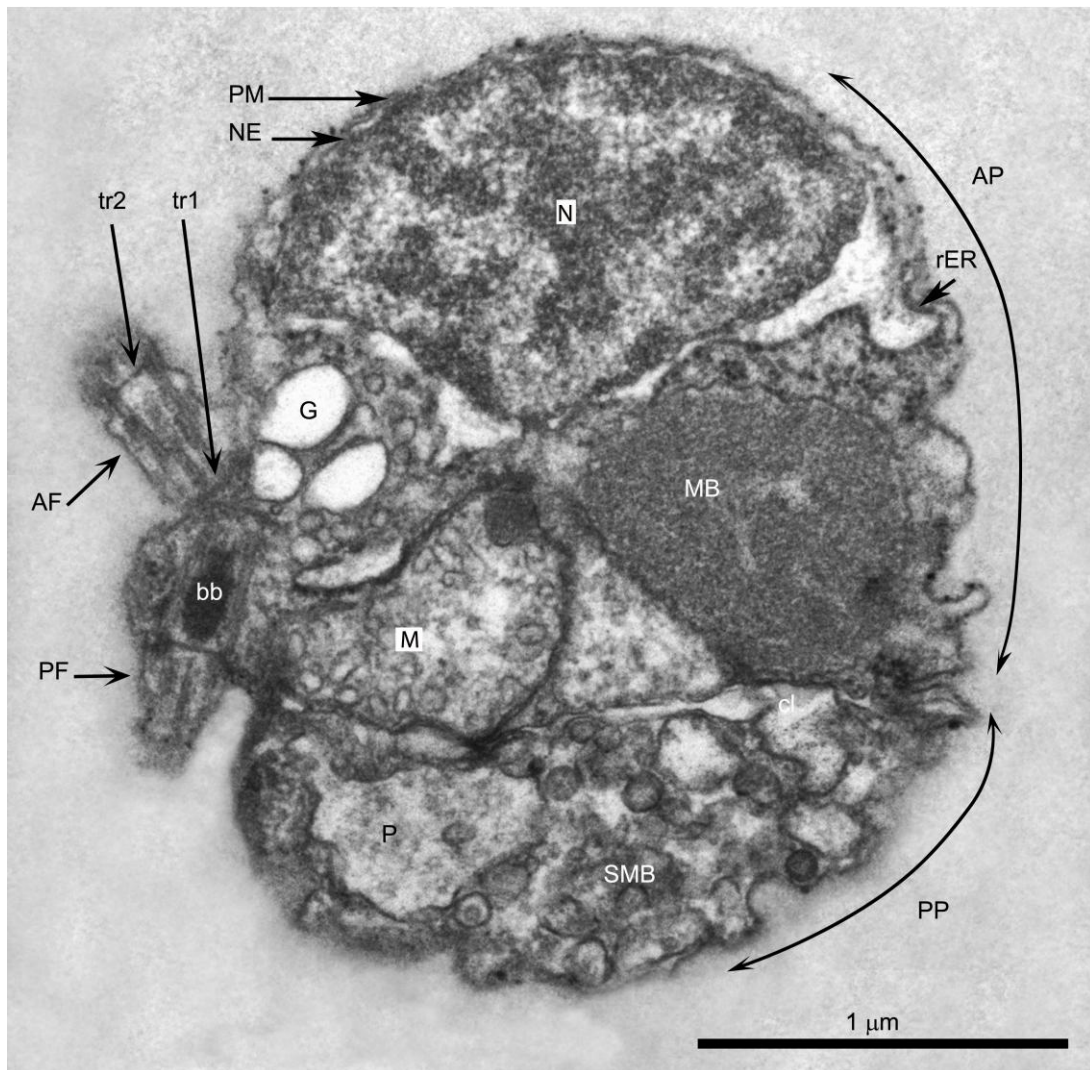


Figure 3.23: Longitudinal TEM section through a ‘picobiliphyte’ cell seen from the cell’s left side. N, Nucleus; NE, Nuclear envelope; PM, Plasma membrane; rER, rough endoplasmic reticulum; G, Golgi body; M, Mitochondrion with tubular cristae; AF/ PF (anterior-/posterior flagellum); AP/PP (anterior /posterior part of the cell); bb, basal body with electron dense lumen; P, posterior digestive body; SMB single membrane body; MB, microbody (‘peroxisome’); ‘cl’, a membrane-bound vacuolar cisterna (‘cleft’) separates the anterior part from posterior part; tr1, tr2, proximal and distal septa of the flagellar transitional region. Scale bar 1 μm.

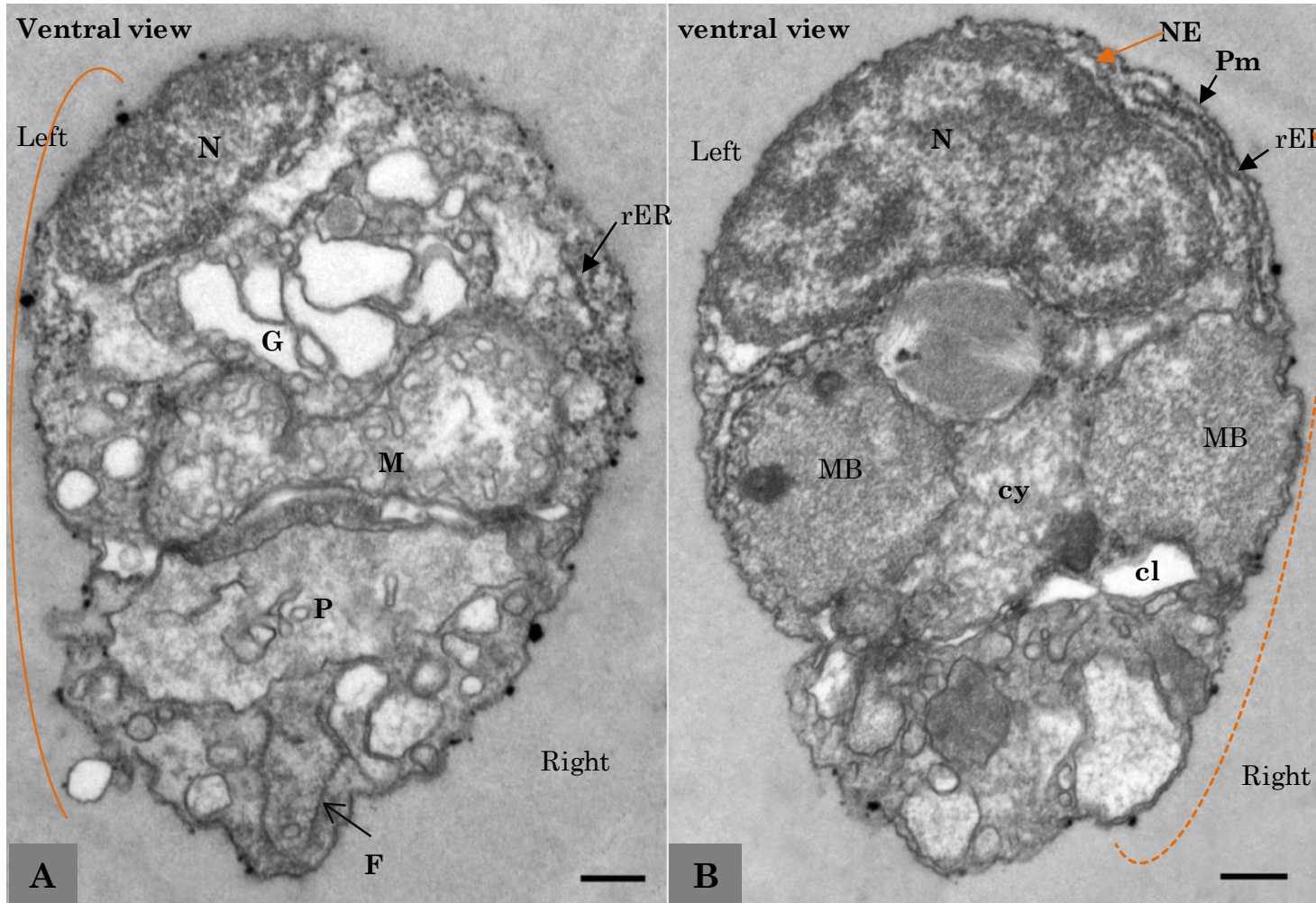


Figure 3.24: Longitudinal non-sequential serial section of *Picomonas* from ventral to dorsal (60 nm sections). **A**, Golgi, Mitochondrion and digestive sac located ventrally **B**, Ventral view into the dorsal part of the cell microbodies preferentially located dorsally. A cleft (Cl) and peroxisome like microbodies (MB) visible at dorsal end of the section. Curved line, cell's left; dotted curved line, cell's right. N, Nucleus; NE, Nuclear envelope; PM, Plasma membrane; rER, rough endoplasmic reticulum; G, Golgi body; M, Mitochondrion; P, posterior digestive body; 'cy', cytoplasm; MB, microbody ('peroxisome'); 'cl', cleft'. Scale bar 200nm.

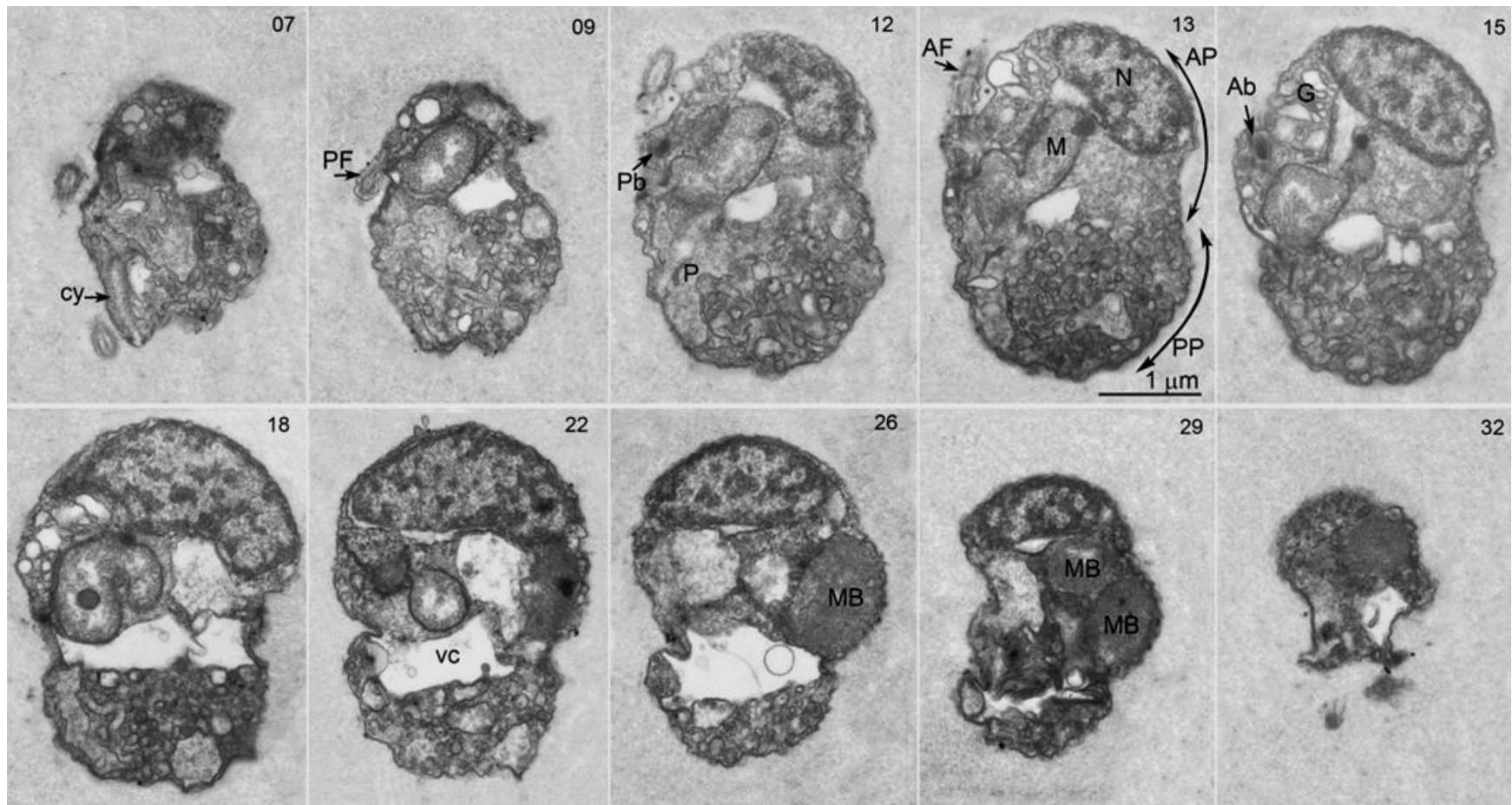


Figure 3.25: Electron micrographs of non-sequential longitudinal serial sections through a *Picomonas* cell from its left to right surface. A complete reconstruction of the cell shows the absence of a plastid and exhibits unique features. Numbers in the upper left corner correspond to discontinuous 60 nm sections from a series of 35 serial sections; N, Nucleus; NE, Nuclear envelope; PM, Plasma membrane; rER, rough endoplasmic reticulum; G, Golgi body; M, Mitochondrion; P, posterior digestive body; MB, microbody; vc, Vacuolar cisterna; AF/ PF (anterior-/posterior flagellum); AP/PP (anterior /posterior part of the cell); Ab/Pb (anterior/posterior basal body); Scale bar 200nm. Scale bar 1 μm .

3.6.6.1 Detailed analysis of structural compartments of *Picomonas judraskeda*

3.6.6.2 Nucleus

The nucleus is hemispherical (N) and occupies a large part of the anterior part of the cell, closely appressed to the anterior plasma membrane, (Fig. 3.23-3.26) and not located centrally in the cell. Approximately, 60% of the nuclear envelope surface (Fig. 3.24, 3.25) is associated to p membrane. The presence of a large nucleus distinguishes the anterior part (AP) from posterior part (PP) of the cell. A reticulate distribution of a dense fibrous chromatin matrix covered with the double layered nuclear envelope is observed within the nucleus; however, a discrete nucleolus is not observed.

A well-developed endoplasmic reticulum (ER) is recognized in the cell with ribosomes (rER) attached to it; however, smooth ER is conspicuous. The rER is continuous with the nuclear envelope, and extends to the inner surface of the anterior part of the cell. Free ribosomes are recognized as well in the anterior part of the cell. Ribosomes (free or ER-bound) and ER are absent in the posterior part thus it is limited to the anterior part (Fig. 3.23- 3.26)

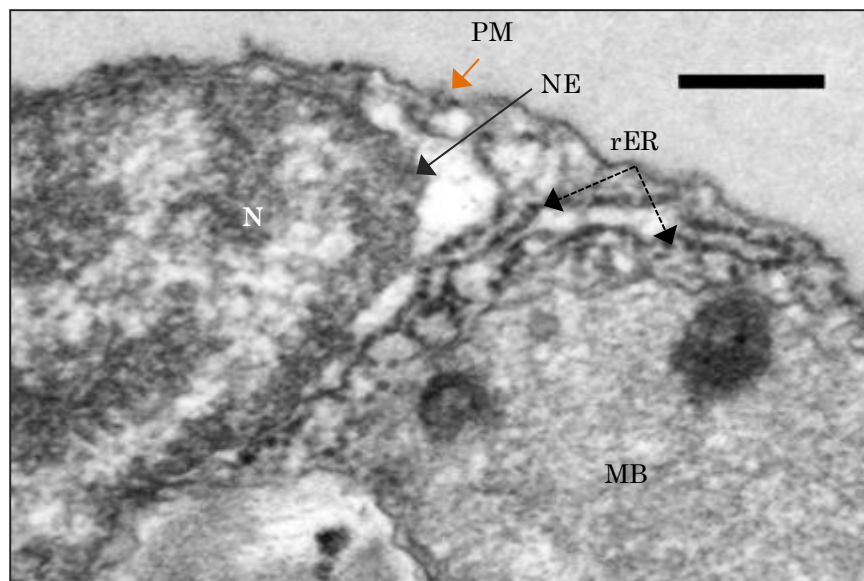


Figure 3.26: Close up view of nucleus (N) with nuclear envelope (NE). Nuclues is appressed with plasma membrane (PM, arrow head), rough endoplasmic reticulum (rER) and microbody (MB). Scale bar 200 nm.

3.6.6.3 Mitochondrion

A cup-shaped, single mitochondrion is observed with tubular cristae which is located ventrally and extended to the central axis of the cell. This is the second largest organelle observed in the cell; it covers partially with the nucleus (N) on top and extends to the posterior digestive sac (P) at the bottom. A ventral view showed that the mitochondrion is slightly elongated from left to right (see Fig. 3.24). Apart from the nucleus, anterior part (AP) is occupied by two major compartments, including A) mitochondrion at the ventral and B) large microbodies at the dorsal part (Fig. 3.23, 3.25). The mitochondrion displays two additional highly distinctive structural differentiations:

(1) There are two membrane-bound inclusions with electron-dense, granular contents located at specific positions inside the mitochondrion (edsm1, edsm2, Fig. 3.27). The first (edsm1) is located at the high back end of the mitochondrion, positioned within the inter-membrane space which is thereby dilated (Fig. 3.27). Appropriately sectioned, this inclusion appeared to be located in the matrix enclosed by a single membrane (the inner envelope membrane). Because the edsm1 could be followed through 7 serial sections (a cell longitudinally sectioned from left to right in Fig. 3.25), the shape of this inclusion could be cylindrical (diameter 150-200 nm, length minimum 400 nm). The second (edsm2) is located in the ventral, left part of the mitochondrion and is enclosed by two membranes (Fig. 3.27). The edsm2 is a tubular invagination of the cytoplasm into the mitochondrial matrix. This inclusion also has contact with the mitochondrial envelope.

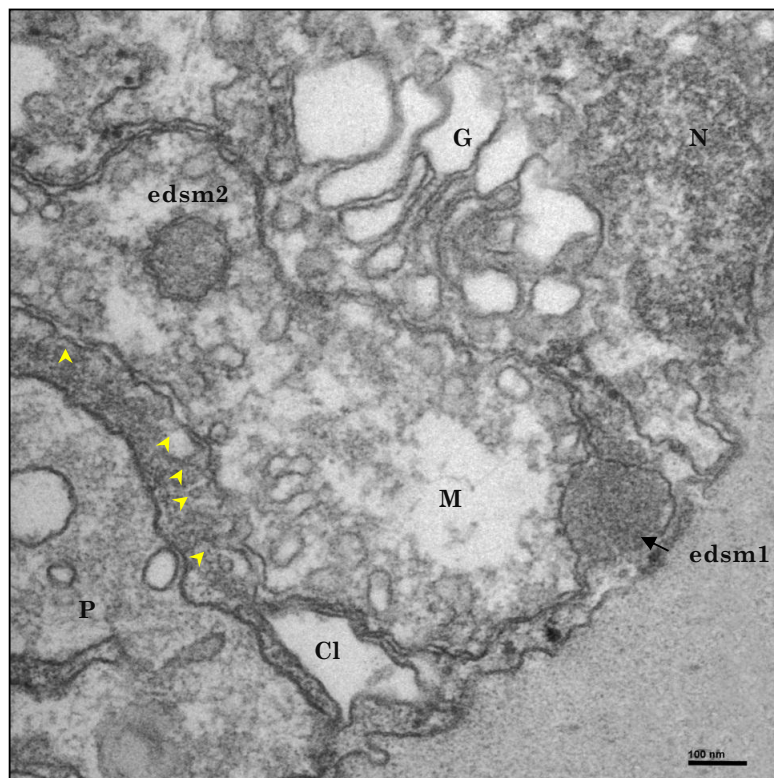


Figure 3.27: Closer view of mitochondrion with two electron dense fibrous material (edsm1; edsm2). The edsm1 enclosed with intermembrane space (arrow). The edsm2 is enclosed with double membrane. 'Mitovilli' are shown in arrow heads. M, Mitochondrion; N, nucleus; G, Golgi body; Cl, cleft; P, posterior digestive sac. Scale bar 100 nm

(2) The lower side of the mitochondrion adjacent to the posterior part of the cell (the bottom of the seating area) displayed another highly unusual specialization. Over an area of $\sim 1 \times 0.6 \mu\text{m}$ (Fig. 3.28), regularly-spaced projections extend from the outer mitochondrial envelope membrane towards the posterior part (PP) for 50-60 nm ($n=30$) after which they terminate in an electron dense granular area that is in contact with the membrane of a large vacuole (the posterior digestive body, P). These projections, termed here “mitovilli,” (approx. 300 mitovilli per mitochondrion) are about 20 nm wide (narrower near their base) and are spaced at 40 nm (Fig. 3.28).

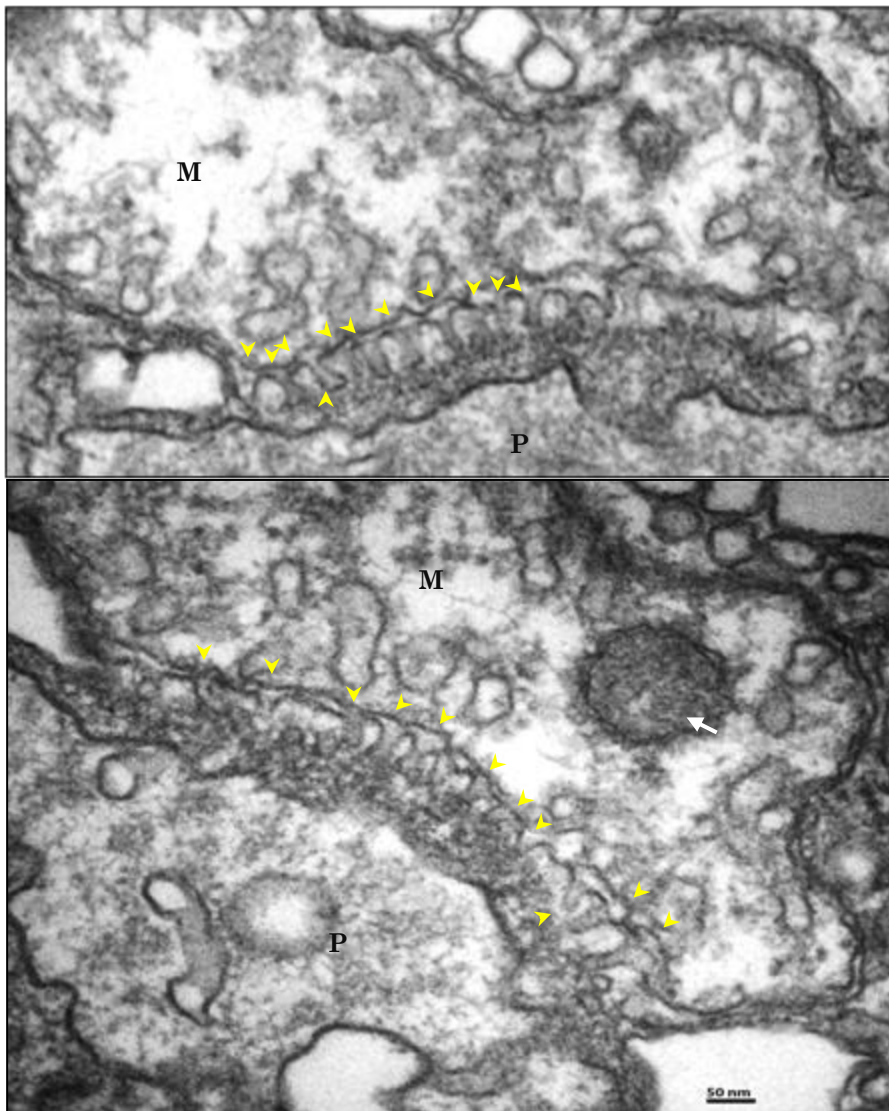


Figure 3.28: Closer view of mitochondrion outer membrane projections ‘mitovilli’ (arrow heads). The mitochondrion double membrane is visible throughout its surface. Upward arrow shows the narrow end of the outer membrane which presumably in contact with electron dense material at the posterior realm. White arrow indicates edsm2. The space between mitovilli and the posterior digestion body (P) filled with electron dense particles. M, Mitochondrion. Scale bar 50 nm

3.6.6.4 Golgi apparatus

A single Golgi body with Golgi vesicles (together forming the Golgi apparatus [GA]) are clearly observed in-between the mitochondrion, the nucleus, and the flagellar apparatus at the ventral side of the cell (Fig. 3.29, 3.30). It contains a series of five to six cisternae; the 'cis' face of the Golgi stacks is recognized near to the ER, possibly attached with nuclear envelope (see appendix 6.7), while 'trans' face is oriented towards the basal bodies. The whole Golgi complex is characteristically positioned in a groove of the mitochondrion facing ventrally.

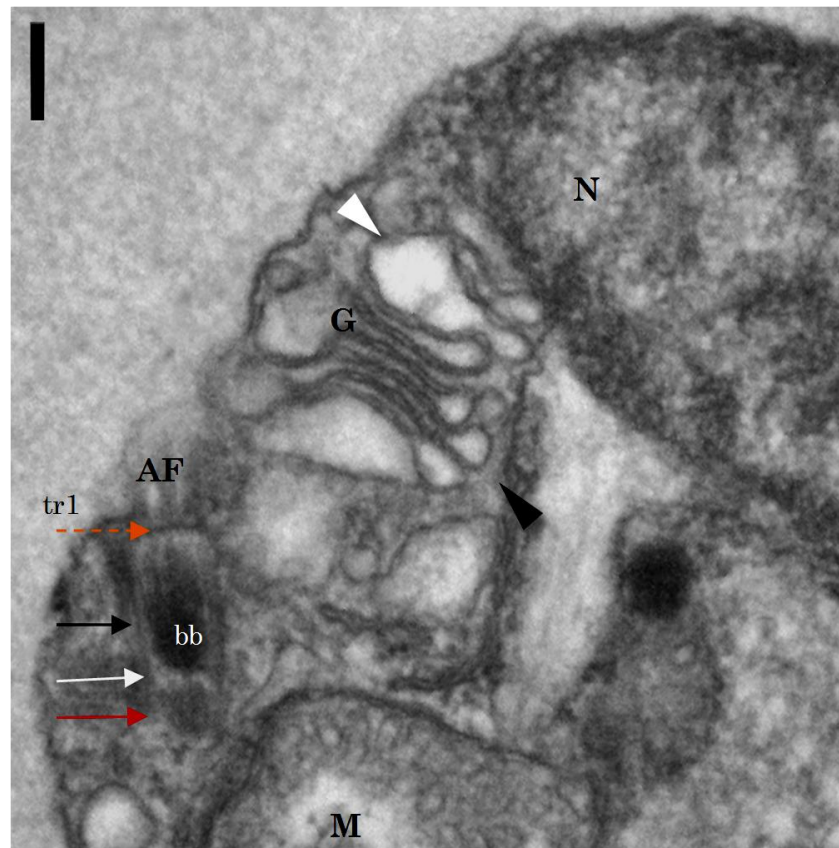


Figure 3.29: The Golgi apparatus. Golgi body with surrounding GA vesicles is located in the Ventral region and placed in the groove of mitochondrion, the cis face attached to the nucleus and the trans face with flagellar apparatus. Red arrow, cartwheel-like structure; black arrow, electron dense lumen of the bb; white arrow, the space between the two electron dense lumens; M, Mitochondrion; N, Nucleus; AF, anterior flagellum; bb, basal body; tr1, transitional region1. Scale bar 200nm

3.6.6.5 Basal body and basal apparatus

The *Picomonas* basal bodies (bb) are positioned between Golgi complex and mitochondrion at the ventral side of the cell and are connected by a proximal connection fiber (pcf). Except for a single proximal connecting fiber both basal bodies were not interconnected by fibrous structures (Fig. 3.30, 1&2). The two basal bodies are displaced against each other by about one basal body diameter, in that the anterior basal body is located more ventrally than the posterior basal body. Each basal body possesses a basal plate (Fig. 3.32, 1A and appendix 6.8), a less electron-dense material at the proximal end (Fig. 3.29 white arrow), microtubular triplets with heavy electron dense materials in the lumen (Fig. 3.29 black arrow), a fibrous material between the two electron dense regions (white arrow) and a pair of microtubular roots at the proximal end. A prominent electron dense fibrous material, (Fig. 3.32, bb1, bb2) is observed within the lumen of both basal bodies over a distance of 200 nm (Fig. 3.29 white to dotted arrow). The length of each basal body extends of approx. 300nm (Fig.3.29, red dotted arrow). Interestingly, the same length has been observed between the tr1 and tr2 transition plates.

The central pair of microtubules starts quite distantly from the tr1 plate and extends through the distal septum of tr2 towards the axonemal tip. Surprisingly, a second transition region (tr2) is observed in this cell, act as a region flagellar shedding (Fig. 3.33). The distance between, at the start of the central microtubules and tr2 (inner surface) is observed with electron dense material (Fig. 3.32, Pic. 2 & 3 with curly bracket) in and around axoneme. At the tip of tr2, the plasma membrane constricts and the presence of a central pair of microtubules is unsure. Interestingly, the central pair of microtubules originate near the tr1 and extend through the tr2 (Fig. 3.32).

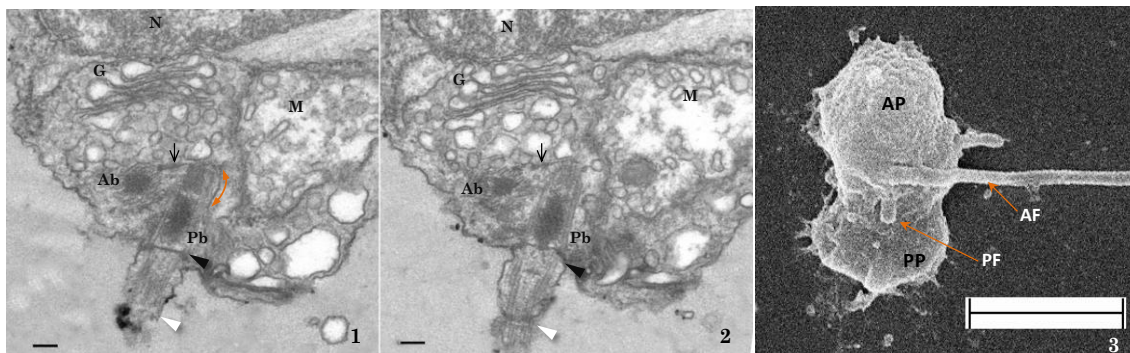


Figure 3.30: 1 & 2, two continuous sections of flagellar basal bodies (bb). Basal bodies (bb) located at the ventral side of the cell and the proximal end is connected by a proximal connection fiber (pcf, arrow). Two transitional regions are observed from both basal bodies (tr1-black arrow, tr2- white arrow). Both basal bodies (Ab, Pb) filled with electron dense fibrous material; double sided arrow show cartwheel-like structure of bb. N, nucleus; G, Golgi apparatus; M, mitochondrion; Ab, anterior basal body; Pb, posterior basal body. Scale bar 100 nm. 3, flagellar bases (AF and PF) imbricated clockwise, when viewed from cell's left. Scale bar 5 μ m.

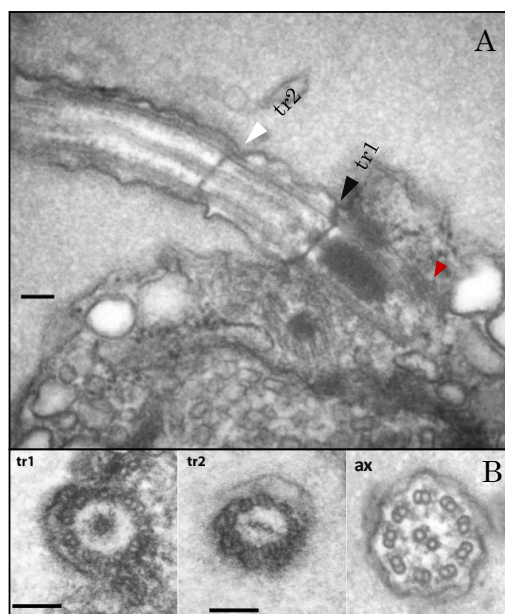


Figure 3.31: A) Longitudinal section of *Picomonas* flagellar system. Two transitional septa (plates) are observed in each flagellum as proximal (tr1-black arrow) and distal plate (tr2-white arrow). The distance between basal plate to tr1 and tr1 to tr2 are almost equal and the length is approximately 300 nm. **B)** Transverse section of flagellum at different positions; tr1, proximal transitional plate connected with basal body; tr2, distal transitional plate, and ax transverse section of axoneme. Triangle indicates the proximal end of tr1. Scale bar 100nm.

3.6.6.6 Transition plate

Transverse sections (60 nm) of the flagellar basal apparatus are composed of nine microtubular triplets with a connection between A and C microtubules (Fig. 3.32 C-E). Both basal bodies form a cylindrical lumen with approximately 300 nm in length and 220 nm in diameter. The lumen of the bb is filled with electron dense material. At the proximal end of the basal body, a basal plate is observed (Fig. 3.32 A, appendix 6.8) which is associated with microtubular roots & proximal connecting fibre (Fig. 3.30 and 3.31, red arrow). In Fig. 3.32 B, the pro-basal body (arrow) is attached with one of the triplets of the basal body.

The doublet and triplet region is observed near the distal end of the basal body in Fig. 3.32 F. The transverse section in Fig. 3.32 G-L comprises the region between tr1 & tr2. The central pair of microtubules starts from Fig 3.32 I, which is about 100 nm away from the tr1 septum. In Figure 3.32 G to K, the plasma membrane is observed quite distantly from nine doublets, and the diameter of the cylindrical column is measured about 300 nm. Interestingly, the plasma membrane at figure 3.32 L&M is appressed with doublets of axoneme. In Fig. 3.32 L, the plasma membrane is confined at lower half than to the upper half (black arrow), and also varies by diameter of the axoneme. The diameter of axoneme in picture G is about 280 nm whereas L is about 220 nm when measured. The exact function of tr2 apart from shedding is unclear (Fig. 3.33). A regular (9x2) +2 pattern is observed as shown in Fig. 32 M, which extends to form the axoneme.

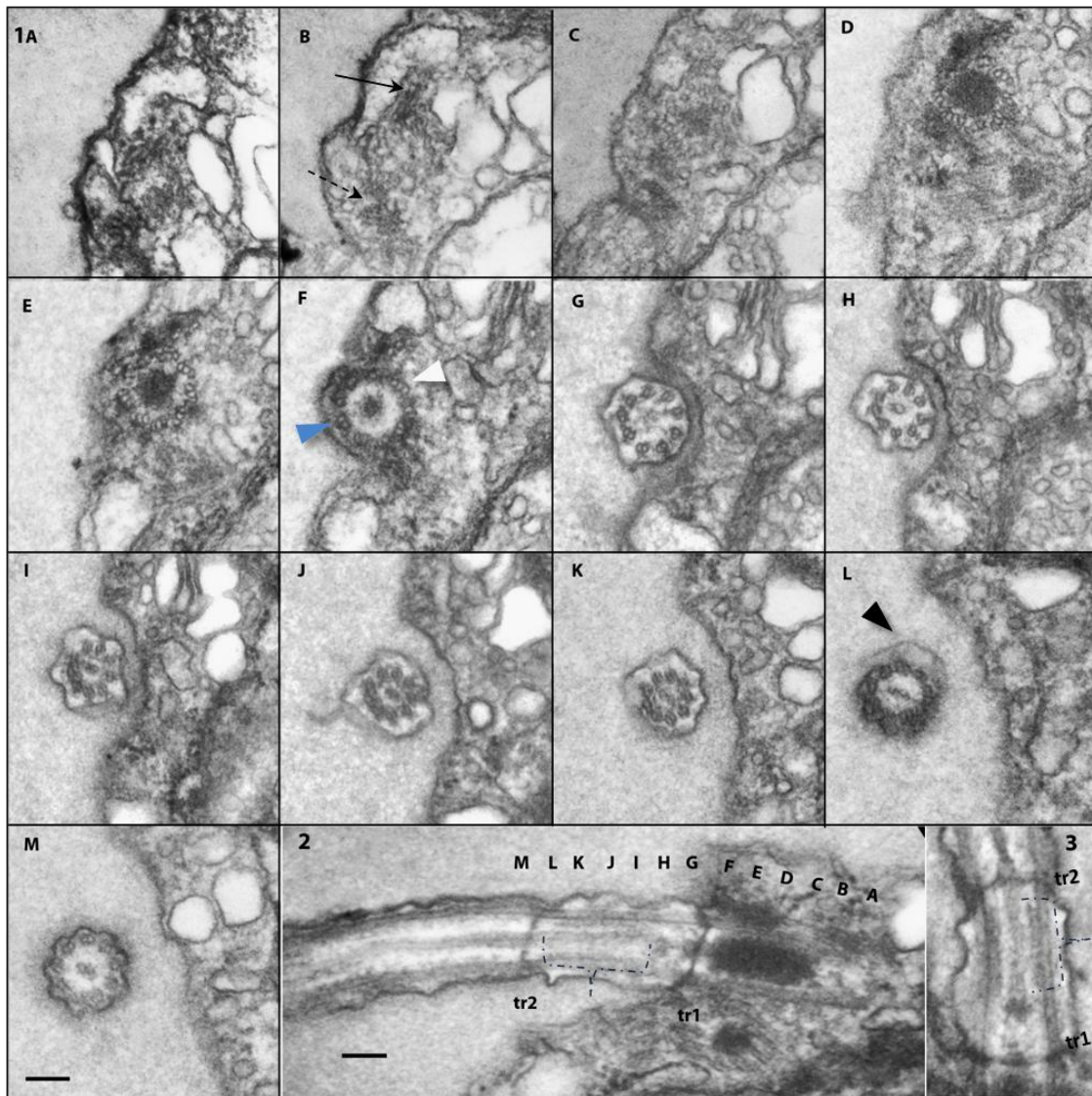


Figure 3.32: 1A-M. Electron micrograph shows sequential transverse section (60nm) of axoneme from proximal to distal. **A** Basal plate, **B** Cartwheel-like structure presumed (see also appendix 6.8) where 9 triplets and pro-basal body starts. **C-E**- electron dense matrix in the lumen, **F** tr1, and a possible distal connecting fibre (double arrow), **G & H**- 9x2 microtubules without central pair of microtubules, **L** tr2 lower side the plasma membrane is appressed but on top PM is distanced (black arrow head), **M**- 9x2 +2 arrangement of the axoneme. Fig. 3.32 2 & 3, **G-K** distance between tr1 and tr2, consisting microtubules surrounded by numerous proteins (dotted bracket) showing a wider plasma membrane around the microtubules; **2**- Longitudinal section of the axoneme, letters refer to levels in the cross section **A-M**, **3**- closer view of tr1 and tr2, electron dense material between axoneme and plasma membrane in tr1. Curly arrow shows electron dense material between central microtubular roots and axoneme. Scale bar 100 nm.

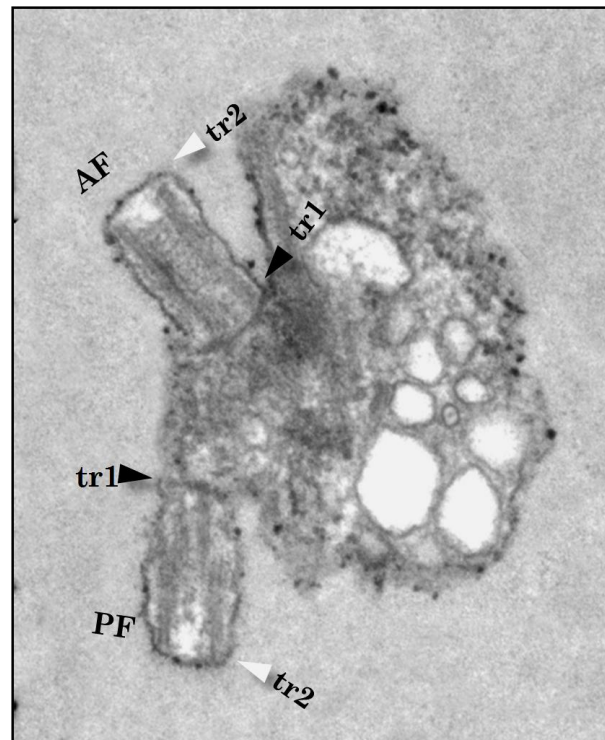


Figure 3.33: Electron micrograph of flagellar shedding. Both anterior (AF) and posterior flagella (PF) shed at the distal transitional region (tr2), making a flagellar stub remain attached.

Both transverse plates (tr1 & tr1) appeared to be structurally identical, however, in our fixation, the distal transverse plate (tr2) constricted the flagellum and axoneme (Fig. 3.33). At this site the flagellum is believed to be shed because often flagellar stumps are observed attached with cell body. In TEM, it clearly shows that the flagellum is terminating at tr2 (Fig. 3.33).

3.6.6.7 Probasal body

During interphase, the basal bodies generally do not appear to be associated with probasal bodies, but in one cell (likely in preparation for cell division), probasal bodies are observed; associated with each basal body (Fig. 3.34A (Ppb, Apb) at 90° angle, the distal end is attached with plasma membrane. Both probasal bodies extended from their parental basal bodies at right angles, and interestingly were oriented towards the same side, closely associated with the ventral surface of the cell (Fig. 3.34A, B)

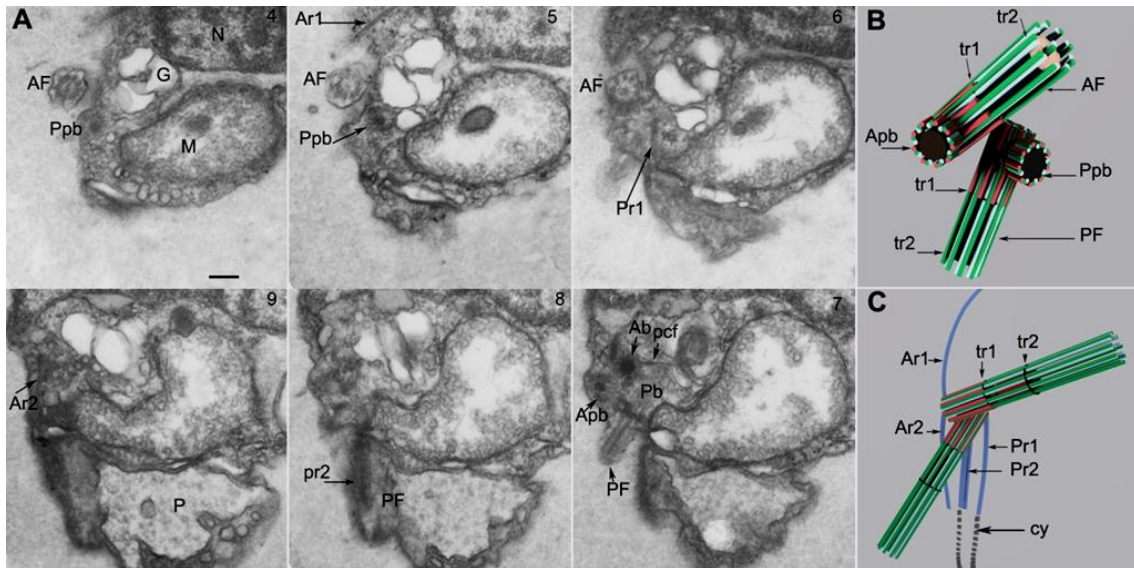
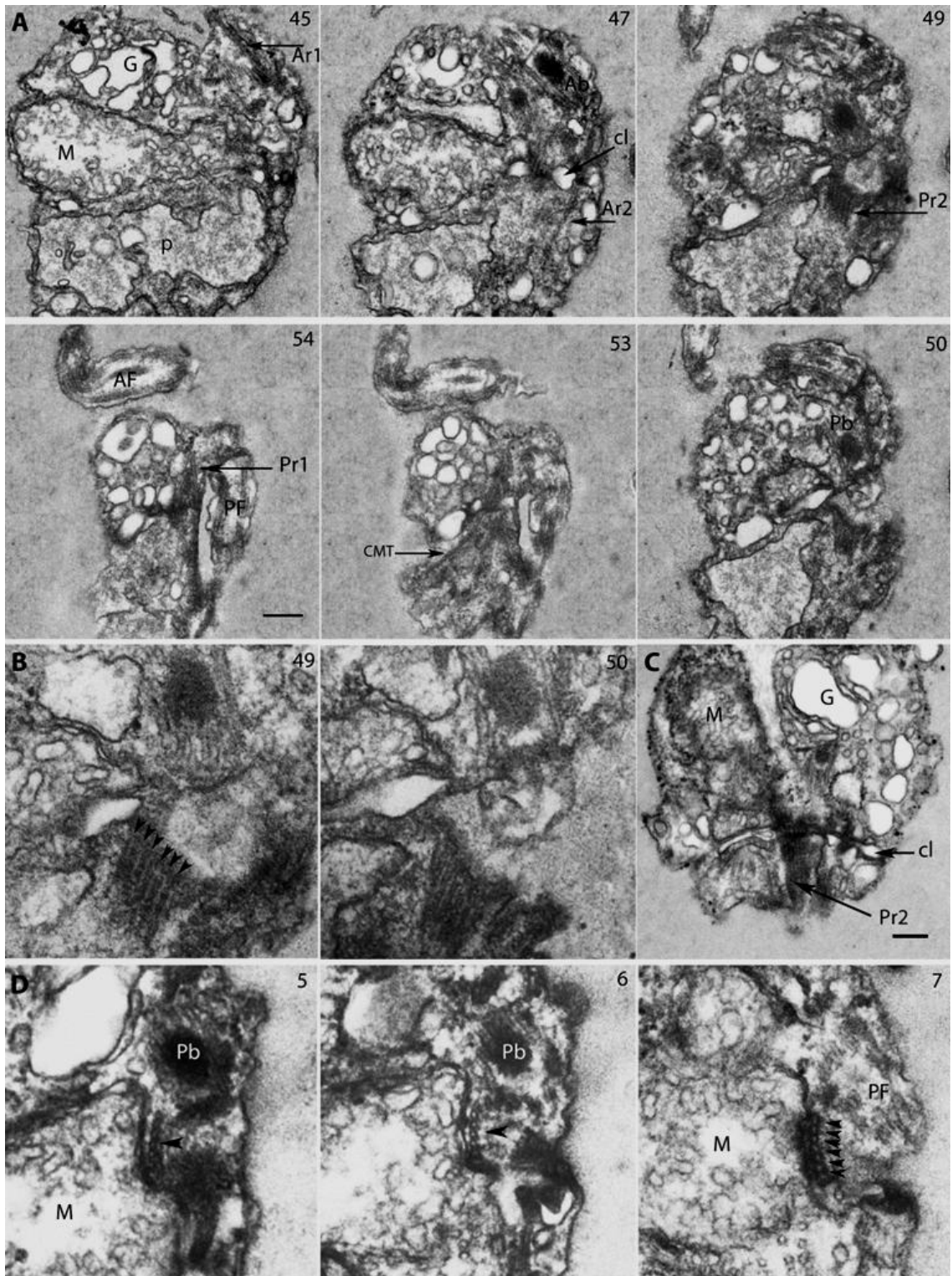


Figure 3.34: Basal apparatus and probasal body. **A.** Electron micrograph shows continuous section of *Picomonas* from ventral to dorsal. Each probasal body is originated from corresponding basal body at 90° angle, the distal end is attached with plasma membrane. **B.** 3D- animation of basal body with probasal body. **C.** Animation of the model of axoneme, basal body with flagellar roots. AF/ PF (anterior-/posterior flagellum); tr₁,tr₂ (distal [tr₂] and proximal [tr₁] flagellar transitional regions); Ab/Pb (anterior-/posterior basal body); Apb/PpB (anterior/posterior pro basal body); pcf (proximal connecting fiber); Ar₁/ Ar₂ (Anterior root 1 and 2); Pr₁/Pr₂ (posterior root 1/ posterior broader root 2); G (Golgi body); N (nucleus); M (Mitochondrion); cy (cytotome). Numbers at the top right indicate the serial section. **Scale bar:** 200 nm.

3.6.6.8 Microtubular flagellar root system

Serial sections revealed the presence of four microtubular flagellar roots, two associated with each basal body; roots originate from anterior basal body is named as Ar1, Ar2, the basal as Pr1, Pr2 (Fig. 3.35; see 3D model in Fig. 3.34 C). The Ar1 consists of two microtubules and runs towards the cell's anterior left (Fig. 3.34 A, section 5). It accompanies the nuclear envelope and terminates before reaching the anterior end of the cell (Fig. 3.34C). The Ar2 also consists of two microtubules, runs beneath the ventral cell surface to the cell's posterior passing the mitochondrion and entering the posterior part (PP) of the cell, terminates near to the anterior end of the cytostome (Fig. 3.34C). The Pr1 originates at the left surface of the posterior basal body near its proximal end (Fig. 3.34), consists of two microtubules, runs posteriorly, along the ventral surface of the cell, and enters the posterior part (PP) of the cell where it terminates near the left side wall of the cytostome (Fig. 3.35). The Pr2 is a broad root consisting of 6 microtubules (Fig. 3.35 B-D) originates the right surface of the posterior basal body. It runs close to the ventral surface of the cell towards the cell's posterior, then traverses the vacuolar cisterna (Fig. 3.35 C), and terminates near the anterior end of the cytostome near its right side wall (Fig 3.34 C). A few additional cytoplasmic microtubules (CMT in Fig. 3.35 A, section 53) originate at an angle of about 45° from the proximal region of the Pr1, to extend to the cell's left. All three posteriorly oriented roots (Ar2, Pr1 and Pr2) run parallel to each other into the posterior part (PP) of the cell, spaced 0.5 μm. The Ar2 seems to terminate before the other roots. At this position, electron dense ribbons associated with the plasma membrane extend from the Pr1 and Pr2 and continue alongside the left (from Pr1) and right (from Pr2) side wall of the cytostome to the cell's posterior end (Fig 3.34; 3.35).

Figure 3.35: Flagellar apparatus. **A.** Longitudinal section of *Picomonas* from ventral to dorsal (sections are oblique from anterior part). Anterior flagellum (AF) and posterior flagellum (PF). The anterior flagellum locates close to the ventral surface followed more interiorly by the posterior flagellum. The basal bodies of both flagella are connected by a proximal connecting fiber (pcf) and exhibit two transitional regions (the proximal is termed 'tr1' and the distal 'tr2'). **B, C.** Consecutive serial cross sections and two serial longitudinal sections of the anterior flagellum. Serial sections of **B** correspond to **C**, denoted in **B_a-j** at the left lower end. **a.** The axoneme with 9 outer doublet and 2 central pair microtubules. **b.** The distal transitional region (tr2) is involved in flagellar shedding (* indicates electron dense material near outer doublets). **f.** the central pair of microtubules originate. **h.** the transitional region 1 (tr1), C-tubules added (arrowhead indicates a microtubular triplet and arrow indicates a microtubular doublet. **i,j.** cross sections through basal body with microtubular triplets arranged in the clockwise direction, the basal body lumen is filled with electron dense material. AF/ PF (anterior-/posterior flagellum); tr1, tr2 (distal [tr2] and proximal [tr1] flagellar transitional regions); Ab/Pb (anterior-/posterior basal body); pcf (proximal connecting fiber); G (Golgi body); N (nucleus); Pr2 (posterior microtubular flagellar root 2). Numbers at the top right indicate the serial section. **Scale bar:** 100 nm. →



3.6.6.9 Cleft

A membrane-bound vacuolar cisterna (vc) (Fig. 3.25-[18; 22; 26], 3.36) forms a 'cleft' separates the two hemispheres (the anterior part and the posterior part). The size of the cleft is not constant, varies among cells. The transverse section of the cell at the juncture (between the two hemispheres) is shown in Fig. 3. 36A. In spite of, searching for a food vacuole in all of 52 cells analysed, no typical food vacuoles are found in *Picomonas*. Furthermore, serial thin sections of the cleft do not show any ingested prey or remnants of bacteria; however, some osmiophilic spherical structures (Fig. 3.37) are observed. Bacteria are seen often close to the sectioned cells and sometimes appeared as attached to the plasma membrane but never inside the cells.

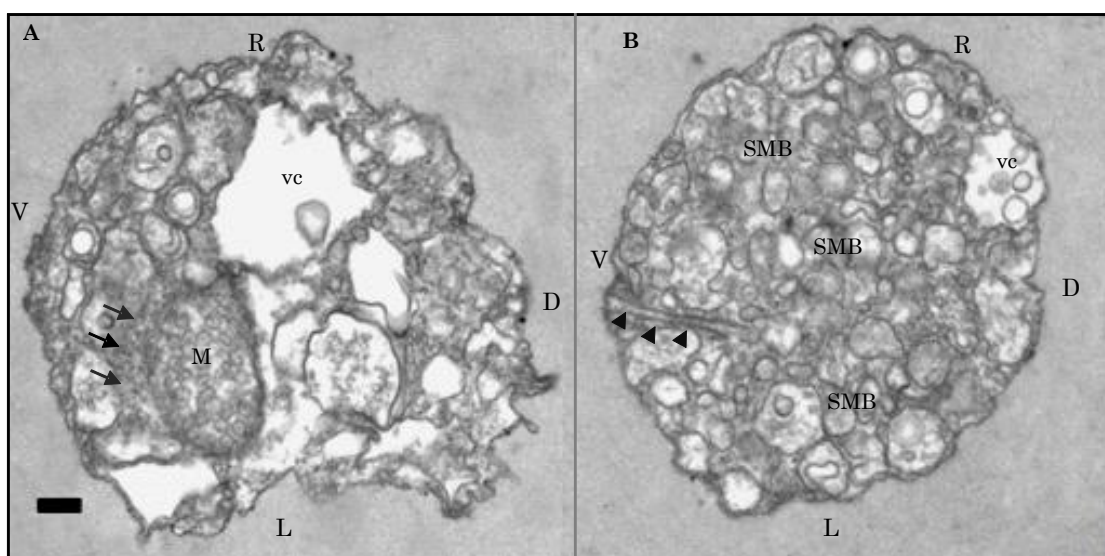


Figure 3.36: Electron micrograph of non sequential cross section of *Picomonas* cell, view from anterior to posterior **A**. Transverse section of a cell in the juncture between anterior and posterior hemisphere revealing mitochondrion (M) and cross section of 'mitovilli' (black arrow) at the ventral side, and vacuolar membrane cisternae (vc) and vesicles (SMB) at the dorsal part. **B**. Transverse section from posterior to anterior direction. The entire volume consists of single membrane bound vesicles (SMB), Feeding basket (non-active feeding stage, arrow heads) observed at the ventral (V) and 'vc' at the dorsal side (D). M, mitochondrion, V- Ventral, D dorsal, L left, R, right side view of the cell. Scale bar 200 nm.

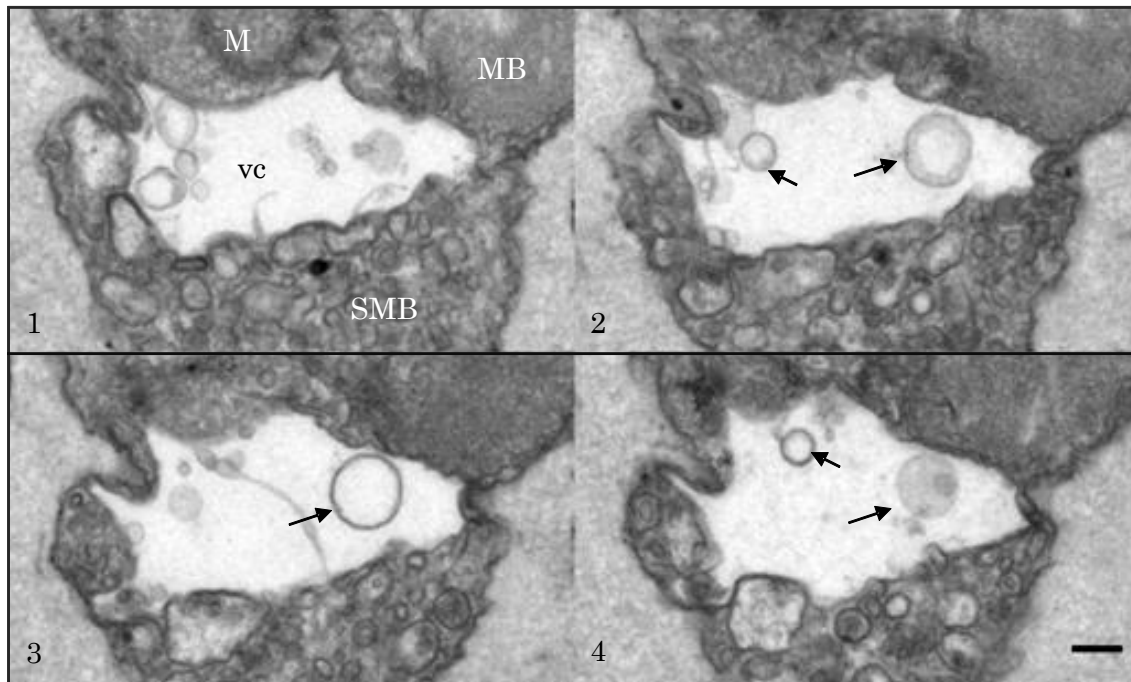


Figure 3.37: Consecutive sections of cleft (perhaps a digestive vacuole or lysosome?). The vacuolar cisterna separates anterior part (AP) from posterior part (PP) at the dorsal side. No digested prey or any remnant inside the vacuole; nevertheless some osmiophilic membrane-bound substances are often observed (arrows). M, Mitochondrion; MB, microbody; vc, vacuolar cisterna; SMB small membrane bound vesicles. Scale bar 200 nm

3.6.6.10 Posterior part

The posterior part varies in size, and comprises of a large single membrane posterior digestive sac (P), putative feeding apparatus (F) and membrane vesicles (SMBs). The posterior digestive body is recognized as a major organelle located at the ventral surface (Fig. 3.38, 3.23, 3.24), occupies up to half the volume of posterior part ($\sim 1 \mu\text{m}$), its depth (from ventral to dorsal) 600-700 nm and its height 400-500 nm. The membrane surface of this vacuole is often highly irregular with invaginations (Fig 3.38). Sometimes these invaginations contain vesicles (Fig 3.38 arrow). The contents of this vacuole consist of irregular, fluffy material of medium electron density and numerous vesicles of various sizes with electron-translucent contents. Though, the anterior part of the posterior digestive sac (P) is situated in a close proximity near 'mitovilli', there no apparent association with Mitochondrion. However, more electron dense particles are always observed between the mitovilli and the digestive sac. The rest of the posterior part is filled with numerous vesicles (Single membrane body (SMB, Fig.3.37B).

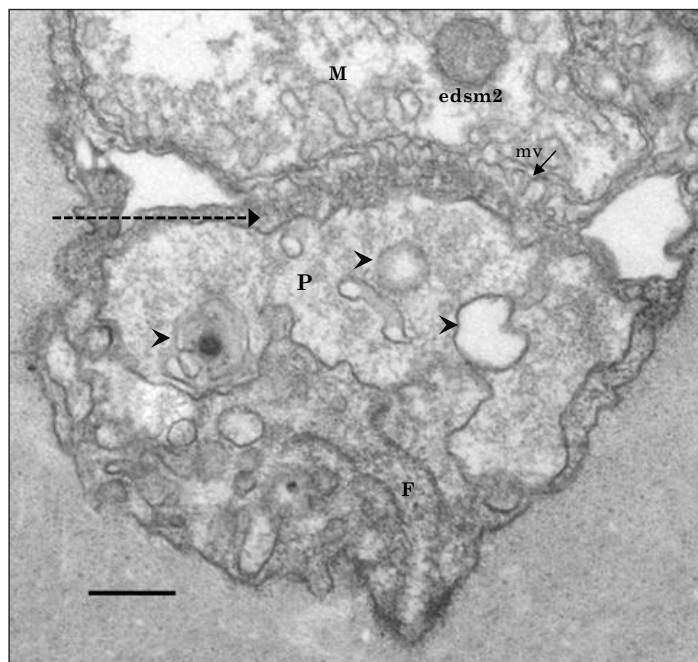


Figure 3.38: Longitudinal section of posterior part. Single vesicles and multi-vesicular bodies (arrow head) are observed. The ‘mitovilli’ (arrow) are adjacent to the posterior digestive body (P), however, no apparent association between these two. P, posterior digestive sac; F, feeding apparatus; mv-‘mitovilli’. Scale bar 200 nm

3.6.6.11 Cytostome like structure

The second conspicuous structure in the posterior part (PP) of the cell is the cytostome/feeding basket that together comprise the feeding apparatus (F, Fig. 3.40). The feeding apparatus is located ventro- posterior to the posterior digestive body (P) and consists of a basket of about 50-60 parallel running fibers (Fig. 3.39A-C (black arrow); diameter of a single fiber: 15 nm, 30 nm repeat structure from one fiber to the next) of varying lengths that extend perpendicular to the anterior-posterior cell axis, from the ventral surface where they are attached to the plasma membrane for up to 1.2 μm enclosing the cytostome, towards the dorsal region where they terminate (Figs 3.41; 3.42). In addition to these major fibers, there is a fine network of very thin fibers that interconnect adjacent fibers irregularly (Fig. 3.41B). The basket is open towards the anterior and dorsal regions of the posterior part (PP), but closed towards the posterior end of the cell (Figs 3.40; 3.41; 3.42) where it sometimes extends into a short tail-like projection of the cell (Figs 3.39; 3.40 B; 3.41B). Towards the dorsal end, the feeding basket gradually widens (up to 500 nm at its dorsal end).

The slit-like cytostome (‘cy’, Fig. 3.39 red arrow head) is formed where the ‘side walls’ of the basket fibers connect to the plasma membrane on the ventral surface (the fibers are anchored in electron-dense ribbons at the plasma membrane; Fig. 3.42, sections 13, 15-18; white arrow head) and extends in the anterior-posterior direction for a length of about 1 μm , its width being on average 150 nm (n=10). In serial sections of some cells it was observed that the anterior-most part of the feeding basket bisected the overlying posterior digestive body (Fig. 3.41, section 11). In these cells (non-feeding stage), the feeding basket appeared to contain mostly small vesicles and multivesicular bodies (Fig. 3.41). In other cells,

possibly during active feeding, the feeding basket contained a single, large vacuole that extended well beyond the basket into the dorsal region of the posterior part (PP) to reach the dorsal plasma membrane (Fig. 3.42, sections 15-18; the length of this vacuole could be up to 1.2 μm). This vacuole contained irregular-shaped, fluffy material of medium electron density (very rarely a vesicle was seen within this vacuole; Fig. 3.40, section 7). This vacuole is named as the “food vacuole (FV).” The food vacuole extended ventrally into the narrow parts of the basket (Fig. 3.42, sections 16-18), where it was sometimes observed to be associated with smaller vesicles (Fig. 3.42, section 17). The anterior end of the cytostome (and thus the feeding basket at the plasma membrane) is linked to the posterior ends of two microtubular flagellar roots (Pr1, Pr2, see below for description of the flagellar apparatus; Fig. 3.41, section 2, 3.42, sections 1, 3; Fig. 3.24C) through the two electron-dense ribbons attached to the plasma membrane that mediate this connection.

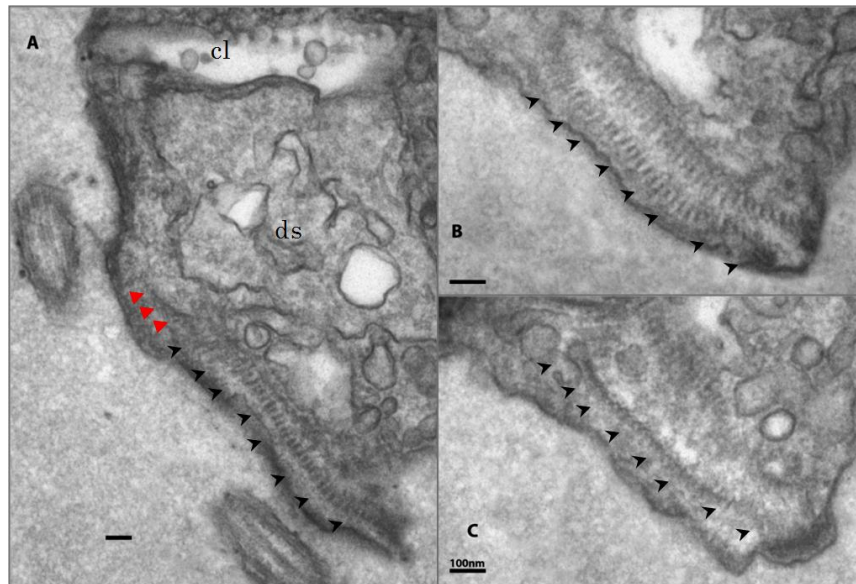


Fig 3.39: Closer view of the cytostome-like structure. Two rows of fibre like structure (left and right fibre) at the ventral surface extends from ventral to dorsal longitudinally, below the digestive sac (P), and proximal end of the fibre is connected with roots (triangles). **A, B, C** three sequential sections through the basket near the cytostome. It shows approx. 60 rows of fibers arranged in parallel (arrows heads depict fibers in the right margin of the basket). Scale bar 100 nm

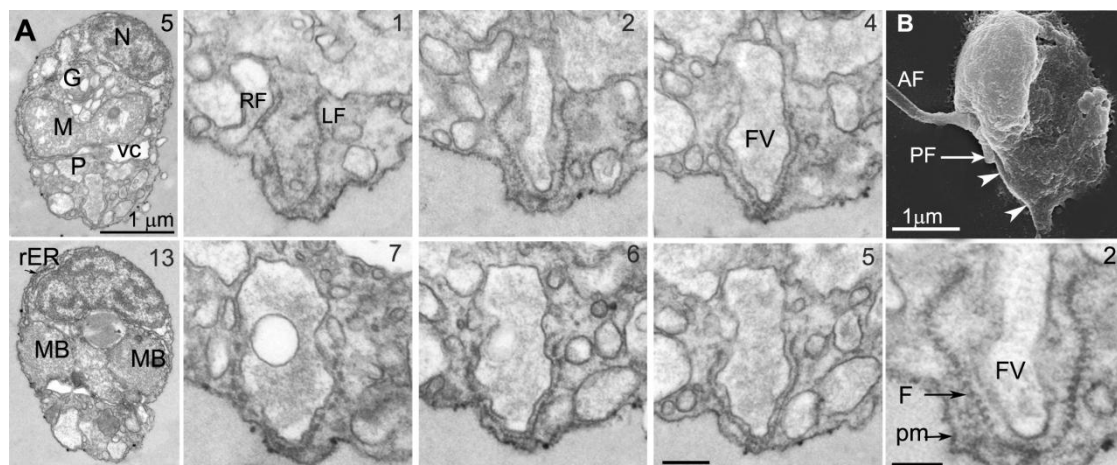


Figure 3.40: Feeding apparatus in Cross section. **A.** Longitudinal sections of a *Picomonas* cell from ventral to dorsal with the feeding apparatus in cross section. Sections 2 to section 7 depict a recently formed food vacuole inside the 'basket' of the feeding apparatus. **B.** An SEM image of *Picomonas* visualizing the left side of the cell. Note that the posterior flagellum has been shed at the tr2; white triangles indicate the cytotome region of the feeding apparatus. AF/ PF (anterior-/posterior flagellum); G (Golgi body); LF/RF (left and right row of fibers of the basket); M (mitochondrion); MB (microbody); N (nucleus); P (posterior digestive body); Ar2 (anterior microtubular flagellar root 2); Pr1 (posterior microtubular flagellar root 1); Pr2 (posterior microtubular flagellar root 2); FV, (food vacuole); vc (vacuolar cisterna); cy (cytostome); F, feeding basket. Numbers at the top right indicate the serial section. **Scale bar:** 200nm; except Fig. 3.40 A, section 2 (100nm).

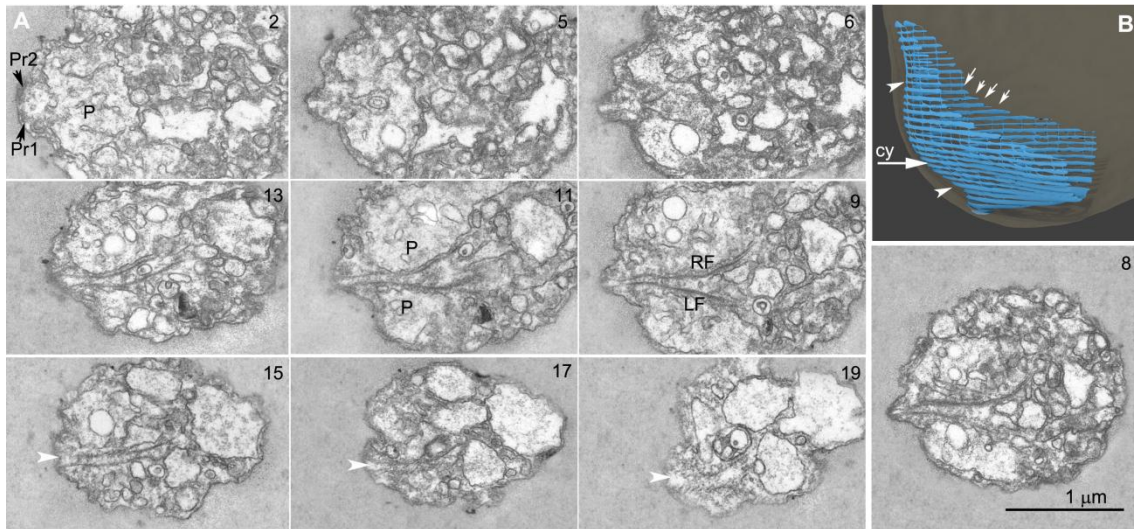


Figure 3.41: Feeding apparatus in longitudinal section. **A.** Cross sections through of *Picomonas* from anterior to posterior; sections begin in the central part of the cell, posterior to the basal bodies. Cell, in the non-feeding mode, without a food vacuole within the basket. **B.** 3D model of the feeding apparatus with rows of fibers in parallel arrangement (white arrows) forming a basket (arrangement of the cell as in **Fig. 3.40A**). Note that the fibers are interconnected by thin filaments. The basket is open towards the top and right (i.e. towards the anterior and dorsal direction of the cell respectively), while it is closed at the bottom (the posterior end of the cell). On the left side of the basket (representing the cell's ventral surface) the fibers are attached to the plasma membrane thus forming the narrow, slit-like cytotome. **Scale bar:** 1 μm

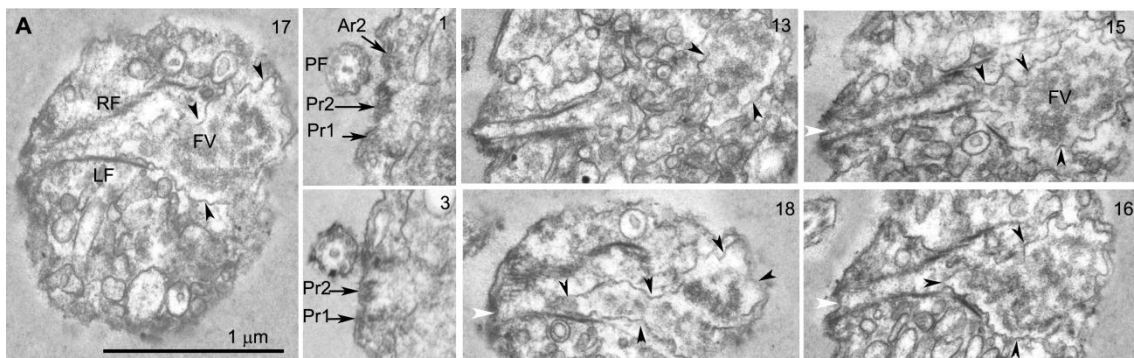


Figure 3.42: Feeding apparatus in longitudinal section. **A.** Cell during active feeding with a large food vacuole within the basket (black triangles); the food vacuole contains irregularly-shaped, 'fuzzy' material, presumably taken up by endocytosis through the cytotome (white triangles). Two rows of fibers representing the left (LF) and right (RF) margins of the basket accompany the food vacuole. **Scale bar:** 1 μm

3.7 Phylogenetic analyses

3.7.1 Phylogenetic analyses of *Picomonas* complete nuclear DNA operon

Phylogenetic tree is constructed for complete ribosomal nuclear operon to understand the phylogenetic position of established *Picomonas* culture (complete nuclear operon of *Picomonas judraskeda*, see appendix 6.10) with available eukaryotic taxa (Fig. 3.41). All sequences in the data set are either from the same species or from the same cell. In addition to *Picomonas* sequence, three environmental ‘picobiliphytes’ sequences are used in this study; in particular, two of them (MS584-5 and MS584-11) are obtained from single cell amplified genome database (SAG) from Yoon et al. 2011. Full length sequence is obtained by a contigs-assembly from SAG database of MS584-5 and MS584-11 (Yoon et al. 2011). The near full length third sequence is obtained from Genbank by concatenating HM595055 and HM595056 sequences (these two have an overlap at the variable region of the large sub unit, without any differences) (Kim et al. 2011). The tree has shown an independent eukaryotic clade (Picozoa) for *Picomonas* along with other three ‘picobiliphyte’ environmental sequences with maximally supported at branch node (Bold branch) by all methods and forms a mono phylum. Tree topology is portrayed that phylum Picozoa has no support assemblage for its close associate's glaucophytes, cryptophytes and katablepharids (Fig. 3.43). Nevertheless, they have shown a weak affinity towards photosynthetic glaucophytes with a little support from Bayesian probability. The alignment includes 100 other eukaryotic nrRNA data set from Genbank, except the ones which are marked with ‘*’ (unpublished data). The data set included Opisthokonta, Chromalveolata, Plantae, Apusozoa, Hacrobia, and Rhizaria; though long branching Amoebozoa and Euglenophyceae are not included in this analysis.

Figure 3.43: Maximum Likelihood phylogenetic tree of 104 eukaryotic taxon samples using complete nuclear encoded SSU, 5.8S and LSU sequences, with 4461 aligned characters for comparisons. Four full-length ‘picobiliphyte’ sequences are grouped under new phylum Picozoa. Published sequences are denoted with accession number, taxon name, followed by strain designation. Unpublished sequences are marked by *. Support values at the branch length are bootstrap partitions from RAxML, ML, neighbor joining, with maximum parsimony and Bayesian posterior probability. Maximal supported branches by all methods are marked in Bold (=100/100/100/1.0). Branch separating opisthokonts are defined as out group. Scale bar denotes 10% substitution per site. →

3.7.2 Diversity of 'picobiliphytes' in marine environment

The complete nuclear operon of the phylogenetic tree suggests that phylum Picozoa forms an independent phylogenetic position as a mono phylum. To assess the biodiversity of 'picobiliphytes', at first, all environmental 18S 'picobiliphytes' sequences (data set-3) are used for the tree construction. To ensure the sequence specificity to 'picobiliphytes', tree is primarily constructed with all other eukaryotic 18S rDNA sequences (Not et al. 2007a; Cuvelier et al. 2008; Heywood et al. 2011; Yoon et al. 2011) includes data set-1 and yielded data set-2. It resulted that all the 'picobiliphyte' sequences form an independent group with existing eukaryotic taxa (data not shown). Sequences from this monophyletic group are taken for the diversity study. Since Picobiliphytes are long branched without prominent support for sister relationship to other eukaryotes groups, an unrooted tree is generated. The sequence of the clonal culture in this study is mentioned as *Picomonas* sp. in these trees. New sequences obtained in this study from taxon specific clone libraries are highlighted in grey in Fig. 3.43. The tree also contained partial 'picobiliphyte' SSU 18S sequences.

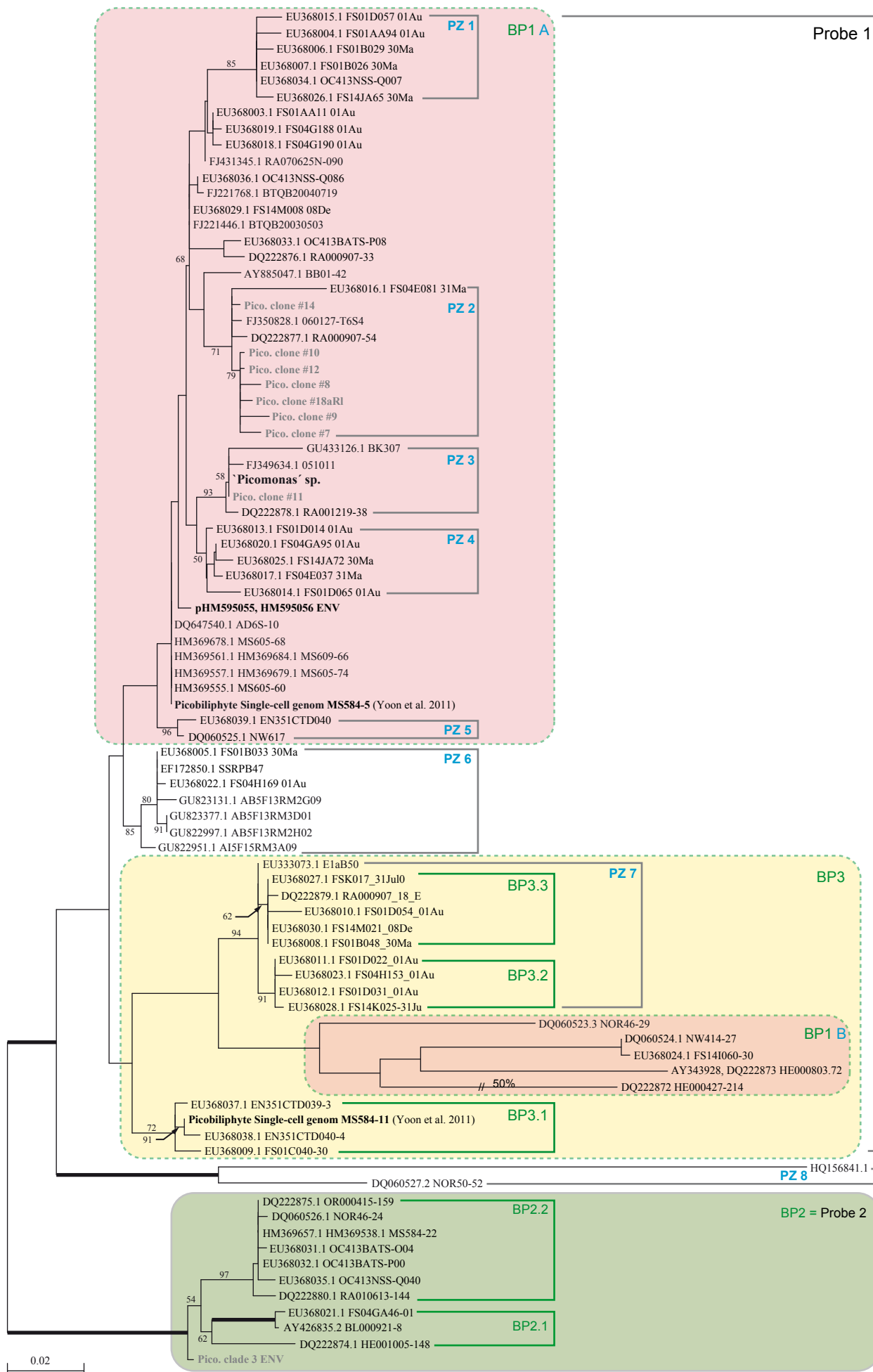
Three possible outcomes are found from this phylogenetic analysis; Sequences obtained from the Helgoland Time Series Station (in this study) are largely grouped together with one sequence in Roscoff ASTAN (Acc.no. DQ222877. 1; clone: RA000907.54), and another sequence from the North Atlantic, forms a monophyletic subclade of the Picozoa (PZ2).

Picomonas sequence along with one environmental sequence from Helgoland form an independent clade PZ3 and they are grouped together with Roscoff ASTAN sequence (Acc.no. DQ222878. 1; clone: RA001219. 38).

The third sequence of tree (Pico. Clade3 ENV) largely supports to clade probe2/ BP2 and forms an independent new clade (PZ11). The formally described clades (Not et al., 2007a; Cuvelier et al., 2008; Kim et al., 2011; Yoon et al., 2011) are plotted on this tree (Fig. 3.44) for better understanding of the biodiversity. Not et al., (2007a) described that the 'picobiliphytes' constitute three clades; clade I & II shown designated as Probe1, and clade III as Probe2. Cuvelier et al., (2008) showed more diversity among 'picobiliphyte' clades by increasing the environmental sequences and suggested that the 'biliphyte' (BP) sequences comprised more possible independent clades with major clades BP1, 2 & 3, which include sub clades (BP2.1, 2.2 and 3.1, 3.2 & 3.3) are marked in green. However, in this study of one of the 'biliphyte' sequences (Acc.no: EU368024; clone: FS14I060-30) from a monophyletic group BP1, diverged and formed a para phyletic group with BP3 (shown as BP1A and BP1B). Of three 'picobiliphyte' sequences from single-cell amplified genome from Yoon et al., (2011) are shown in dotted line, filled with pink, yellow and green colours for MS584-5, MS584-11 and MS584-22 respectively. Two sequences (Acc. No: DQ060527.2 & HQ156841. 1) are highly diverged and strongly supported at the base node and forms a monophyletic sub clade PZ8. Another sequence from Helgoland environmental sample (Pico.Clade3 ENV) forms independent branch with strong support at the basal node (BP2=Probe2). Thus, the

tree with increasing number of sequences resulted in a prediction of at least eight new sub clades with formally existing clades from this analysis.

Figure 3.44: Unrooted 'picobiliphyte' tree based on the 18S rDNA. Randomized accelerated maximum likelihood (RAxML) phylogeny for 86 'picobiliphytes' taxa (85 are from environmental sequencing and 1 from my clonal culture) with 1775 aligned characters are used in this study. The length of the branch is equal to the number of substitution; the scale bar indicates 2% substitution per site. The tree topology was calculated by RAxML maximum likelihood. Bold branches show 100% bootstrap support. The discontinuous branch (//) has been shortened to 50% of the branch length. PZ- Picozoa clade, BP- 'biliphytes' clade (Cuvelier et al. 2008), Probe 1&2 'picobiliphytes' clade (Not et al., 2007a), coloured rectangle boxes- Single Amplified Genome sequence (Yoon et al. 2011). →



4 Discussion

4.1 'Picobiliphyta': A cell with enormous mystery

Plankton, both micro- and nano-plankton are easily visible under a light microscope, providing a wealth of features that are mostly adequate to identify the taxa to which they belong. However, little is known about the morphological and functional characteristics of the very small cells ($< 3 \mu\text{m}$) which comprise the picoplankton, a fraction that dominates the biomass of the biosphere (Pace 1997; L K Medlin et al. 2006). This lack of knowledge is rooted in our general inability to culture these organisms. The biodiversity and abundance of picoplankton have been mainly monitored using a molecular approach (18S rRNA clonal libraries), but this cannot reflect the true diversity because of PCR biases (Stepanauskas & M. E. Sieracki 2007; Heywood et al. 2011) and other artefacts such as FISH. However, molecular analyses have aided the identification of new protists from environmental samples by allowing successful phylogenetic analyses. This has revealed an inordinate diversity among these organisms, thus many new taxa have been discovered with increasing list of awkwardly long branched independent/associated lineages (Giovannoni et al., 1988; Amann et al., 1990; Díez et al., 2001; Not et al., 2002; Not et al., 2007b; Biegala et al., 2003; Massana et al., 2004; Lovejoy et al., 2006; Medlin et al., 2006). Sequences from three different coastal areas (in the North Atlantic, on the European coast and in the Arctic Ocean) indicated a distinct independent lineage comprising three clades, which collectively had a weak association with algae possessing secondary endosymbiont, such as cryptophytes (Hoef-Emden & Melkonian 2003; Novarino 2003; Medlin et al. 2006) and katablepharids (colorless flagellates (Inouye & Noriko Okamoto 2005; Noriko Okamoto et al. 2009). These sequences led to synthesis two oligonucleotide probes (Not et al., 2007a), which are used to identify organisms belonging to this new clade (from here on referred to as 'picobiliphytes'), and are applied to samples on $0.2 \mu\text{m}$ membrane filters following $3 \mu\text{m}$ prefiltered sea water (TSA-FISH, (Not et al., 2007a)). Cells with positive signals has been observed as unicellular, and contained one or two plastids, the pigments of which are not completely removed by alcohol dehydration steps of FISH (Such pigmentations are only found when phycobilins are present). A single DAPI stained body was observed in the plastid, (in general the plastid DNA was not so condensed) showing that the cells have a reduced nucleus, termed the nucleomorph, similar to that of cryptophytes (Not et al. 2007a). Fig. 4.1 shows a schematic representation of 'picobiliphytes'.

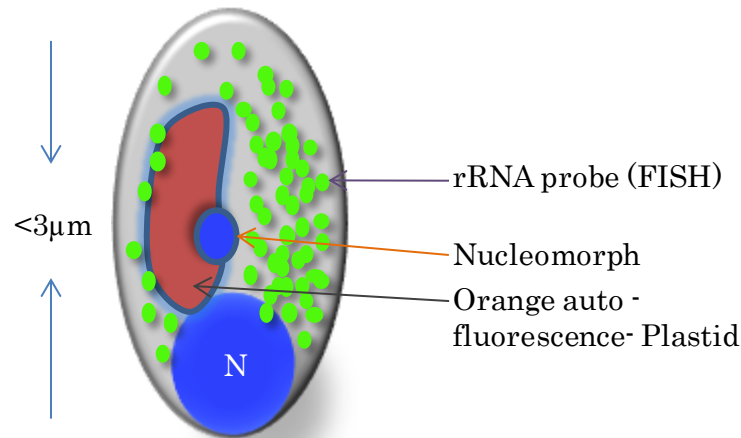


Figure 4.1: Schematic representation of the structure of 'picobiliphytes' according to Not et al., 2007a. The green fluorescence represents FISH by taxon specific probes (PICOBI01/PICOBI02), the orange fluorescence highlights phycobilin in the plastids and the DAPI stains the nucleus (N) and reduced nucleomorph in the plastid/s.

Since the publication of Not et al., 2007a, speculation was rife about the size and structure of the 'picobiliphytes'. The first observations suggested that the cells do harbor plastids (orange fluorescence observed by FISH), but they are bigger than pico-sized, and hence termed 'biliphytes' (Cuvelier et al. 2008). Although the authors showed no FISH images in their study, they recorded 'biliphyte' cells are ranging from $3.5 \pm 0.9 \times 3.0 \pm 0.9 \mu\text{m}$ ($\pm\text{SD}$, $n = 45$), for probe BP2 and $4.1 \pm 1.0 \times 3.5 \pm 0.8 \mu\text{m}$ ($\pm\text{SD}$, $n = 60$), for probe BP1. However, it is hard to estimate the cell size with fluorescence images (fluorescence signals from membrane filters) and thus that the dimensions provided are purely speculative with no further substantial experimental confirmation.

On the contrary, Kim et al. has suggested that 'biliphytes' are not an obligate photoautotrophs but rather facultative mixotrophs or phagotrophs, with any transient detection of orange fluorescence representing ingested prey (e.g., the cyanobacterium *Synechococcus*). The highly punctate phycobilin-like (orange) fluorescence as reported previously (Not et al., 2007a; Cuvelier et al., 2008) was not detected with the hybridized (referring to cells allowed to interact with the fluorochrome) cells. The 'biliphytes' and rappemonads are initially thought to be the same but that rappemonads are not 'biliphytes' (Kim et al. 2011).

The single-cell amplification of various heterotrophic protists by FACS from the Gulf of Maine is indicated that 'picobiliphytes' consisted of a significant fraction in the environment. However, the optical properties of these cells intimated that the absence of phototrophic pigments; therefore, suggests the possibility of a heterotrophic lifestyle (Heywood et al. 2011). Recently, the whole genome amplification for single cell amplified genome (SAG) analysis for three individual cells of 'picobiliphytes' also has not shown any evidence of plastid genes (Yoon et al. 2011) in their genomes. Despite their observation that 'picobiliphytes' are coexisted with single-stranded DNA viruses and bacteria, the DNA of which is

found in their genome data, hypothesised that ‘picobiliphytes’ may once have been photosynthetic (derived from plastid-containing ancestors) as has been suggested for ciliates (Reyes-Prieto et al. 2008) and telonemids (Okamoto et al. 2009).

The plethora of controversies and speculations around the ‘picobiliphytes’ make it highly desirable to resolve the trophic status of these protists. Thus, only by isolating and studying the features (both morphological and functional) of such a cell, the true relationship of its position in the ecosystem can be revealed.

4.2 Abundance and diversity of ‘picobiliphytes’

The reported, abundance of ‘picobiliphytes’ has not only varied with ecophysiological conditions and distributions in the ecosystem, but also has been influenced by the methods are used. Of a total picoeukaryotic cell count in the English Channel, 1.6 % are determined as being ‘picobiliphytes’ (Not et al., 2007a). In two coastal regions of the Atlantic Ocean (Sargasso Sea & Florida current) the ‘biliphytes’ are estimated to contribute, about 28 ± 6 % of total phytoplankton population in the eddy-influenced surface waters (Cuvelier et al. 2008). However, the representation of ‘picobiliphyte’ abundances are biased with the methods are being applied, for e.g. *18S rDNA* clonal library (2.9% ‘picobiliphytes’), which was much less compared to the *18S rRNA* clonal library (12.8%) from the same Mediterranean Sea water sampling site (Not et al. 2009; L. Li et al. 2008). Then again, the ‘picobiliphyte’ sequences obtained by SAG are much higher and efficient than all PCR based approach (17%), as the samples from the same site did not show any ‘picobiliphytes’ sequences in *18S rDNA* clonal library (Heywood et al. 2011). Recurrent sampling for ‘picobiliphytes’ during this study (July to October 2007) in Helgoland sampling Site by sing taxon-specific primers (*PicoBI01F/PicoBI02F*), shown that ‘picobiliphytes’ are frequently encountered at higher level (67% occurrence of total sampling period as PCR positives found elsewhere).

4.3 Molecular approach: an advantage or disadvantage?

Culture-independent *18S rDNA* clonal libraries have been considered as a useful tool for conducting surveys of the microbial population in the biosphere. Whenever, the diversity of plankton community has been investigated using this method, a high degree of new sequences appears (Giovannoni et al., 1988; Amann et al., 1990; Díez et al., 2001; Not et al., 2002; Biegala et al., 2003; Massana et al., 2004; Medlin et al., 2006; Not et al., 2007b). However, this application is significantly skewed by PCR biases by either the high number of copies of the *rDNA* operon or the persistence of DNA in extracellular materials. Thus, alternative methods have been introduced to resolve the better diversity (Not et al. 2009), metagenomics and Single cell Amplified Genome sequences (SAG) (Not et al. 2009; Heywood et al. 2011; Yoon et al. 2011). These methods, alone or in combination can resolve new plankton groups and biodiversity, their resilience and

have also inform the choice of designing taxon-specific probes (rDNA probes). Using these taxon-specific probes, aiding to increase the spectrum of diversity among the specific taxa (phylum, division, class, or genus), and intimating their functional and morphological features by FISH (Simon et al. 1995; Simon et al. 2000; Not et al. 2002; Biegala et al. 2003; Not et al. 2007a; Kim et al. 2011). Although, these techniques are often considered the gold standard for identifying new taxa, they may mislead researchers. At least where in the study of 'picobiliphytes', which at first considered as putative photosynthetic secondary endosymbionts (Not et al. 2007a; Cuvelier et al. 2008), now uncovered as heterotrophic (Kim et al. 2011; Heywood et al. 2011; Yoon et al. 2011).

4.4 Flow cytometry: as an approach for protists

In early 1980s, analytical flow cytometry (AFC) was applied for the first time to phytoplankton cells from sea water. Since then, the application of AFC has increased dramatically to isolate a cell from both marine and fresh water, and subsequently, it has been successfully used to sort the phytoplankton (micro and nano-plankton) and to establish axenic cultures (Veldhuis & Kraay 2000; Gasol & Giorgio 2000; Sensen et al. 1993). AFC has recently been recognized as an important tool for enumeration of picoplankton communities by using their optical properties (Fuller et al. 2006; F. Le Gall et al. 2008; Surek & Melkonian 2004). The use of taxon-specific probes (FISH with rDNA probes) combined with flow cytometry has enhanced population studies and also enabled the visualization of cells (R. I. Amann et al. 1992; Sekar et al. 2004; Not et al. 2002; Biegala et al. 2003). These methods (Flow cytometry using autofluorescence and FISH) are although limited to photosynthetic protists, more recently a novel technique has been used in flow cytometry, enabled the way for sorting of heterotrophic protists too. In this approach, heterotrophic eukaryotic cells are stained with molecular markers (*Lysotracker* - green fluorescence, which stains the food vacuoles) and single cells are sorted against green fluorescence (FL1), and side scatters (SSC) (Heywood et al. 2011). Although, photosynthetic cells can also be stained with *Lysotracker* (due to the presence of a food vacuole), they are easily eliminated by use of their other optical properties in Flow cytometry. Still, the viability of cells sorted by using such markers is unknown. Alternatively, *Mitotracker* GreenFM (Molecular marker, Invitrogen) has also been used to sort not only heterotrophic cells for molecular analysis, but also given the possibility of obtain a clonal culture from it (though, the growth is solely depends on the nutrient requirements of the sorted individual cells). This can be broadly used as a novel approach for sorting uncultivable heterotroph and establishing successful clonal cultures.

4.5 The elusive clonal culture

Fractionated Sea water from Helgoland is enriched by using various culture media. PCR-based identification of enriched cultures has showed only 36 % as positive for 'picobiliphytes' using the PCR approach, but no phycobilin-like autofluorescence either by FACS or FISH are ever detected for the enriched (appendix 6.2). Serial sub-culturing of these PCR-positive enrichments showed a reduction in the percentage of 'picobiliphytes' to the overall plankton. Has any of these enriched cultures harboured any plastids, as suggested in previous studies (Not et al., 2007a; Cuvelier et al., 2008), they would have been successfully sorted by FACS (phycobilin) after enrichment, and their growth would have been steadied in the presence of phototropic medium provided. The results from culturing experiments clearly showed the continuous fall of cell growth over a period of time. Taken together, these results clearly show that 'picobiliphytes' are not autotrophic as reported earlier, but are heterotrophic in nature.

4.5.1 Heterotrophic cell culture

Heterotrophic protists can be isolated either by serial dilution or by capillary pipetting methods (Klaveness et al. 2005). Culturing heterotrophic cell is not as easy as in the case for autotrophs, they predominantly dependent on other cells (two members culturing) for grazing. Most of the contaminants in picobiliphyte' enriched culture are removed by serial dilution, except two *Goniomonas* species (*Goniomonas* sp1, & sp2), which are consistently persistent. Many trails are made to eliminate these contaminants; however they were extremely sturdy in comparison to 'picobiliphytes' or in other hand 'picobiliphytes' sequences were not detected in the absence of *Goinomonas* species. This led to a hypothetical conclusion that; there may be an interaction at cellular level or symbiotic relationship between 'picobiliphytes' and *Goniomonas*. In general, the phagotrophic heterotrophs show high specificity in their feeding preferences. Some feed on algae (eukaryotrophs) for example *Telonema antraticum* feeds on *Rhodomonas* sp (Klaveness et al. 2005); *Katablepharis japonica* and *Leucocryptos marina* feed on the haptophyte *Chrysochromulina* sp. (N Okamoto 2005), while others feed on bacteria (bacteriotrophs) example *Goniomonas* sp. (Martin-Cereceda et al. 2009) and *Palpitomonas bilix* (Yabuki et al. 2010). To determine the cellular or symbiotic interaction between 'picobiliphytes' and *Goniomonas*, FACS-based heterotrophic cell sorting (one cell/well in a 96well plate) has been applied; cells are sorted with forward scatter (FSC) and side scatter (SSC) window. Despite successful isolation of these two contaminants (*Goniomonas* species), neither 'picobiliphyte' cells nor 'picobiliphyte' sequences are not detected in any of these resultant isolates, concluded no such organismal interaction of 'picobiliphytes' with *Goniomonas* species.

The second possibility is that can 'picobiliphytes' grow by feeding on a particulate organic matter from the medium with the presence of *Goniomonas*. In order to obtain enriched growth of 'picobiliphytes', nutrient content has been increased by adding soil extract, leaf extract, rice, wheat and double strength of K

medium, etc., thus increasing organic source. Under these conditions, the *Goniomonas* growth was vigorous, though the 'picobiliphytes' are unable to grow. This resulted that 'picobiliphytes' are dependent on specific organic matter, which could possibly available only in the marine ecosystem, for example marine viruses. The identification of 'picobiliphytes' has become impossible and isolation has also become impractical, despite of constant sub culturing with fresh FSSW, until they were observed by scanning electron microscope. The *PicoPCR*-positive enriched cultures are subjected for complete scanning in SEM and a unique anisokont biflagellate are observed that differed from *Goniomonas* (Fig. 3.11). They found in very low abundance (approx. 1 in 500 other cells) in SEM and that probably accounted for the fact that they are not detected by the light microscope.

To establish the clonal cultures of these unique biflagellate, two alternate approaches are performed to the sample; First with Percoll density gradient centrifugation, which has been successfully used for cell fractionation and organelle isolation in mixed cultures (Putzer et al. 1991; Cho et al. 2002). During in this experiment, unique flagellates are observed in 20 % and 40 % Percoll gradient fraction (Fig. 3. 12b) and these were later confirmed by *PicoPCR* and sequencing. Although, these fractions yielded high numbers of expected flagellates, their subsequent growth development in culture was further inhibited by faster-growing bacterial and *Goniomonas* populations or by an endotoxin from Percoll. *Goniomonas* cells are mainly recovered from the 60 % Percoll fraction, indicating that the 'picobiliphytes' have a less buoyant density than *Goniomonas* but higher than bacteria (Fig. 3.12b). Second approach was by using antibiotics' (β -lactam peptidoglycan inhibitors; i.e. Ampicillin and Carbenicillin), to inhibit the marine bacterial growth (Ferris & Hirsch 1991). This method is employed to restrict the *Goniomonas* growth by restricting bacterial population, and ensure the growth of 'picobiliphytes' does not get affected. As expected, the 'picobiliphytes' are grown under these condition while *Goniomonas* population declined (Fig. 3. 12c). However, using antibiotics may cause mutations thus not recommended for isolation, which may leads to physiological variations of the wild type, the method was dropped for isolating 'picobiliphytes'.

4.5.2 Fluorescence markers

The use of molecular fluorescence markers to target the specific organelles in a cell for sorting picoplankton, in particular, to non-photosynthetic eukaryotes has not been reported until recently. Lysotracker a green fluorescence marker has been used for staining the food vacuole and are sorted marine heterotrophic protists successfully. In these studies, Lysotracker-stained cells are sorted with green fluorescence (FL1) and SSC, and the isolates are sequenced using single-cell amplified genome analysis (SAG) (Heywood et al. 2011; Yoon et al. 2011). However, the viability of such sorted cells in the presence of fluorescent markers has not been investigated so far.

Mitotracker Red CMXRos / GreenFM, (Invitrogen, Pendergrass et al. 2004) is similar type of molecular marker specifically stains the mitochondrion of all eukaryotic cells. The advantage of using Green FM against *Mitotracker* Red

CMXRos is that the GreenFM fluoresces only when it binds to the mitochondrial membrane and no longer retained in the cell which can easily be used for cell sorting with Argon laser under blue excitation (488nm). *Goniomonas* sp. has been used as a model species and *Mitotracker* Green FM has been applied for sorting and to test their viability, the cells were intact as evidenced by their morphology and motility (Fig. 3.14).

Similarly, ‘picobiliphytes’ have also been sorted by using *Mitotracker* Green FM into 96 and 24 well plates. The results has shown that ‘picobiliphytes’ grew faster in the presence of *Goniomonas* than they did in clonal culture, but as mentioned earlier; bacteria are ultimately out-competed the ‘picobiliphytes’ in clonal samples. Both samples are tested positive for ‘picobiliphytes’ using *PicoPCR*, and the establishment of an exclusive clonal culture has proven by using universal eukaryotic 18S rDNA primers and sequencing (appendix 6.4). Subcultures of these cultures are performed every two weeks to maintain them successfully. However, the growth has not been uniform across all conditions (e.g. growth was not consistent in triplicates).

Without further knowledge of the feeding behaviour of ‘picobiliphytes’, the cells are maintained as liquid clonal cultures and that is only possible by frequent transfer using filtered sea water with soil extract.

4.6 Microscopic studies

4.6.1 Light microscopy

The ‘picobiliphyte’ cells (referred to a new genus, ‘*Picomonas*’), as seen using phase contrast optics, are slightly elongated with two hemispherical extremities, and possess two unequal flagella. The use of *Mitotracker* and DAPI staining of *Picomonas* failed to show either plastid-encoded autofluorescence or a nucleomorph as reported by Not et al. 2007a; Cuvelier et al. 2008. The combination of fluorescent staining is shown that the nucleus and mitochondrion are both found in the anterior hemisphere which could be a functional character in identification of this organism.

4.6.2 Electron Microscopy

Electron microscopy studies are used to investigate the *Picomonas* at the ultrastructural level. The scanning electron microscope is shown that the two unequal flagella are inserted on a flat surface of the mid-ventral side of the cell. This is unlike other Hacrobian, where the cells most commonly have an invagination (groove or pocket), and the flagella are inserted on its edge (Okamoto et al. 2009; Yabuki et al. 2010; Heywood 1988). However, heliozoan has a distinct axopodium extending from the centrosome without clear cell invaginations (Yabuki et al. 2012). The flagella are naked, with no flagellar appendages (mastigoneme or non-tubular hairs), which could be considered as a common characteristic of

katablepharids (Okamoto et al. 2009), even though, there is no shared morphological synapomorphy. During flagella shedding, conspicuous flagellar protrusions remain attached to the cell, which is one of the uncommon findings in this cell. Each flagellum has two evident transition plates (tr1 & tr2) and flagella shed at the level of the more distal tr2. The transverse section of tr2 is more constricted than tr1. A recent study focused on the flagellar apparatus among all 'Hacrobian' super-group covered two possible transition regions, on at least one of the two flagellar basal bodies (Yabuki et al. 2012). It is certain that *Palpitomonas* (Yabuki et al. 2010), katablepharids (Okamoto 2005), cryptophytes (Oakley & Dodge 1976; Hibberd David J. 1979) and *Goniomonas* (see appendix 6.8) all display two transition regions in their flagella, with constriction being restricted at the second transition plate (tr2). The Two transition plates are also found in Haptophyta (Yoshida et al. 2006), telonemids (Klaveness et al. 2005; Shalchian-Tabrizi et al. 2006) and Heliozoa (Cavalier-Smith 1993), but the proximal one is inconspicuous and distal might have simplified its transition zone, which is thus likely a common ancestral feature for all Hacrobian (Yabuki et al. 2012), and that possibly includes *Picomonas* within Hacrobia super-group. However, the ultrastructural features of *Picomonas* show little resemblance to other Hacrobian, thus it is very likely independent to other members of Hacrobian. In comparison with cryptophytes, *Picomonas* are never observed with any membrane invagination, ventral furrow, and periplasts-like structures which are characteristic features for cryptomonads (Novarino 2003; Martin-Cereceda et al. 2009).

4.6.3 Ultra-structural character of *Picomonas*

The Ultrastructure of *Picomonas* was analysed in detail by serial ultra-thin sections exploring the distinctive features of the cell. Three dimensional reconstructions of *Picomonas* cells illustrated in Fig. 4.2 and Fig. 6.9. That ventral side is where flagella inserted, dorsal opposite to this. Anterior region is forward facing when the cell swims –direction of anterior (longer) flagellum, posterior side is that contains vacuoles. The Left and right as defined– view from dorsal, the left side is on the left, and the right is on the right (opposite to ventral).

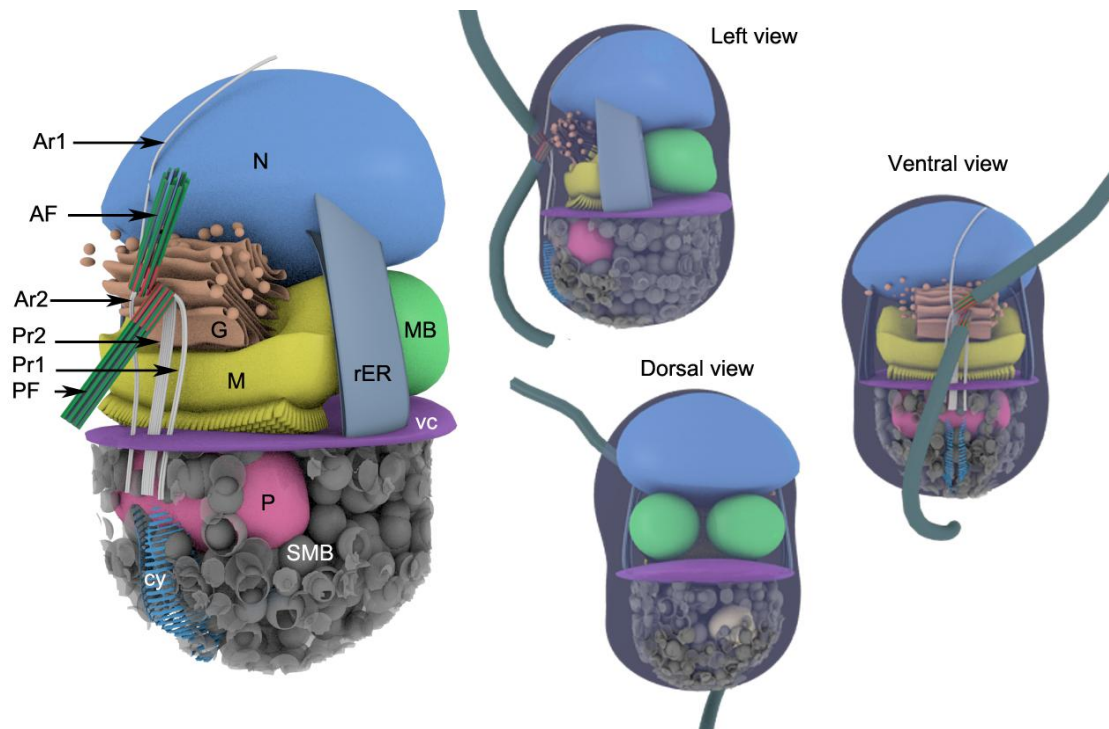


Figure 4.2: 3D model system of *Picomonas* sp. The left view depict all cell components, the ventral view shows all cellular organelles and the arrangement of the basal bodies and the dorsal view with nucleus, and microbodies. AF, Anterior flagellum, PF posterior flagellum, N nucleus, G Golgi body, M Mitochondrion, vc vacuolar cisternae, P posterior digestive part, SMB single membrane vesicles, MB microbody. Ar1&2 and Pr1&2 the flagellar roots arise from anterior and posterior basal body respectively.

In general, all the cell constituents, as expected for flagellates, occupy defined positions in the cell (the only variable feature was the size and content of the posterior-digestive body (P), and the size and number of the microbodies). A single Golgi stack was located inside a groove sandwiched between the nucleus, mitochondrion and flagellar basal bodies. Numerous GA vesicles are observed around the Golgi and near the plasma membrane. Two basal bodies (bb) located on the ventral side, formed an angle exceeding 90° relative to one another and are connected by a proximal connecting fibre. Two transitional septa (plates) in each flagellum is observed, a proximal septum (named tr1) marking the distal end of the basal body where the flagellum emerges from the cell. Interestingly, the central pair of microtubules extended through the distal septum and terminated shortly before reaching the proximal septum, which was not clearly observed among other described hacrobian representatives (Oakley & Dodge 1976; Hibberd David J. 1979; Noriko Okamoto & Inouye 2005; Noriko Okamoto et al. 2009; Yabuki et al. 2010; Yabuki et al. 2012). The hacrobian genera are, however, morphologically distinct and phylogenetically long-branched, but now are considered as one group with one common feature, the distal septum (tr2). The presence of a prominent, fibrous electron-dense matrix in the lumen of both basal bodies is the other distinctive component of *Picomonas* and not observed in other eukaryotes as so condensed.

In *Picomonas* four (non rhizostyle-like) microtubular flagellar roots (two associated with each basal body) are observed. In addition, two more non-microtubular flagellar roots are observed in the microtubular organization centre (MTOC) associated with the posterior basal body. These roots run all the way along the ventral surface in the cell and into the posterior part, where they curve towards the dorsal side and terminate near to a complex apparatus that is reminiscent of a cytostome or the base of an axopodium.

4.7 Novel features of the cell

Picomonas can be characterized microscopically by the presence of certain special features;

1. A peroxisome-like microbody: Each cell contains more than one putative microbody (Fig. 3.24B) located at the dorsal side of the anterior part, extending from the posterior edge of the nucleus to the cleft 'cl'. These specialized structures surrounded by a single membrane may well be vesicles with containing a mucilaginous substance, or the content may be granular and further investigation is required to determine their function.

2. The posterior part: The posterior part (PP) of the *Picomonas* cell consists of a digestive sac (P), 'Single-membrane bodies (SMB)' and 'a cytostome (cy, see below)'. These components are thought to be involved in particulate food intake, and break down and are collectively termed, the posterior part. The 'P' is variable in size, sometimes occupying more than half the volume of the digestive body, and contains single and double-membrane bounded substances, which at present are functionally uncharacterized. The SMB vesicles are thought to be involved in food (prey, detritus or particulate organic matters) transport or membrane recycling. The SF present in the posterior end of the digestive body contains the putative ingestion apparatus (Fig. 3.39, and 4.3).

3. The cleft (cl): This is a membrane-bound vacuolar cisterna that separates the two hemispheres (the anterior part (AP) and the posterior part (PP)). It contains osmiophilic substances. Despite of an intensive search, no typical food vacuoles nor did any ingested bacteria or remnants found. Although bacteria are often encountered close to the sectioned cells and even at times attached to the plasma membrane, they are never found inside the cells.

4.8 Feeding behavior and Food Sources

Whereas the heterotrophic nature of the Picozoa is now beyond doubt, their mode of feeding remains essentially unknown. Kim et al. (2011) speculated that phycoerythrin fluorescence in Picozoa may have been the result of phagotrophic feeding of Picozoa on cyanobacteria, e.g. *Synechococcus* sp., whereas Yoon et al. (2011) discussed the possibility that the reported plastid and nucleomorph (Not, et al. 2007a) may have "come from a kleptoplastid or cryptophyte alga captured as food" by Picozoa. In their study on single-cell amplified genomes of three individual

cells of Picozoa isolated from seawater Yoon et al. (2011) discovered high abundances of specific single-stranded and double-stranded DNA viruses as well as DNA from marine bacteria of the Bacteroidetes, Proteobacteria, and Firmicutes groups. Furthermore, the three cells differed with respect to the associated viruses and bacteria. The authors concluded that they had studied “complex biotic interactions among previously uncharacterized marine microorganisms”, and regarding one cell, a “virus infection captured *in-situ*”, although they did not rule out passive attachment of viral and bacterial DNA to the surface of the cells. In conclusion, Yoon et al. suggested that Picozoa might feed on Proteobacteria, Bacteroidetes and large DNA viruses (Yoon et al. 2011).

Do our electron microscope observations shed light on the feeding behavior and the likely food source of the Picozoa? One of the most unusual structural features of *P. judraskeda* is the subdivision of the cell into two parts, an anterior part housing almost all cell constituents and a posterior part, containing a digestive system including the feeding apparatus. Interestingly both parts are separated by a large vacuolar cisterna that leaves larger spaces only for interaction of the posterior digestive body with the single mitochondrion and for passage of three microtubular flagellar roots that presumably position the cytostome (see Results). We serially sectioned 52 cells, but never encountered an intact or recognizable bacterium within the putative food vacuole inside the feeding apparatus, in the posterior digestive body or in any other part of the cell. Because we fixed a growing culture, we would expect to encounter bacteria, if they were a suitable food source for *P. judraskeda*. Although we cannot exclude the possibility that a specific bacterium, that was not present in our bacterized culture, could serve as a selective food item for *P. judraskeda*, there are other reasons to believe that *P. judraskeda* does not, and in fact cannot, feed on bacteria (feeding of *P. judraskeda* on *Synechococcus* sp. can be excluded, because we never encountered chlorophyll/phycoerythrin autofluorescence in sorted cells that were shown to yield ‘picobiliphyte’-specific DNA after PCR amplification with the respective primers). We apparently fixed cells for electron microscopy at different stages in the feeding cycle as evidenced by the presence or absence of a food vacuole within the feeding basket (see Results). We measured the width of the cytostome (the region marked by the attachment of the fibers of the feeding basket to the plasma membrane) at these different stages in the feeding cycle and found that it did not change, always being around 150 nm. We conclude that the slit-like cytostome is a rigid structure that cannot take up particles that are larger than its width, thus excluding bacteria. This conforms with the peculiar motile behavior of the cells, which is very unlike that of e.g. bacterivorous nanoflagellates (W. K. W. Li 1990; Matz et al. 2002). We propose that *P. judraskeda* feeds on particles smaller than 150 nm that are taken up by a fluid phase, bulk flow mechanism. This generates a single food vacuole of enormous size (it can be estimated that the membrane area of a large food vacuole corresponds to about 30-40% of the total plasma membrane surface of the posterior part of the cell) arguing for rapid membrane turnover.

At present, we can only speculate about the force(s) that initiate the fluid phase flow mechanism. The close association of the posterior flagellum with the cytostome slit (see Results) may indicate that flagellar motility (perhaps during the drag movement) could be involved. Regarding the possible food source, we note that the contents are irregular aggregates of ‘fuzzy’ material that resemble <120 nm marine colloids, which are dispersed widely in seawater (Erken et al. 2012) and may contain lipopolysaccharide material of bacterial membranes (Wells & Goldberg 1991). The Picozoa may thus be specially adapted to exploit < 120 nm marine colloids as a food source. The ‘skedaddle’ movement could then be envisaged not primarily as a phobic response to escape predators, but rather as a mechanism to explore new food resources once grazing at a specific location has depleted resources. The abundance and spatial distribution of marine colloids may also explain the relatively low number of Picozoa that we observed in our culture of *P. judraskeda* (30-40 cells/ml) as well as reported in natural samples using FISH (55 cells/ml in Not et al. 2007a and up to 300 cells/ml in Cuvelier et al. 2008). This also suggests that filter-sterilized seawater (0.1 μm filters) could have been the major source of most of the colloidal food particles necessary to support growth of *P. judraskeda*, although a contribution by the bacterial population is also likely. We assume that the unusual structures observed in the mitochondrion (mitovilli and electron dense inclusions in the intermembrane space) may also be involved in the processing of specific, perhaps mostly lipidic molecules derived from small colloidal food particles. The two prominent microbodies could be involved in the degradation of fatty acids derived from such lipidic molecules.

Could Picozoa perhaps feed on viruses as well as suggested by Yoon et al. (2011)? Viruses constitute the most abundant group of nucleic acid-containing particles in the ocean and up to 10^8 virus particles per ml have been recorded in productive coastal surface waters (Wakeham 2003). Although filtration of natural seawater through 0.1 μm filters would likely exclude the larger size class of marine viruses, the smaller size class (30-60 nm), which is 4- to 10-fold more abundant, would easily pass through a 0.1 μm filter (Suttle 2005). If we assume that *P. judraskeda* feeds on < 150 nm particles by a fluid-phase bulk flow mechanisms, then it is likely that small viruses, such as circular single-stranded DNA viruses (Nanoviridae, Circoviridae; (Dominique Marie et al. 1999)) would be taken up as well. This might explain their prevalence in the single-cell genome amplification of Picozoa (Yoon et al. 2011), although virus particles or DNA attached to the surface of a cell or even co-sorted with such a cell (given the high number of viral particles present in seawater, a sorted droplet of on average 10 picoliters (Rosario et al. 2012), could still contain one or two co-sorted virus particles) should not be dismissed. Although we did not recognize viral particles inside food vacuoles of *P. judraskeda*, we do not exclude the possibility that Picozoa take up small size-class viruses during feeding. Whether these are digested as proposed by Yoon et al. (2011) or exocytosed unaltered during the feeding cycle needs further investigation. We note, however, that the large vacuolar cisterna separating the anterior from the posterior part of the cell would be ideally positioned to prevent access of endocytosed viral particles to the cell’s nucleus.

4.9 Evidence for the new phylum

Phylogenetic analyses of, 18S rDNA sequences (Not et al. 2007a; Cuvelier et al. 2008; Yoon et al. 2011) and of the complete nuclear-encoded rDNA operon ((Kim et al. 2011) & this project) indicate that the ‘picobiliphytes /*Picomonas*’ are highly distinctive and phylogenetically deep-branched eukaryotes, with a weak affinity to eukaryotic super-group, ‘Hacrobia’. However, morphological and ultra-structural evidence shows that they are sufficiently novel to warrant the establishment of a new phylum for these abundant eukaryotic picoplankters.

4.9.1 Justification for a new phylum –Picozoa

The heterotrophic protist *Picomonas judraskeda* gen. nov., sp. nov., described here as a member of a new protist phylum, the Picozoa, has apparently not yet been studied before; the living cell and its morphology by light and electron microscopy were unknown. Gene sequences obtained from environmental clone libraries, however, previously identified a unique pico- or nanoplanktonic eukaryotic lineage that has broad thermal and geographic distribution and became known under the names ‘picobiliphytes’ (Not, et al. 2007a) or ‘biliphytes’ (Cuvelier et al. 2008). Originally envisaged as a novel photosynthetic lineage with affinities to katablepharids/cryptophytes (Not, et al. 2007a, Cuvelier et al. 2008), recent whole-genome shotgun sequence data of three ‘(pico)biliphyte’ cells sorted by FACS from an environmental sample, did not find any evidence of plastid DNA or of nuclear-encoded plastid-targeted genes in these genomes, and concluded that ‘(pico)biliphytes’ were likely heterotrophic (Yoon et al. 2011). All previous phylogenetic studies using environmental sequence comparisons, however, agreed that these organisms comprise a genetically unique and diverse novel eukaryotic group to be delineated at a high taxon level. In the recently proposed revised classification of eukaryotes, ‘(pico)biliphytes’ have been placed into “Incertae sedis Eukaryota” (Adl et al. 2012) and denoted as “Poorly characterized, known only from environmental samples, and no species or genera described.” We established a single cell-derived culture of a ‘(pico)biliphyte’ and characterized it by light and electron microscopy. Our results support the conclusion of Yoon et al. (2011) that these organisms are heterotrophic because no plastids were found. In addition, we revealed a set of highly unusual behavioral and structural features of the cells that to the best of our knowledge have not yet been reported for any other eukaryotic cell. Among these features we list: (1) flagellate cells exhibit a stereotypic pattern of motility consisting of three phases, “jump, drag and skedaddle,” (2) each cell is separated into two parts of almost equal size, an anterior part containing the compartments/organelles typical of a eukaryotic cell, and a posterior part that consists exclusively of vacuoles/vesicles and the feeding apparatus. (3) A single, large vacuolar cisterna physically “seals” both parts of the cell except for a specialized region in which regular projections of the outer mitochondrial envelope, termed “mitovilli,” mediate direct contact between both cell parts. (4) a feeding apparatus consisting of a large basket of fibers that terminate at the ventral cell surface thereby defining the boundaries of a long, slit-like cytostome, which allows formation of a large food vacuole containing only particles of less than 150 nm in

size, (5) finally, three of the four microtubular flagellar roots enter the posterior part of the cell, being closely spaced, and terminate near the anterior end of the cytostome.

All these characteristics of *Picomonas* are sufficient to place this heterotrophic protist into a new phylum, as depicted below

Phylum- Picozoa

Class- Picomondea

Order- Picomonadida

Family- Picomonadidae

Genus- *Picomonas*

Species- *judraskeda* (provisional name)

Etymology: “Pico” (retained the name from “pico”biliphyte) + “monas” (wanderer) refers to pico-sized single cell organism.

“ju” (jumping) + “dra” (dragging) + “skeda” (skedaddle movement) refers to the swimming behaviour of the cell

The classical taxonomical description of *Picomonas judraskeda* (under the International Commission on Zoological Nomenclature -ICZN) has been formally introduced in the original manuscript “Seenivasan et al. 2012, *Picomonas judraskeda* gen. et sp. nov.: the first identified member of the Picozoa phylum nov., a widespread group of picoeukaryotes, formerly known as ‘picobiliphytes’ PLoS ONE (in press).”

The hunt for ‘picobiliphyta’ are rather yielded unexpected results in our findings, these ‘picobiliphyta’ are neither ‘bili’ nor ‘phyta’ and only marginally ‘pico’ considering their high vacuolation properties. Albeit with so much controversy around picobiliphyta, a new phylum named with prefix “Pico” (starved cells are considered) and added “zoa” for its heterotrophic nature hence, a novel name for the phylum, the Picozoa, was created.

4.10 Conclusion

During the last decade, culture-independent molecular surveys based on rDNA clone libraries, phylogenetic analyses, and fluorescence *in-situ* hybridization have revealed numerous novel, high-ranking picoeukaryotic (< 3 μm) lineages in the oceans. This new knowledge is rapidly altering our understanding of marine microbial food webs, and the biogeochemical significance of marine protists (M. Sieracki et al. 2005). Although culture-independent techniques have been essential for the discovery of picoeukaryotic biodiversity, for an understanding of the biology of the organisms involved, they should be complemented by studies of the respective organisms in culture. Here, we provided evidence that a genetically diverse and apparently widespread group of picoeukaryotes in the world's oceans, hitherto known as 'picobiliphytes' or 'biliphytes', and here formally described as Picozoa phylum nov., display highly unusual structural and behavioral characteristics that match their isolated position in the eukaryotic phylogenetic tree. Based on, the characteristics described for *Picomonas judraskeda* gen. nov., sp. nov., we conclude that Picozoa are heterotrophic and feed on small (< 150 nm) particles by a novel fluid-phase, bulk flow uptake mechanism. Further studies on other members of the Picozoa are needed to substantiate this conclusion. We strongly recommend that more effort should be made to cultivate the vast 'uncultured' diversity of eukaryotic microbes in the sea.

5 References

- Adl, S. M., A. G. B. Simpson, M. a Farmer, R. a Andersen, O. R. Anderson, J. R. Barta, S. S. Bowser, G. Brugerolle, R. a Fensome, S. Fredericq, T. Y. James, S. Karpov, P. Kugrens, J. Krug, C. E. Lane, L. a Lewis, J. Lodge, D. H. Lynn, D. G. Mann, R. M. McCourt, L. Mendoza, O. Moestrup, S. E. Mozley-Standridge, T. a Nerad, C. a Shearer, A. V. Smirnov, F. W. Spiegel, and M. F. J. R. Taylor.** 2005. The new higher level classification of eukaryotes with emphasis on the taxonomy of protists. *The Journal of eukaryotic microbiology* **52**:399-451.
- Amann, R. I., B. Zarda, D. a Stahl, and K. H. Schleifer.** 1992. Identification of individual prokaryotic cells by using enzyme-labeled, rRNA-targeted oligonucleotide probes. *Applied and environmental microbiology* **58**:3007-11.
- Amann, R. I., L. Krumholz, and D. A. Stahl.** 1990. Fluorescent-oligonucleotide probing of whole cells for determinative, phylogenetic, and environmental studies in microbiology. *Journal Of Bacteriology. Am Soc Microbiol* **172**:762-770.
- Bassøe, C.-F., N. Li, K. Ragheb, G. Lawler, J. Sturgis, and J. P. Robinson.** 2003. Investigations of phagosomes, mitochondria, and acidic granules in human neutrophils using fluorescent probes. *Cytometry. Part B, Clinical cytometry* **51**:21-9.
- Biegala, I. C., F. Not, D. Vaultot, N. Simon, and M. Curie.** 2003. Quantitative Assessment of Picoeukaryotes in the Natural Environment by Using Taxon-Specific Oligonucleotide Probes in Association with Tyramide Signal Amplification-Fluorescence In Situ Hybridization and Flow Cytometry. *Society* **69**:5519-5529.
- Buchmann, K., and B. Becker.** 2009. The system of contractile vacuoles in the green alga *Mesostigma viride* (Streptophyta). *Protist. Elsevier* **160**:427-43.
- Cavalier-Smith, T.** 1993. The Protozoan Phylum Opalozoa. *The Journal of Eukaryotic Microbiology* **40**:609-615.
- Cavalier-Smith, T.** 2004. Only six kingdoms of life. *Proceedings. Biological sciences / The Royal Society* **271**:1251-62.
- Cavalier-Smith, T., and E. E.-Y. Chao.** 2003. Molecular phylogeny of centrohelid heliozoa, a novel lineage of bikont eukaryotes that arose by ciliary loss. *Journal of molecular evolution* **56**:387-96.
- Cho, J.-young, J.-suk Choi, I.-soo Kong, S.-il Park, and R. G. Kerr.** 2003. A procedure for axenic isolation of the marine microalga *Isochrysis galbana* from heavily contaminated mass cultures. *Journal of Applied Phycology* 385-390.
- Cuvelier, M. L., A. Ortiz, E. Kim, H. Moehlig, D. E. Richardson, J. F. Heidelberg, J. M. Archibald, and A. Z. Worden.** 2008. Widespread distribution of a unique marine protistan lineage. *Environmental microbiology* **10**:1621-34.
- Díez, B., C. Pedrós-Alió, and R. Massana.** 2001. Study of Genetic Diversity of Eukaryotic Picoplankton in Different Oceanic Regions by Small-Subunit rRNA Gene Cloning and Sequencing. *Applied and Environmental Microbiology. American Society for Microbiology* **67**:2932-2941.
- Doyle J. J., Doyle J. L.** 1990. Isolation of plant DNA from fresh tissue. *Focus* **12**:13–15.

- Doyle, J. J., and J. L. Doyle.** 1990. Isolation of plant DNA from fresh tissue. *Focus* **12**:13-15.
- Drebes, G., and D. Schulz.** 1989. *Anaulus australis* sp. nov. (Centrales, Bacillariophyceae), a new marine surf zone diatom, previously assigned to *A. birostratus* (Grunow) Grunow. *Botanica Marina. De Gruyter* **32**:53-64.
- Elwood H. J., Olsen G. J., Sogin M. L.** 1985. The small-subunit ribosomal RNA gene sequences from the hypotrichous ciliates *Oxytricha nova* and *Stylonychia pustulata*. *Molecular biology and evolution* **2**:399-410.
- Eppley, R., F. Reid, and J. Strickland.** 1970. The ecology of the plankton off La Jolla, California, in the period April through September, 1967. *Bulletin of the Scripps Institution of Oceanography* **17**:33.
- Erken M., Farrenschon N., Speckmann S., Arndt H., Weitere M.** 2012. Quantification of Individual Flagellate - Bacteria Interactions within Semi-natural Biofilms. *Protist In Press*:632-42.
- Ferris, M. J., and C. F. Hirsch.** 1991. Cyanobacteria Method for Isolation and Purification of Cyanobacteria. *Applied and Environmental Microbiology* **57**:1448.
- Fuhrman, J. A., and G. B. McManus.** 1984. Do bacteria-sized eukaryotes consume significant bacterial production? *Science* **224**:1257-1260.
- Fuller, N., C. Campbell, D. Allen, F. Pitt, K. Zwirgmaier, F. Le Gall, D. Vaultot, and D. Scanlan.** 2006. Analysis of photosynthetic picoeukaryote diversity at open ocean sites in the Arabian Sea using a PCR biased towards marine algal plastids. *Aquatic Microbial Ecology* **43**:79-93.
- Gasol, J. M., and P. A. D. E. L. Giorgio.** 2000. Using flow cytometry for counting natural planktonic bacteria and understanding the structure of planktonic bacterial communities *. *Methods In Cell Biology* **64**:197-224.
- Geimer, S., and M. Melkonian.** 2004. The ultrastructure of the *Chlamydomonas reinhardtii* basal apparatus: identification of an early marker of radial asymmetry inherent in the basal body. *Journal of cell science* **117**:2663-74.
- Giovannoni, S. J., E. F. DeLong, G. J. Olsen, and N. R. Pace.** 1988. Phylogenetic group-specific oligodeoxynucleotide probes for identification of single microbial cells. *Journal Of Bacteriology. Am Soc Microbiol* **170**:720-726.
- Gonzalez, J. M., and C. A. Suttle.** 1993. virus-sized particles : ingestion and digestion. *Marine Ecology Progress Series* **94**:1-10.
- Heywood, J. L., M. E. Sieracki, W. Bellows, N. J. Poulton, and R. Stepanauskas.** 2011. Capturing diversity of marine heterotrophic protists: one cell at a time. *The ISME journal. Nature Publishing Group* **5**:674-84.
- Heywood, P.** 1988. Ultrastructure of *Chilomonas paramecium* and the phylogeny of the cryptoprotists. *Bio Systems* **21**:293-8.
- Hibberd David J.** 1979. THE STRUCTURE AND PHYLOGENETIC SIGNIFICANCE OF THE FLAGELLAR TRANSITION REGION IN THE CHLOROPHYLL c-CONTAINING ALGAE. *Biosystems* **11**:243-261.

- Hoef-Emden, K., and M. Melkonian.** 2003. Revision of the Genus *Cryptomonas* (Cryptophyceae): a Combination of Molecular into a Long-Hidden Dimorphism. *October* **154**:371-409.
- Hoef-Emden, K., B. Marin, and M. Melkonian.** 2002. Nuclear and nucleomorph SSU rDNA phylogeny in the Cryptophyta and the evolution of cryptophyte diversity. *Journal of molecular evolution* **55**:161-79.
- Inouye, I., and N. Okamoto.** 2005. Changing concepts of a plant : current knowledge on plant. *Plant Biotechnology* **514**:505-514.
- Jeong, H. J., K. A. Seong, Y. D. Yoo, T. H. Kim, N. S. Kang, S. Kim, J. Y. Park, J. S. Kim, G. H. Kim, and J. Y. Song.** 2008. Feeding and grazing impact by small marine heterotrophic dinoflagellates on heterotrophic bacteria. *The Journal of eukaryotic microbiology.* Lawrence, Kan.: Society of Protozoologists, c1993- **55**:271-288.
- Jürgens, K., and R. Massan.** 2008. Protist grazing on marine bacterioplankton. *Microbial Ecology of the Oceans*, Second edn.
- Karsten U., Schumann R., Rothe S., Jung I., Medlin L.** 2006. Temperature and light requirements for growth of two diatom species (Bacillariophyceae) isolated from an Arctic macroalga. *Polar Biology* **29**:476–486.
- Keller, M. D., R. C. Selvin, W. Claus, and R. R. L. Guillard.** 1987. Media for the culture of oceanic ultraphytoplankton. *Journal of Phycology* **23**:633-638.
- Kim, E., J. W. Harrison, S. Sudek, M. D. M. Jones, H. M. Wilcox, T. a Richards, A. Z. Worden, and J. M. Archibald.** 2011. Newly identified and diverse plastid-bearing branch on the eukaryotic tree of life. *Proceedings of the National Academy of Sciences of the United States of America* **108**:1496-500.
- Klaveness, D., K. Shalchian-Tabrizi, H. A. Thomsen, W. Eikrem, and K. S. Jakobsen.** 2005. *Telonema antarcticum* sp. nov., a common marine phagotrophic flagellate. *International journal of systematic and evolutionary microbiology* **55**:2595-604.
- Le Gall, F., F. Rigaut-Jalabert, D. Marie, L. Garczarek, M. Viprey, a Gobet, and D. Vaultot.** 2008. Picoplankton diversity in the South-East Pacific Ocean from cultures. *Biogeosciences* **5** 203-14.
- Lepère, C., D. Vaultot, and D. J. Scanlan.** 2009. Photosynthetic picoeukaryote community structure in the South East Pacific Ocean encompassing the most oligotrophic waters on Earth. *Environmental microbiology* **11**:3105-17.
- Li, L., Q. Huang, S. Wu, D. Lin, J. Chen, and Y. Chen.** 2008. The spatial and temporal distribution of microalgae in the South China Sea: evidence from GIS-based analysis of 18S rDNA sequences. *Science in China. Series C, Life sciences / Chinese Academy of Sciences* **51**:1121-8.
- Li, W. K. W.** 1994. Primary production of prochlorophytes, cyanobacteria, and eucaryotic ultraphytoplankton: Measurements from flow cytometric sorting. *Limnology And Oceanography.* The American Society of Limnology and Oceanography **39**:169-175.
- Liu, H., I. Probert, J. Uitz, H. Claustre, S. Aris-Brosou, M. Frada, F. Not, and C. de Vargas.** 2009. Extreme diversity in noncalcifying haptophytes explains a major pigment paradox

- in open oceans. Proceedings of the National Academy of Sciences of the United States of America **106**:12803-8.
- Loeblich, A. R., and V. E. Smith.** 1968. Chloroplast pigments of the marine dinoflagellate *Gyrodinium resplendens*. Lipids **3**:5-13.
- Lovejoy, C., R. Massana, and C. Pedro.** 2006. Diversity and Distribution of Marine Microbial Eukaryotes in the Arctic Ocean and Adjacent Seas †‡. APPLIED AND ENVIRONMENTAL MICROBIOLOGY **72**:3085-3095.
- Martin-Cereceda, M., E. C. Roberts, E. C. Wootton, E. Bonaccorso, P. Dyal, A. Guinea, D. Rogers, C. J. Wright, and G. Novarino.** 2009. Morphology, ultrastructure, and small subunit rDNA phylogeny of the marine heterotrophic flagellate *Goniomonas* aff. *amphinema*. The Journal of eukaryotic microbiology **57**:159-70.
- Massana, R., M. Pernice, J. A. Bunge, and J. Del Campo.** 2011. Sequence diversity and novelty of natural assemblages of picoeukaryotes from the Indian Ocean. The ISME journal. Nature Publishing Group **5**:184-195.
- Massana, R., V. Balagué, L. Guillou, and C. Pedrós-Alió.** 2004. Picoeukaryotic diversity in an oligotrophic coastal site studied by molecular and culturing approaches. FEMS microbiology ecology **50**:231-43.
- Matz C., Boenigk J., Arndt H., Jürgens K.** 2002. Role of bacterial phenotypic traits in selective feeding of the heterotrophic nanoflagellate *Spumella* sp. Aquatic Microbial Ecology **27**:137–148.
- Medlin L., Elwood H. J., Stickel S., Sogin M.L.** 1988. The characterization of enzymatically amplified eukaryotic 16S-like rRNA-coding regions. Gene **71**:491–9.
- Medlin, L. K., K. Metfies, H. Mehl, K. Wiltshire, and K. Valentin.** 2006. Picoeukaryotic plankton diversity at the Helgoland time series site as assessed by three molecular methods. Microbial ecology **52**:53-71.
- Moestrup, O., and M. Sengco.** 2001. Ultrastructural Studies on *Bigelowiella Natans*, Gen. Et Sp. Nov., a Chlorarachniophyte Flagellate. Journal of Phycology **37**:624-646.
- Moon-Van Der Staay, S. Y., R. De Wachter, and D. Vault.** 2001. Oceanic 18S rDNA sequences from picoplankton reveal unsuspected eukaryotic diversity. Nature. Nature Publishing Group **409**:607-610.
- Not, F., J. Del Campo, V. Balagué, C. De Vargas, and R. Massana.** 2009. New Insights into the Diversity of Marine Picoeukaryotes. PLoS ONE. Public Library of Science **4**:7.
- Not, F., K. Valentin, K. Romari, and C. Lovejoy.** 2007a. Picobiliphytes: a marine picoplanktonic algal group with unknown affinities to other eukaryotes. Science (New York, N.Y.) **315**, 253.
- Not, F., N. Simon, I. C. Biegala, and D. Vault.** 2002. Application of fluorescent in situ hybridization coupled with tyramide signal amplification (FISH-TSA) to assess eukaryotic picoplankton composition. Aquatic Microbial Ecology **28**:157-166.
- Not, F., R. Gausling, F. Azam, J. F. Heidelberg, and A. Z. Worden.** 2007b. Vertical distribution of picoeukaryotic diversity in the Sargasso Sea. Environmental Microbiology. Wiley Online Library **9**:1233-1252.

- Novarino, G.** 2003. A companion to the identification of cryptomonad flagellates (Cryptophyceae = Cryptomonadea). *Hydrobiologia* **502**:225-270.
- Oakley, B. R., and J. D. Dodge.** 1976. The Ultrastructure of Mitosis in *Chroomonas salina* (Cryptophyceae). *Protoplasma* **88**:241-254.
- Okamoto, N.** 2005. The Katablepharids are a Distant Sister Group of the Cryptophyta: A Proposal for Katablepharidophyta Divisio Nova/Kathablepharida Phylum Novum Based on SSU rDNA and Beta-Tubulin Phylogeny. *Protist* **156**:163-179.
- Okamoto, N., and I. Inouye.** 2005. A Secondary Symbiosis in Progress? *October* **310**:2005-2005.
- Okamoto, N., C. Chantangsi, A. Horák, B. S. Leander, and P. J. Keeling.** 2009. Molecular Phylogeny and Description of the Novel Katablepharid *Roombia truncata* gen. et sp. nov., and Establishment of the Hacrobia Taxon nov. *PLoS ONE. Public Library of Science* **4**:11.
- Pace, N. R.** 1997. A Molecular View of Microbial Diversity and the Biosphere. *Science. AAAS* **276**:734-740.
- Parfrey, L. W., E. Barbero, E. Lasser, M. Dunthorn, D. Bhattacharya, D. J. Patterson, and L. a Katz.** 2006. Evaluating support for the current classification of eukaryotic diversity. *PLoS genetics* **2**:e220.
- Pendergrass, W., N. Wolf, and M. Poot.** 2004. Efficacy of *Mitotracker* Green and CMXrosamine to measure changes in mitochondrial membrane potentials in living cells and tissues. *Cytometry. Part A : the journal of the International Society for Analytical Cytology* **61**:162-9.
- Putzer, K. P., L. a Buchholz, M. E. Lidstrom, and C. C. Remsen.** 1991. Separation of methanotrophic bacteria by using percoll and its application to isolation of mixed and pure cultures. *Applied and environmental microbiology* **57**:3656-9.
- Reyes-Prieto, A., A. Moustafa, and D. Bhattacharya.** 2008. Multiple genes of apparent algal origin suggest ciliates may once have been photosynthetic. *Curr Biol.* **18**:956-962.
- Romari, K., and D. Vaultot.** 2004. Composition and temporal variability of picoeukaryote communities at a coastal site of the English Channel from 18S rDNA sequences. *Limnology And Oceanography. JSTOR* **49**:784-798.
- Rosario K., Duffy S., Breitbart M.** 2012. A field guide to eukaryotic circular single-stranded DNA viruses: insights gained from metagenomics. *Archives of Virology.*
- Seenivasan R., Sausen N., Medlin L. K., Melkonian M.** 2012, *Picomonas judraskeda* gen. et sp. nov.: the first identified member of the Picozoa phylum nov., a widespread group of picoeukaryotes, formerly known as 'picobiliphytes' *PLoS ONE* (in press).
- Sekar, R., B. M. Fuchs, R. Amann, and J. Pernthaler.** 2004. Flow Sorting of Marine Bacterioplankton after Fluorescence In Situ Hybridization. *Society* **70**:6210-6219.
- Sensen, C. W., K. Heimann, and M. Melkonian.** 1993. The production of clonal and axenic cultures of microalgae using fluorescence-activated cell sorting. *European Journal of Phycology* **28**:93-97.

- Sieracki M., Poulton N., Crosbie N.** 2005. Automated isolation techniques for microalgae. In Andersen RA (Ed) *Algal Culturing Techniques*, p. 101–116. *In* Elsevier, Burlington MA.
- Simon, N., L. Campbell, E. Ornofsdottir, R. Groben, L. Guillou, M. Lange, and L. K. Medlin.** 2000. Oligonucleotide probes for the identification of three algal groups by dot blot and fluorescent whole-cell hybridization. *The Journal of eukaryotic microbiology* **47**:76-84.
- Simon, N., N. LeBot, D. Marie, F. Partensky, and D. Vaultot.** 1995. Fluorescent in situ hybridization with rRNA-targeted oligonucleotide probes to identify small phytoplankton by flow cytometry. *Applied and environmental microbiology* **61**:2506-13.
- Stamatakis, A.** 2006. RAxML-VI-HPC: maximum likelihood-based phylogenetic analyses with thousands of taxa and mixed models. *Bioinformatics (Oxford, England)* **22**:2688-90.
- Stepanuskas, R., and M. E. Sieracki.** 2007. Matching phylogeny and metabolism in the uncultured marine bacteria, one cell at a time. *Proceedings of the National Academy of Sciences of the United States of America* **104**:9052-7.
- Stockner, J. G., and N. J. Antia.** 1986. Algal picoplankton from marine and freshwater ecosystems: A multidisciplinary perspective. *Canadian Journal of Fisheries and Aquatic Sciences*. NRC Research Press **43**:2472-2503.
- Surek, B., and M. Melkonian.** 2004. CCAC – Culture Collection of Algae at the University of Cologne: A new collection of axenic algae with emphasis on flagellates. *Nova Hedwigia* **79**:77-92.
- Suttle C. A.** 2005. Viruses in the sea. *Nature* **437**:356–361.
- Thomas, P., and H. Arndt.** 1996. Uptake of sub-micrometre- and micrometre-sized detrital particles by bacterivorous and omnivorous ciliates. *Aquatic Microbial Ecology* **10**:45-53.
- Tobe, K., L. K. Medlin, and G. Eller.** 2006. Automated detection and enumeration for toxic algae by solid-phase cytometry and the introduction of a new probe for *Prymnesium parvum* (Haptophyta: Prymnesiophyceae). *Journal of Plankton Research* **28**:643-657.
- Vaultot, D., F. L. Gall, D. Marie, L. Guillou, and F. Partensky.** 2004. The Roscoff Culture Collection (RCC): a collection dedicated to marine picoplankton. *Nova Hedwigia* **79**:49-70.
- Veldhuis, M. J. W., and G. W. Kraay.** 2000. Application of flow cytometry in marine phytoplankton research: current applications and future perspectives. *In Vivo*. Consejo Superior de Investigaciones Cientificas **64**:121-134.
- Vigil, P., P. Countway, J. Rose, D. Lonsdale, C. Gobler, and D. A. Caron.** 2009. Rapid shifts in dominant taxa among microbial eukaryotes in estuarine ecosystems. *Aquatic Microbial Ecology*. Inter-Research, Nordbunte 23 Oldendorf/Luhe 21385 Germany, **54**:83-100.
- Wakeham S.** 2003. Hydroxy fatty acids in marine dissolved organic matter as indicators of bacterial membrane material. *Organic Geochemistry* **34**:857–868.
- Wells M. L., Goldberg E. D.** 1991. Occurrence of small colloids in sea water. *Nature* **353**:342–344.

- Woyke, T., G. Xie, A. Copeland, J. M. González, C. Han, H. Kiss, J. H. Saw, P. Senin, C. Yang, S. Chatterji, J.-F. Cheng, J. a Eisen, M. E. Sieracki, and R. Stepanauskas.** 2009. Assembling the marine metagenome, one cell at a time. *PloS one* **4**:e5299.
- Yabuki, A., E. E. Chao, K.-ichiro Ishida, and T. Cavalier-smith.** 2011. *Microheliella maris* (Microhelida ord . n .), an Ultrastructurally Highly Distinctive New Axopodial Protist Species and Genus , and the Unity of Phylum Heliozoa. *Protist*. Elsevier **163**: 356-388.
- Yabuki, A., Y. Inagaki, and K.-ichiro Ishida.** 2010. *Palpitomonas bilix* gen. et sp. nov.: A novel deep-branching heterotroph possibly related to Archaeplastida or Hacrobia. *Protist*. Elsevier **161**:523-38.
- Yoon, H. S., D. C. Price, R. Stepanauskas, V. D. Rajah, M. E. Sieracki, W. H. Wilson, E. C. Yang, S. Duffy, and D. Bhattacharya.** 2011. Single-cell genomics reveals organismal interactions in uncultivated marine protists. *Science (New York, N.Y.)* **332**:714-7.
- Yoshida, M., M.-H. Noël, T. Nakayama, T. Naganuma, and I. Inouye.** 2006. A haptophyte bearing siliceous scales: ultrastructure and phylogenetic position of *Hyalolithus neolepis* gen. et sp. nov. (Prymnesiophyceae, Haptophyta). *Protist* **157**:213-34.
- Zhu, F., R. Massana, F. Not, D. Marie, and D. Vaultot.** 2005. Mapping of picoeucaryotes in marine ecosystems with quantitative PCR of the 18S rRNA gene. *FEMS microbiology ecology* **52**:79-92.

6 Appendix

6.1 Sample collection in Helgoland time series station (Helgoland reede)

Field sample are collected in Helgoland time series site from July-October 2007 which shown in table 5.1. The samples are fractionated with series of membrane filters and 3 μm filtered sea water are filtered on 0.2 μm filter for genomic DNA extraction. Genomic DNA from these filed samples was used for PCR in search of 'picobiliphytes'. Table 6.2 shows the number of 'picobiliphyte' positives for environmental sample in Helgoland station.

Field samples from July 2007 to October 2007	
1. Pico070716	29. Pico070910
2. Pico070717	30. Pico070912
3. Pico070718	31. Pico070914
4. Pico070719	32. Pico070917
5. Pico070731	33. Pico070919
6. Pico070801	34. Pico070921
7. Pico070802	35. Pico070924
8. Pico070803	36. Pico070927
9. Pico070806	37. Pico071001
10. Pico070807	38. Pico071002
11. Pico070808	39. Pico071004
12. Pico070809	40. Pico071005
13. Pico070814	41. Pico071008
14. Pico070815	42. Pico071009
15. Pico070816	43. Pico071010
16. Pico070817	44. Pico071011
17. Pico070820	45. Pico071012
18. Pico070821	46. Pico071017
19. Pico070822	47. Pico071019
20. Pico070823	48. Pico071022
21. Pico070824	49. Pico071023
22. Pico070827	50. Pico071024
23. Pico070828	51. Pico071025
24. Pico070829	52. Pico071026
25. Pico070830	53. Pico071029
26. Pico070903	54. Pico071030
27. Pico070905	55. Pico071031
28. Pico070907	M- 1kb ladder
	M1- I/HindIII/EcoRI

Table 6.1: Total sample collection at Helgoland time series station between July to October 2007

Slno	Sample ID	PCR positive	Slno	Sample ID	PCR positive
1	Pico070710	+	23	Pico070823	+
2	Pico070711	+	24	Pico070829	+
3	Pico070716	+	25	Pico070910	+
4	Pico070717	+	26	Pico070912	+
5	Pico070718	+	27	Pico070914	+
6	Pico070719	+	28	Pico070919	+
7	Pico070720	+	29	Pico070927	+
8	Pico070723	+	30	Pico071001	+
9	Pico070724	+	31	Pico071002	+
10	Pico070725	+	32	Pico071004	+
11	Pico070726	+	33	Pico071005	+
12	Pico070727	+	34	Pico071008	+
13	Pico070806	+	35	Pico071009	+
14	Pico070807	+	36	Pico071010	+
15	Pico070808	+	37	Pico071011	+
16	Pico070809	+	38	Pico071012	+
17	Pico070813	+	39	Pico071023	+
18	Pico070814	+	40	Pico071024	+
19	Pico070815	+	41	Pico071025	+
20	Pico070816	+	42	Pico071026	+
21	Pico070817	+	43	Pico071030	+
22	Pico070821	+			

Table 6.2: PCR positive samples for 'picobiliphytes' in the environment samples, out of 55 filed collection 43 samples showed positive to Taxon specific primers (PicoBI01R and PicoBI02R) indicated 'picobiliphytes' are widely distributed during summer and fall.

6.2 'Picobiliphytes' from enriched cultures

'Picobiliphyte' cells are searched in enriched cultures from K (Keller et al. 1987), GP5 (Loeblich & Smith 1968), IMR (Eppley et al. 1970), Drebes (Drebes & Schulz 1989) by 'picobiliphyte' specific PCR. Not, all showed 'picobiliphyte' positive to PCR amplification with specific primers. Table 6.3 shows the number of positive samples for different enriched flasks and different collection time. Results showed that 'picobiliphyte' are present in all media which was used. The positive flask are used for further analysis like cell sorting, TSA-FISH.

Sno	Sample ID	PCR positive	Culture positives with picoprimer			
			K	GP5	IMR	Drebes
1	Pico070710	+				
2	Pico070711	+				+
3	Pico070716	+		+	+	+
4	Pico070717	+	+	+	+	
5	Pico070718	+	+	+		
6	Pico070719	+				
7	Pico070720	+				+
8	Pico070723	+				+
9	Pico070724	+				
10	Pico070725	+				
11	Pico070726	+				
12	Pico070727	+				
13	Pico070806	+				+
14	Pico070807	+		+		+
15	Pico070808	+			+	
16	Pico070809	+	+	+	+	
17	Pico070813	+				+
18	Pico070814	+		+	+	+
19	Pico070815	+	+	+	+	+
20	Pico070816	+			+	
21	Pico070817	+				+
22	Pico070821	+		+		
23	Pico070823	+	+	+		
24	Pico070829	+				
25	Pico070910	+				
26	Pico070912	+				
27	Pico070914	+	+			
28	Pico070919	+		+		+
29	Pico070927	+	+		+	
30	Pico071001	+	+			+
31	Pico071002	+	+			
32	Pico071004	+		+		+
33	Pico071005	+	+			
34	Pico071008	+		+		
35	Pico071009	+			+	+
36	Pico071010	+	+	+	+	+
37	Pico071011	+				
38	Pico071012	+	+	+	+	+
39	Pico071023	+			+	
40	Pico071024	+				+
41	Pico071025	+	+		+	
42	Pico071026	+		+		+
43	Pico071030	+	+	+		+

Table 6.3: Taxon specific primers applied to search for 'picobiliphytes' form enriched samples; and the result showed, about 36% of the samples are turned Positives. These positive samples are used in FACS and in search of phycoerythrin autofluorescence (FL2)

'Picobiliphyte' positive flasks are re-transferred into new medium and the remains are used for cell sorting targeting its orange autofluorescence (Phycobilin contain Phycoerythrin) as mentioned by Not et al. 2007a. Cells are in 96 well plates for further enrichment, and also sorted directly into PCR tube for 'picobiliphyte' specific PCR amplification (many regions are used in FACS for sorting to understand the region where 'picobiliphytes' will be grouped). However the data showed that not only 'picobiliphytes' are grown further in flasks but also failed show their autofluorescence in FACS. TSA-FISH experiments for both on membrane filter (cells on 0.2 μm membrane filter) and the sorted cells are inconclusive. In addition, high orange fluorescence or phycoerythrin (PE) containing cells (Fig. 6.1A & B) are failed to amplify with 'picobiliphyte' specific primers, indicated that 'picobiliphytes' may not be having photosynthetic organelles.

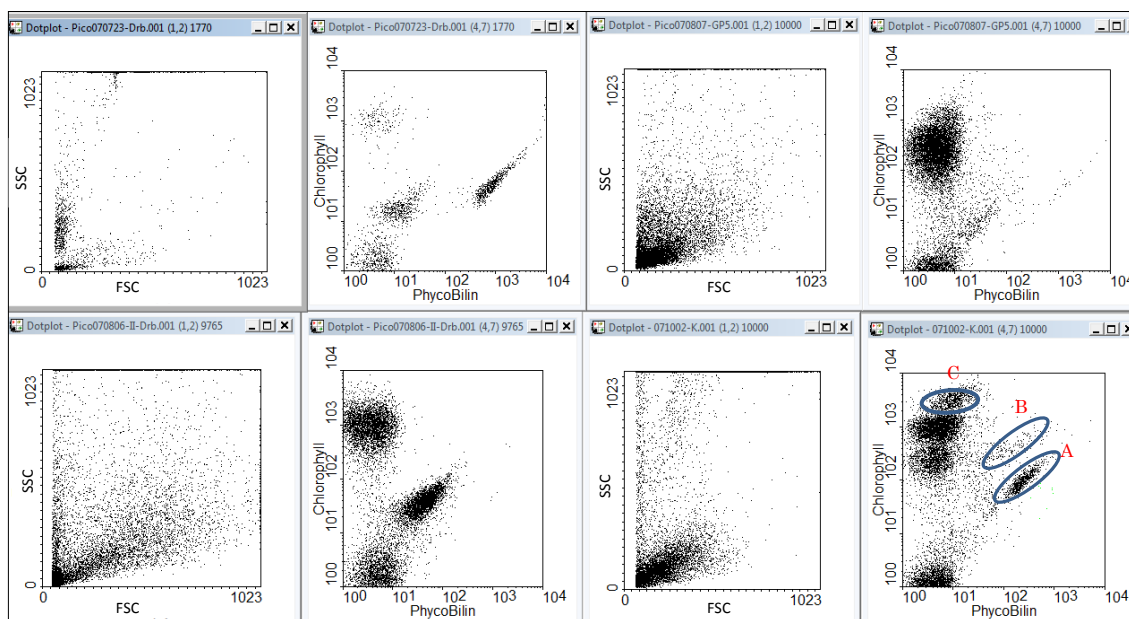


Figure 6.1: Positive samples from enriched culture are subjected to cell sorting against all possible fields as shown in the cytograms like Forward scatters (FSC), Side scatters (SSC), chlorophyll (FL3) and Phycoerythrin (PE) /Phycobilin (FL2). However, the results showed that 'picobiliphytes' never observed in PE fractions (A, B), in addition, the cell sorted from other regions are also failed to show 'picobiliphytes' in PCR (C).

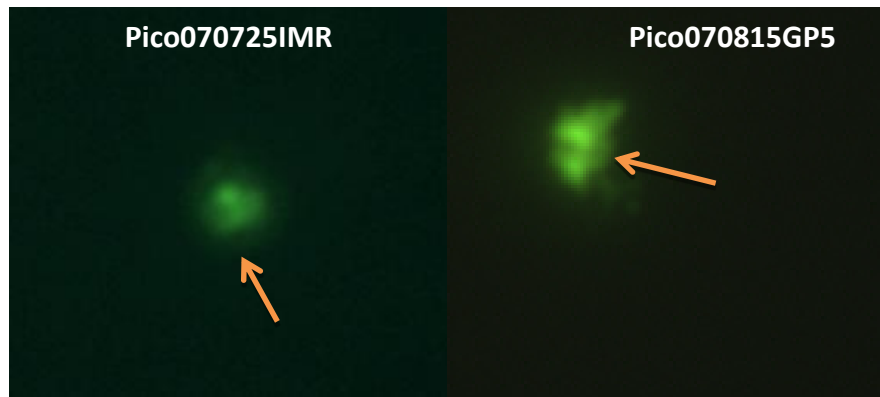


Figure 6.2: TSA-FISH reaction for cells filtered on 0.2µm membrane with taxon specific probes (PicoBI01 and PicoBI02). Few cells showed green fluorescence for probes, however, neither DAPI nuclear body nor orange autofluorescence (phycobilin) observed on these cells.

6.3 Specificity of ‘picobiliphytes’

In order to understand the ‘picobiliphyte’ specificity, the ITS region was amplified from environmental samples with *PicoBi01F* (clade I & II, Not et al. 2007a) and 28S large subunit primer L52R. The 2.5kb amplified PCR product was cloned into pGEM-TEasy vector. Positive clones are then sequenced and non-redundant sequences are used for alignment. In addition ‘picobiliphyte’ specific ITS primers (PicoITS1F/1R, PicoITS1FII/1RII and PicoITS2F/2R) are designed to enhance the specific ‘picobiliphyte’ sequences from environmental samples.



Figure 6.3a: Schematic diagram of primers (PicoBi01F/L52R) used for construction of Taxon specific clonal library construction.

Sequence alignments for ITS region and ‘picobiliphyte’ specific ITS primers are shown below.

6.4 Sequence comparison of *Picomonas* clonal culture

Chromatogram for three *Picomonas* clonal cultures (2, 3 & 4) established show clean peaks for nucleotides, from common eukaryotic 18S rDNA primers and sequence of these cultures showed high similarities with 'picobiliphyte' environmental sequences (Not et al., 2007a). The chromatogram 1 shows contamination from two membrane culture (*Picomonas* and *Goniomonas* sp2).

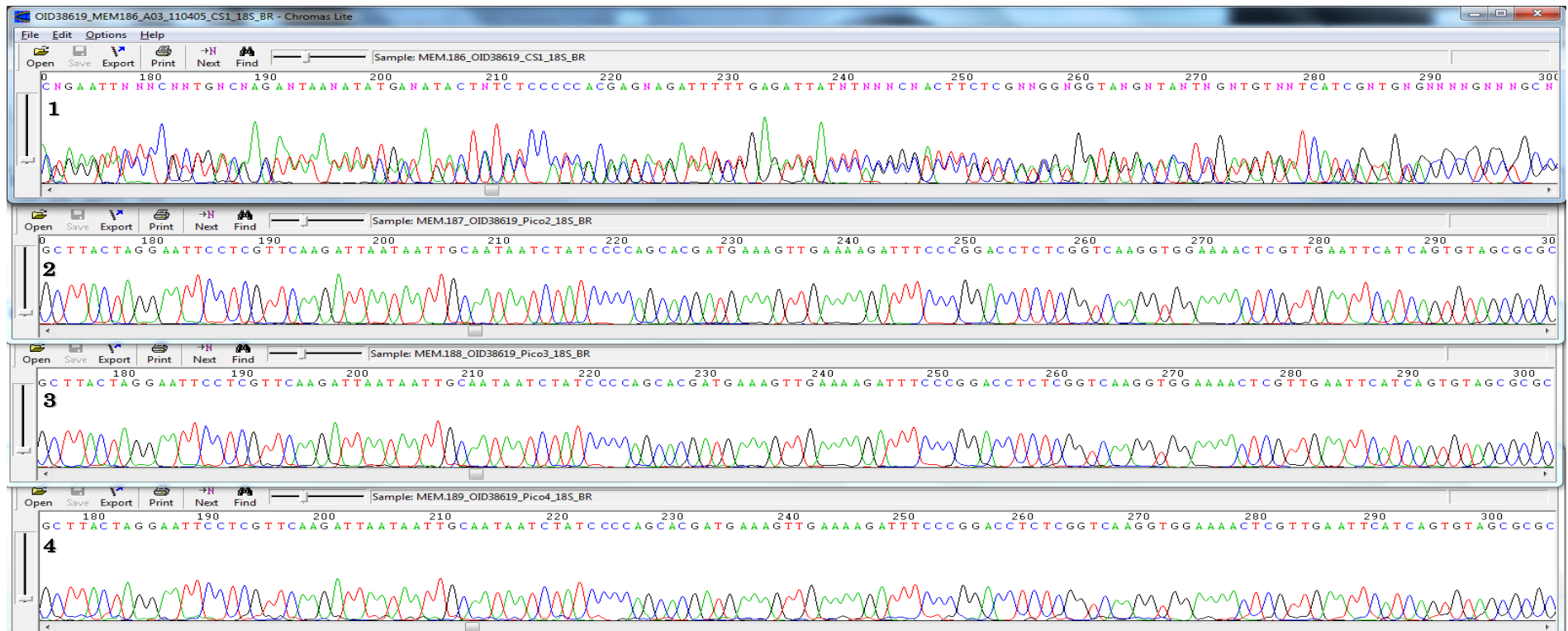


Figure 6.4: Comparisons of chromatogram of three *Picomonas* clonal cultures (2-4) with one contaminant (1) (*Picomonas*+ *Goniomonas* sp2) using eukaryotic primers. Sequences are searched for similarities in Genbank showed to uncultured photoeukaryotic clone RA001219.38 (Not et al., 2007a) which was grouped with 'picobiliphytes' clade I.

6.5 FACS cell sorting using Mitotracker GreenFM

Molecular / fluorescent probe *Mitotracker* Green FM was used for ‘picobiliphyte’ positive cultures and cell are sorted in different regions. Initially the cells are collected in PCR tube which contained 10 μ l of 1X PCR buffer. The cell numbers are different for sorting, depending on their population in each region (region R2, R6 and R7 sorted with 500 cells, and for R1, R3, R4, R5, R8 and R9 approximately 200 cells are sorted), are sorted for *PicoPCR* (Fig. 6.5a). However, reamplification was needed to amplify the fragments (*PicoBI1F/1005R*). This experiment was repeated and results are reproduced (Fig. 6.5b).

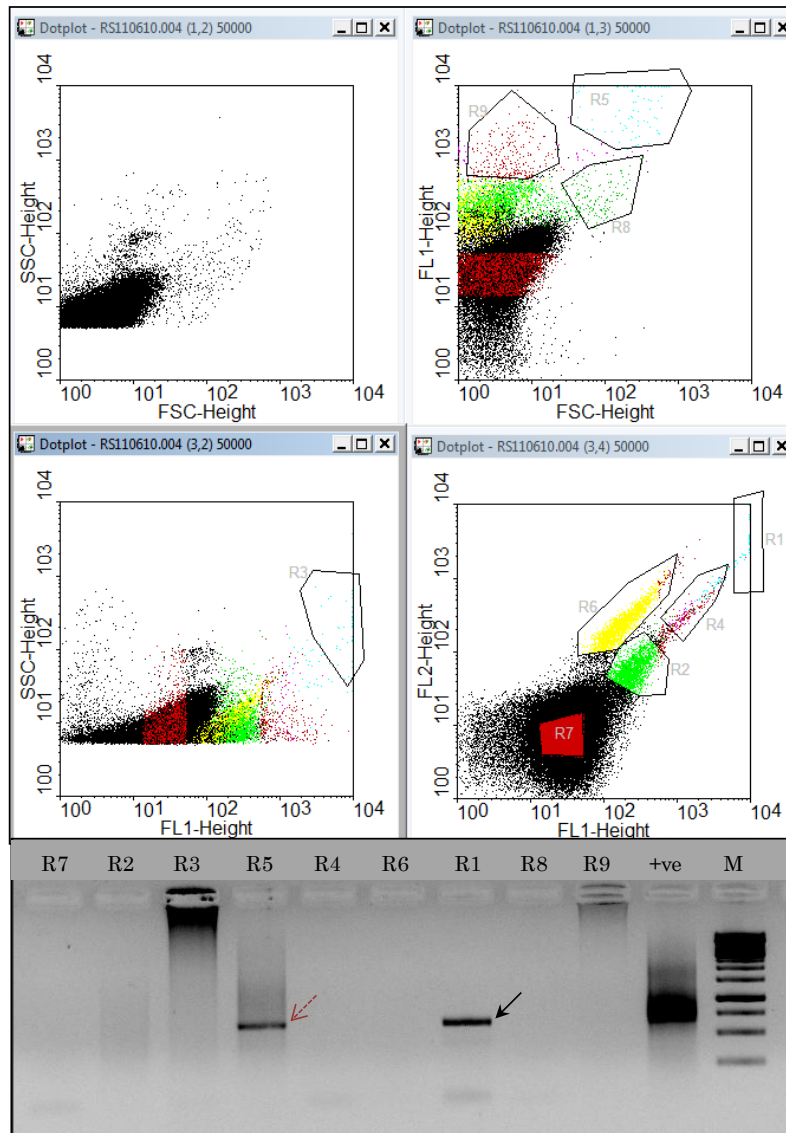


Figure 6.5a: Region R1 to R9 was used for sorting into PCR tubes; PCR results shown to corresponding regions. ‘Picobiliphyte’ cells are sorted in Region R1 and R5. (Note. Region R1 is same as R5 in FSC and FL1 window). FSC, forward scatter; SSC, side scatter; FL1, green fluorescence; FL2 orange fluorescence. M- 1kb ladder, arrow positive PCR product ~650bp.

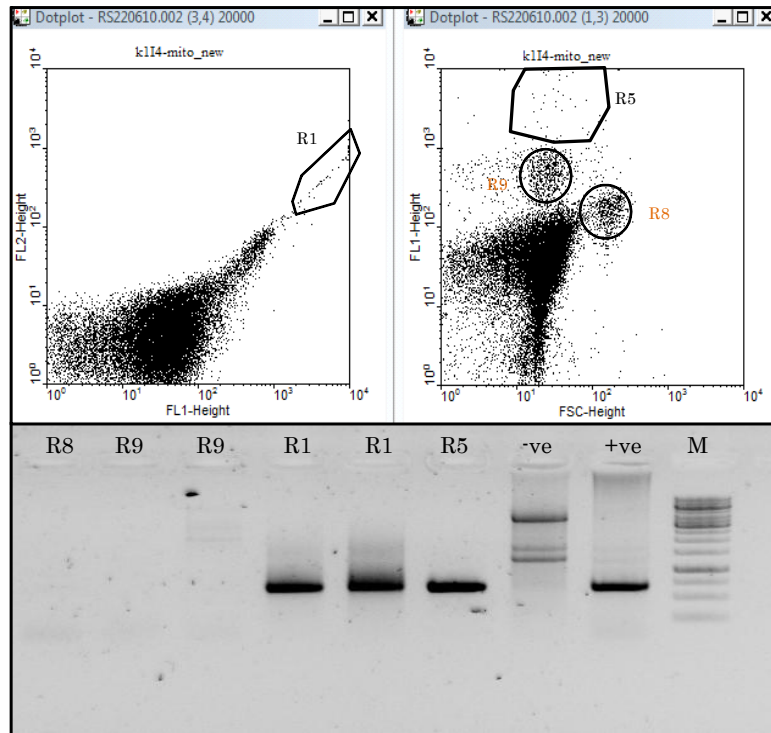


Figure 6.5b: Region R1, R5, R8 and R9 are sorted again for the second batch of ‘picobiliphytes’ positive cultures and PCR was performed as mentioned earlier. The gel image was clearly shown Region R1 and R5 positives to ‘picobiliphytes’. FSC, forward scatter; SSC, side scatter; FL1, green fluorescence; FL2 orange fluorescence. M- 1kb ladder, arrow positive PCR product ~650bp.

6.6 Picomonas cell view form ventral to dorsal

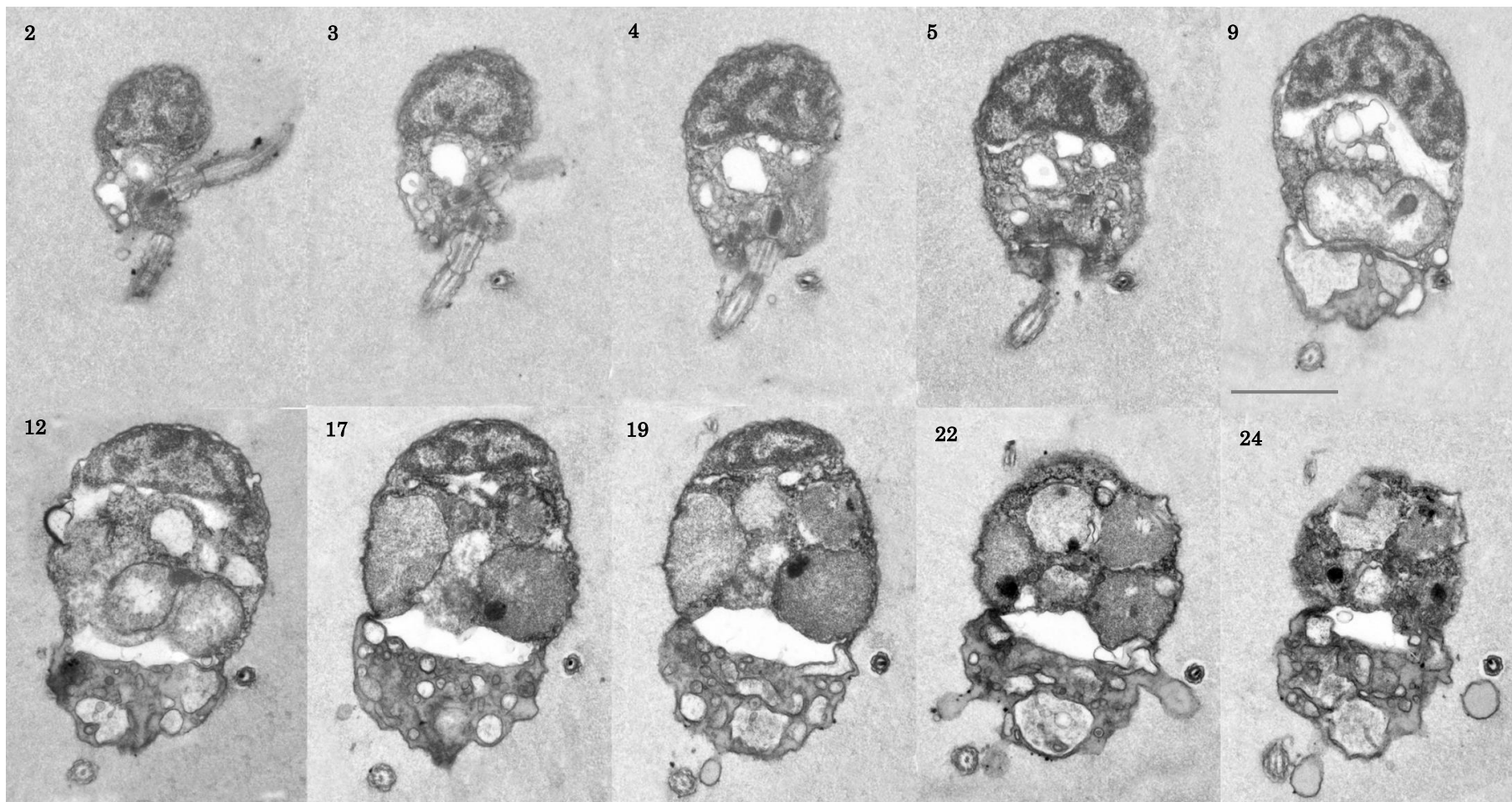


Figure 6.6: Non sequential sections of *Picomonas* cell sectioned from ventral to dorsal has shown a complete organelle arrangement of a single cell. Numbers indicate section numbers. 100nm sections; Bar 1μm.

6.7 Golgi apparatus

Longitudinal section of Golgi clearly showed they are located at the ventral surface of the cell. Golgi apparatus was observed with six cisternae stack, where two stacks, ('cis') facing to the nucleus (attached with nuclear envelope) and others ('trans') are facing towards the basal bodies (Fig.6.7).

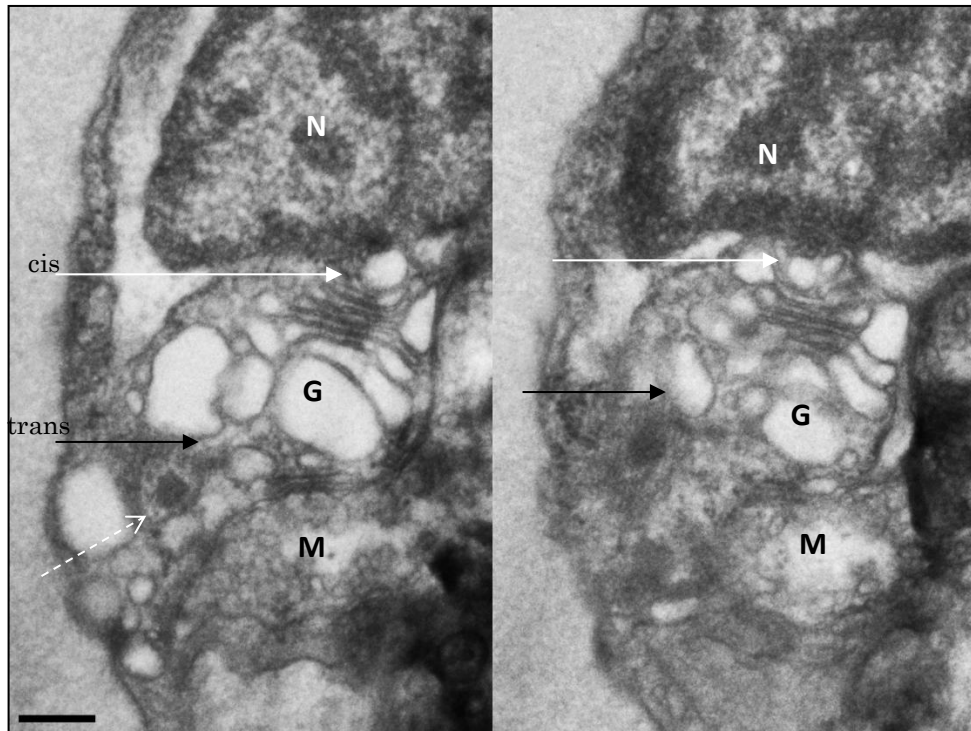


Figure 6.7: Electron micrograph shows consecutive longitudinal sections of *Picomonas*. The two cisternae, 'cis' face of Golgi is connected with nuclear envelope and the other cisternae, 'trans' face is observed near basal body of two flagella. Dotted white arrow, basal plate. Scale bar 200nm

6.8 The Cross section of basal apparatus

Longitudinal serial sections of another *Picomonas* cell show the flagella located at the ventral surface and located in between nucleus, Golgi and Mitochondrion. Though, the basal plate (Fig. 6.8 pict5) is clearly visible, could not detect any cartwheel-like structure at the proximal end of the basal body. However it is observed as less electron dense matrix (red arrow Fig. 3.29) at the proximal end only next to basal plate. Figure 6.8 shows the cross section of the anterior flagellum and longitudinal section of the posterior flagellum with two transition plates.

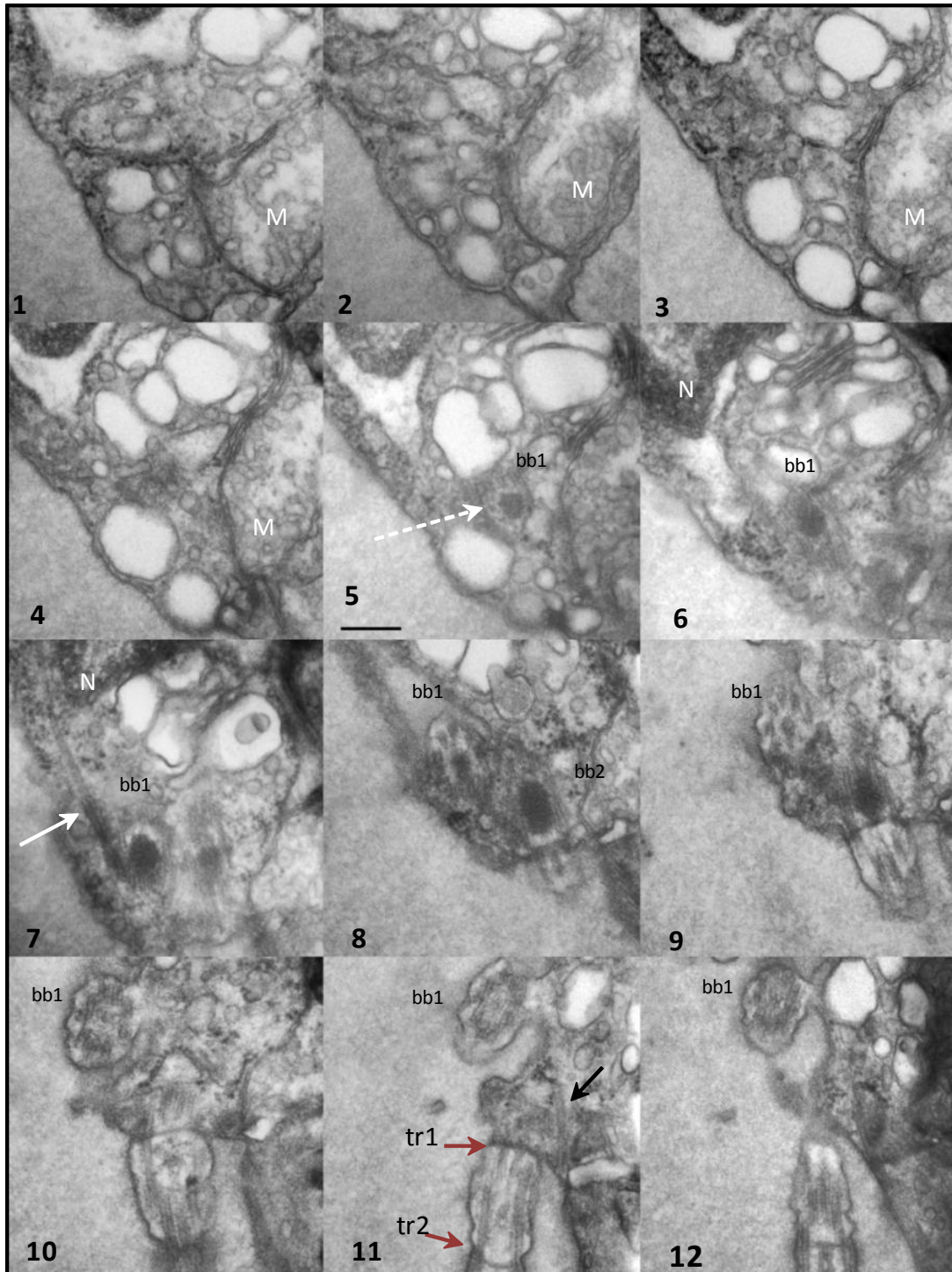


Figure 6.8: Electro micrograph shows sequential sections (100nm) of *Picomonas* at the ventral surface (1-12). The basal plate of the anterior flagellum is observed in picture 5 (white dotted arrow), the anterior microtubular roots are observed in picture 7 (white arrow), whereas posterior microtubular flagellar roots are seen picture 11 (black arrow), and two flagellar transition region (tr1, tr2) of the posterior flagellum are visible in picture 11. M mitochondrion, N nucleus, bb1 anterior basal body, bb2 posterior basal body. Scale bar 200nm.

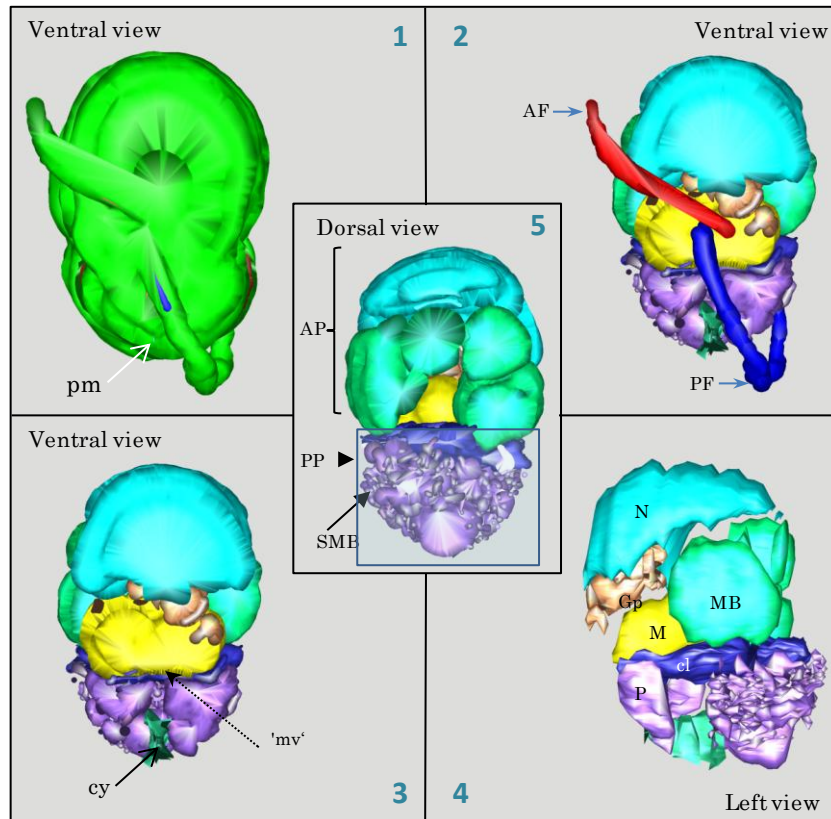
6.9 Three dimensional reconstruction of *Picomonas*

Figure 6.9: Three dimensional reconstruction of *Picomonas* by IMOD from serial sections, 1, 2 & 3 are ventral views of a single cell, with plasma membrane (pm), without pm and without flagella, respectively. 4 & 5 are views of the left side and dorsal side of the cell respectively, AF anterior flagellum, PF posterior flagellum, M. mitochondrion, G. Golgi complex, P. peroxisome like structures, mv mitovilli (mitochondrial appendages), SF- striated fibre, SMB single-membrane body (vesicles) , cl cleft and ds digestive sac, Pd- Posterior part (boxed area).

6.10 Full length nuclear operon of *Picomonas* sp

Construction of full length ribosomal operon is as follows. 100µl of Pico cells are pelleted and amplified with Eu1F and L52R primers. One µl of PCR product was reamplified with PicoBI01F and L52R. The product was cloned and sequenced with PicoBI01F, 1055F/R, BR, L52R. To extend further large subunit (LSU), next round of PCR amplification was performed with P01ITS1F and LSU1433 primer and the PCR product was reamplified using P01ITS2FII with LSU1433. This product was cloned into pGEMTeasy vector and clones are sequenced with the following primers P01ITS2FII, L336F and LSU1433R. This aided to design two internal specific primers (PiLSU-D15F, PiLSU-D21F) for 'picobiliphyte'. Large subunit was further amplified with PiLSU-D15F and LSU2933R followed by reamplification and sequencing with PiLSU-D21F and LSU2933R. The 3' end of the LSU operon was amplified and sequenced with newly designed 28S_PicoG4For primer and common eukaryotic LSU3356 reverse primer. All the chromatogram was aligned with 'DNA star' software using Megalign programme to construct the full length operon. Thus, a total of 5.8 kb was constructed from the *Picomonas* and used for the Phylogenetic analyses.



Figure 6.10A: Full length nuclear encoded ribosomal operon constructed by primer walking; total of 5.8 kb was obtained later used for Phylogenetic analyses.

Full length sequence of *Picomonas* complete nuclear ribosomal operon

```

5'TTGATCTGCCAGTAGTCATATGCTGTCTCAAAGATTAAGCCATGCATGTCTAAGTATAAGCACCTTACTGTGAAACTGCGAATGGCTCATTAAATCAGTTATCG
TTTATTTGATGATCTCTGTCTACTTGGATACCCCGTGGTAATCTAGAGCTAATACATGCGACAACACCCGACTTCTGGAAGGGTGGTATTTATTAGATAAAAAACCTAC
TCGCTTCGGCGATCCTCGTGATTATAAATACTTTTGAAGTGCATGACCTTGTGTGCGGCGTGGTTCATTCAAATTTCTGCCCTATCAACTTTTCATGTTAGGATAG
AGGCCTACCATGGTGGTAACGGGTAACGGGAGAATAGGGTTCGATTTCCGGAGAGGGAGCCTGAGAGACGGCTACCACATCCAAGGAAGGCGAGCGCGCAAAT
TACCCAATCCTGACACAGGGAGGTAGTGACAAAAAATACCAATACAGGGCATTACATGTCTTGAATTGGAATGAGAACAATTTAAATCCCTTATCGAGGATCCATTG
GAGGGCAAGTCTGTTGCCAGCAGCCGCGTAATCCAGCTCCAATAGCGTATATTAAGTTGTGTCAGTTAAAAAGCTCGTAGTCGGATTTTGGCATCAGCCGCTACT
GTCTGCCGATTGGTATGCACGGTTTGGCGGGTCTTCTCCGGAGGCTGTTCCCTCCTTAAGTGAAGGTTCTGTTGGTTCGGTCTTTTACTTTGAGAAAAATTAGA
GTGTTCAAAGCAGGCCATATGCTCTGAATAGGTTAGCATGGAATAATAGAAATAGGACTTTGGTCTATTTTGTGGTTTCTAGGACCGAAGTAATGATTAAATAGGGACA
GTTGGGGGCTTCAATTTCCATTGTACAGGGTAAATCTTGATTAACGGAAGATGAATCTTCCGAAAGCATCTGCCAAGGATGTTTTTCATTGATCAAGAACGAAA
GTTAGGGATCGAAGACGATCAGATACCGTCTGAGTCTTAACATAAACTATGCCGACTAGGGATGTGGAGGTGTTAAGTCTGTACGACCTCCATGCACCTTATGAG
AAATCAAAGTCTATGGTTCCGGGGGGAGTATGGTCCGCAAGGCTGAACTTAAAGGAATTGACGGAAAGGGCACCCAGGAGTGGAGCTGCGGCTTAAATTTGACT
CAACACGGGAAAATACCAGGTCCAGACATAGTTAGGATTGACAGATTGAGAGCTTCTTCTGATTCTATGGTGGTGGTGCATGGCCGTTCTTAGTTGGTGGAGT
GATTTGTCTGGTTAATTCGATAACGAAACGAGACCTTAACTGCTAAATAGTAGTCCGATGATTTCTTATCGTGTGACTTCTTAGAGGGACTACGTTGCTAACCG
ATGGAAGTTTGGAGCAATAACAGGTCTGTGATGCCCTTAGATGTTCTGGGCGCACGCGCTACACTGATGAATCAACGAGTTTTCCACCTTGACCGAGAGGTTCCG
GGAAATCTTTCACTTTCATCGTGTGGGATAGATTATGCAATATTAATCTTGAACGAGGAATCCTAGTAAGCGGAGTCACTAGCTCGCGTTGATTACGTCCC
TGCCCTTTGTACACACCCCGCTGCTACTACCGATTGAGCATTAGGGTGAATCTTCCGACCGTGGCATACTTCTGGCTTAGCCAGTCTTTGTCGGTGGGAGTCCGT
TAAATCTGATGCTTAGAGGAAGTAAAGTTCGTAACAAGGTTTCCGTAAGTGAACCTGCGGAAGGATCATTACCACATTTCTGCCAGTGGCTTTTCCCGCTCGTGC
GGGTTGGTCTGCTGGCGATATCCACCCACGTAACATTGAGATGTTCCAGCATTCAATAATCTCACCCCTTGAACAAACCACTGATTGTAGATTGAGTGTCT
CAGTGTGTGAGCCCTTTGCTTACGCGCGCGCTTACGCATAAAGCCTCAAGACCACATAACCCAAACAAACTCTAACGATGATATCTGGTCTCGCAACGATG
AAGAACGCGAGCAATGCGATACGCAAGTTCGAGAATTCAGTGAATCATCAGAACTTGAACGCATATTCGCGCTGAGGATTCCTCAGAGCATGTTGTCT
CAGTGGCATCTCCCTCTCCCGTGGGTTGCTTCCCTCGTGAAGCAGCTCGGTAGGGCGGCGAGGACTCGAGCCGTCAGAGGTCCTCATCTGATGAGTGTG
GGATCTCTGTCCTCAAGAGCAGAGTTGGCCGCTTGGCGACACATCTCAAATGTCTGTGCGCAGCGTAGCGTGGTAGTGGGTCCTCCGCTCAATGAGTTTAA
GCTGTGCTGTGTGCACTGTAGGCGGGTGTGTCATTGAAGAGCGGTGTTCCGGCTAGGTGCGATGGCTCGGTGTTCTGTGTCGCGAGCCAGTCTCGTGTGCGG
GTTGGATCGAGTGTCTAAGCTTCACTATCTTGCCCTGAGATCAAGCAAGGCTACCCGCTGAATTAAGCATATAACTAAGCGGAGGAAAAGAACTAACAGGATT
CCCCTAGTAAGGGCGACTGAAGCGGGAAGAGCTCAAGCCTAGAATCTGCATGTTTCGCATGCGCAATTGTAGTCTATCGAGTTGTCGTTCTCCGCGCGCGAGGAT
AAGTCTTTTGAACAAGGCATATAGAGGGTGAAGATCCCGTTTGTACTTGCCTGCGTCCGCTTGTATCGACATCTGGCGAGTCAGGTTTTCGAGATTGACGC
CTAAAATGGGTGGTAAATTTCACTAAAGCTAAATATAGGCGAGAGACCGATAGCGAAACAAGTACCGTGAGGAAAAGATGCAAAAGAACTTTGAAAAGAGAGTTAAA
AAGTCTTGAATTTGTTAGGAGGGAAGCGGATCGAACCAAGTGTTCGCGAGTAAGGACCGGAGGCTGGCGCTTCCATACGCTTCTGTCGCGATGCCAGCATCAGTC
GTTCCGCGATATAAGCGGATTCTGACCACTTCTCTGTGCTGTGCTGATAAGACTGAGGAGTTCGACGGGCGCTTATGCGTTACTGTGCTTTCAGTGTCTCACCAT
TCTGGGACTACATGATGTCGGGTTTTGTCTGGCGGCTCTGGCTGCAGTTTTCTGCCGCTGGCGATGTTGGCAAATGCTTCGCTCCGCGCGCTTGAACACGGA
CCAAGGAGTCTAACATGTGTGCGAGTATTGTGGTGGCAACCATGGTGCAGCAATGAAAGTAAAAGGGTGGGTGCACCCGCCGACCGACCATGATCTTCTGTGAAAAG
TTTGAGTAAGAGCATCTCTTGGGACCCGAAAGATGGTGAATGCTGCTGAGTAGGGGAGGAACTCTGGTGGAGCTGTGAGCGTACTGACGATGACGTTGTC
AAATCGTTTCTGCAAACTTGGGTATAGGGGGCGAAAGACTAATCGAACTATCTAGTAGCTGGTCCCTCCGAAAGTTTCCCTGAGGATAGCTGAGCTCAATGAGTTTAT
CAGGTAAGCGAATGATTAGAGGCATTGGGGTTGAACAACCTGCACCTATTTCAAATTTAAATGGGTAAGATGCCCTTCGCTTCTAACCGAGCGTGGGGTGC
ATCGGAGCTCTAGTGGGCCATTTTGGTAAGCAGAACTGGCGATGCGGGATGAACCGAAAGCGGAGTTAAAGTGGCGGACTGCAGCTCATCCAGATACCAAAA
AGGTGTTGATTCACTGACAGCAGGACGGTGGTATGGAAGTCAAAATCCGCTAAGGAGTGTGTAACAACTCACCTGCCGAATGAATAGCCCTGAAAATGGAT
GCGCTCAAGCGTGCAGCTACTCGCCATCAGGGCAATGCGATGCCCTGATGAGTAGGAGGGCGTGGGGTCTGTAAGCAGCCCGCGCGTGGAGCGGGGTG
aAACGTGCTAGTGCAGATCTGGTGGTAGTACAAATATTCAAATGAGAACTTTGAAGACTGAAGTGGAGAAAGGTTCCATGTGAACAGCACTTGGACATGGGT
AGTCCGCTCAAGCGATAGGAAAATCCGTTTTAAAGACGCTTTTTTGGCGTATAGCGGAAAGGGAATCGGGTAAATATCCCGAACGGGATGTGGGTAATGT
GTGGTAACACAACAGAACGCGGAGAGCTGGCGGGAGCCCTGGGAAGTCTCTTTTTCTTTAACTGCTTACCCTGGAAATCAGATTACCTGGAGATAGGGTTA
CACGGCAGGAAAAGCACCTTACGCTTGTAGGTGTCCGGTGGCTCTGACGCGCCCTTGAATCCCGGGACAGGATTATCATACGCCCGCGCTACTATAACCG
CATCAGGTCTCAAGGTGAACAGCCTTAGTCGATAGAACAATGTAGGTAAGGGAAGTCCGCAAAATAGATCCGTAACCTCGGAAAAGGATTGGCTTAAGGGTT
GGTCTAGGGGTCTGCGCAAGAAGCCGAGGCTGTGTGCGACTAGCGGGGCTTACGCGGCTGCTGTCGACCGCGTACGGCCGAAACGCGGACGGCCGCA
GAACGCTTACGGCTTTCCCTAGGCAATGAACAACCGACTTAGAACTGGTACGACAAAGGGGAATCCGACTGTTAATTTAAACAAGCAATTCGATGGCCGCAACC
GGTGTGACGCAATGTGATTTCTGCCAGTCTCTGAATGTCAAAGTGAAGAAATCAACCAAGCGGGTAAACGGCGGGAGTAACTAGCTCTCTTAAGGTAGC
CAATGCTCGTCTAATAGTAGCAGCATGAATGATTAACGAGATTCCCACTGTCCCTATCTACTATCTAGCGAAACACAGCCAAAGGGAACGGGCTTGAAT
AATCAGCGGGGAAAGAACCCCTGTTGAGCTTACTAGTCTGACTTGTGAAATGAGCTTCCGGGTGTAGCATAAGTGGGAGCTCCGGCCCAATGAAAATACCA
TACTGTTGTCTGTTTTACTTATTCATGATGTAAGCGGTCTCTGACCTCTTCTAGCATTAAAGCACTGCGATCTAAGTGGAAAGACATTGTAGGTTGGGAGTTTG
GCTGGGCGGCACATCTGTTAAACAATAACGCAAGGTGCTCAAGATGAGTCAATGAGAACAAGAACTCTATGGAACAACAAAGGGTAAAGGCTCATTGATTGTTGA
TTTTAGTACGAATAACAACGCGAAAGCATGGCCTATCGATCCTTAGCCTTAAAGAAATTTAAGTAGAGGTGTGAGAAAAGTTACCACAGGGATAACTGGCTGT
GGCAGCAAGCGTTCATAGCGAGTGTCTTTTGTCTTCTGATGTCGGCTTCTCTATCATTGTGACGCAAGTCAACAAAGTGTGGATTGTTACCCCGCAATAGG
GAACGTGAGTGGGTTAGACCGTCTGAGACAGGTTAGTTTTACTACTGATGAAAGTGTATCGCAATAGTAACTAACTAGTACGAGAGGAAACCGTTGATTAC
ATACTTGGTATTTTCACTAGCTGAACAGCTAATGGTGAAGCTATCATGTGATGAGGATTACGGCTGAACGCCTTAAAGCCGGAATCCATGCTAGATCGCGATGATTA
TTACCGCTCTCTATCAGTGCACAACAATAGGCTTCCGGCCAACGCATACTGATTTCAATCGAAATTTGAGAGCGATAAATCCTCTGACAGCACTTAGCAGGG
AACAGAGTACTGAAGGAGTAGAGTAGCCTTGTGCTAC3

```

Figure 6.10B: Full length sequence of *Picomonas* sp complete ribosomal nuclear operon (5.8kb)

6.11 Ultrastructure of *Goniomonas* flagellar transition region

Goniomonads, heterotrophic biflagellate with unique features; include a distinctive swimming behaviour (gliding), and the absence of a plastid and nucleomorph (Novarino 2003; Martin-Cereceda et al. 2009). The molecular phylogenetic studies suggested that goniomonads could have diverged before the acquisition of the complex plastid of photosynthetic cryptomonads (Hoef-Emden et al. 2002). Despite a wealth of ultra-structural studies on cryptomonads, *Goniomonas* taxonomic features are not fully understood (Novarino 2003; Martin-Cereceda et al. 2009). Although, morphologically, both cryptophytes and goniomonads share many common features (Novarino 2003), the ultrastructure of goniomonads are not well studied, in particular the flagellar transition region. The structure of the transition region is one of characteristic feature in newly erected super group 'Hacrobia' which includes cryptomonads, katablepharids, telonemids, and palpitomonas (Yabuki et al. 2010 & 2011). The longitudinal section of *Goniomonas* clearly showed two transitional zones at the base of the flagellum. A distinct constriction of the flagellar membrane from the cell surface (proximal transitional region (tr1)) to that the level the central pair of microtubules terminates (second transitional region (tr2)) as seen in cryptophytes (Moestrup & Sengco 2001)(Hibberd David J. 1979) (Fig. 6.11). Thus, indicating that *Goniomonas* and cryptophytes are shared common flagellar transition features with other groups in Hacrobia.

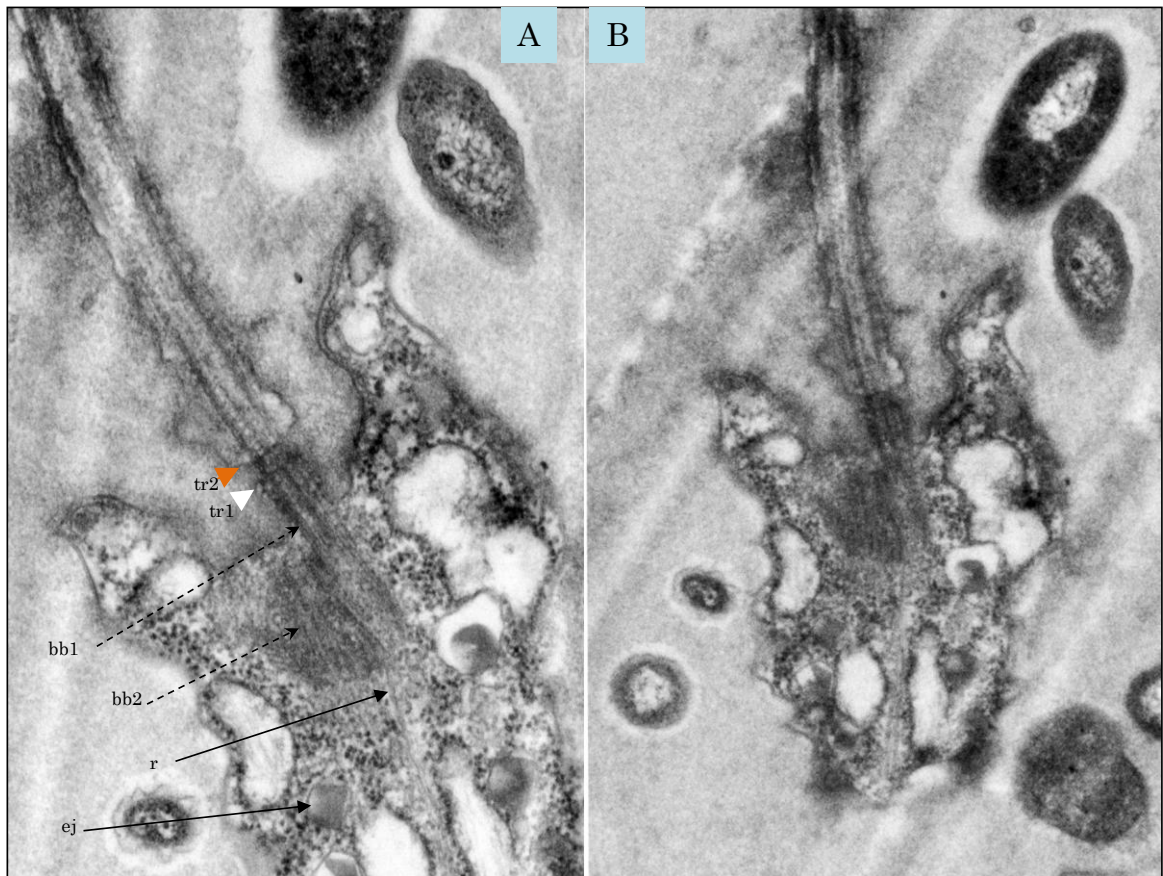


Figure 6.11: Electron micrograph shown longitudinal section of *Goniomonas* sp. tr1, transition region 1 (proximal end, white arrow head; tr2, constricted distal transitional region; bb basal body of flagella (1&2); r microtubular roots; ej, ejectosomes. **B** Longitudinal section of *Goniomonas* sp.

7 Abbreviations

7.1 A1: General

%	Percent
°C	Temperature (in Grad Celsius)
μ	micro-
bd	distilled twice
Acc.no.	Accession number
bp	base pairs
BSA	bovine serum albumin
C	carbon
c	Concentration
ca.	circa
cDNA	copy DNA
Cell PCR	PCR directly on pelleted cells
DAPI	4'-6-diamidino-2-phenylindole
dATP	2-Desoxyadenosintriphosphate
DIC	Differential interference contrast
DMF	Dimethylformamide
DMSO	Dimethylsulfoxide
DNA	Desoxyribonucleic acid
dNTP	2-Desoxynucleoside triphosphate
DTT	1,4-Dithiothreitol
<i>E. coli</i>	<i>Escherichia coli</i>
EDTA	Ethylendiamine tetra acetate
ER	Endoplasmic reticulum
FISH	Fluorescent InSitu Hybridisation
FSSW	0.1μ Filter Sterilzed sea water
g	Gram
GFP	Green fluorescent protein
Glc	Glucose
HEPES	N-2-Hyroxythylpiperazin-N'-2-ethansulfonic acid
HPLC-H ₂ O	pure water
IPTG	Isopropyl-β-D-thiogalactopyranoside
kb	kilo base
kDa	kilo Dalton
K	Keller medium
L	Litre
LM	Light microscopy
LB	Luria/Bertani medium
M	Molar (mol/l)

m	milli-
ML	Maximum Likelihood
MP	Maximum Parsimony
MeOH	Methanol
min	Minutes
mRNA	messenger RNA
n	nano
N	nitrogen
NJ	Neighbour Joining
nm	nanometer
OD	Optical density
p	Pico
PCR	polymerase-chain reaction
Pico PCR	PCR with 'picobiliphyte' primers (PicoBI01F/ITSR)
RNA	Ribonucleic acid
rpm	rounds per minute
rRNA	ribosomal RNA
RT	Room temperature
RT-PCR	Reverse Transcription Polymerase Chain Reaction
SDS	sodium dodecylsulfate
SEM	Scanning Electron Microscopy
Ta	annealing temperature
TAE	Tris acetate EDTA
Taq	DNA polymerase (from <i>Thermophilus aquaticus</i>)
TBE	Tris borate EDTA
Tris	Tris-(hydroxymethyl)-aminomethane
TEM	Transmission Electron Microscopy
Trp	Tryptophan
TSA-FISH	Tyramide Signal Amplification -FISH
Tyr	Tyrosine
UV	ultraviolet
w/v	Weight per volume
X-Gal	5-bromo-4-chloro-3-indolyl-beta-D-galactopyranoside

7.2 A2: Cellular organelle abbreviations

'ds'	Digestive sac
A	Anterior part
AF	Anterior Flagellum
bb	Basal body
cl	Cleft
Cy	Cytoplasm
edsm	Electron dense membrane
G	Golgi complex

M	Mitochondrion
mv	Mitovilli
N	Nucleus
NE	Nuclear Envelope
P	Posterior part
p	Peroxisome/ microbody
pbb	Probasalbody
pcf	proximal connecting fiber
PF	Posterior Flagellum
Pm	Plasma membrane
r	Flagellar roots
rER	rough Endoplasmic Reticulum
SF	Striated Fiber
SMB	Single Membrane Body
tr1	Transition region 1
tr2	Transition region 2

8 Acknowledgements

Foremost, I would like to express my sincere gratitude to my supervisor, Prof. Dr. Michael Melkonian for the continuous support of my Ph.D study and research, for his patience, especially when I use the phrase 'it's there but not yet to be seen', and his motivation, enthusiasm and immense knowledge. His guidance helped me in all the time of research and writing my thesis. I could not have imagined having a better advisor and mentor for my study.

I am grateful to Prof. Dr. Linda Medlin and Dr. Nicole Aberle-Malzahn for their impeccable support and advice for sample collection and processing in Bremerhaven and Helgoland.

I would like to thank Nicole Sausen who has done molecular phylogenetic analysis which is part of my thesis and Jixin Chen for constructing environmental clonal libraries. Without their help, this PhD thesis would not have been completed.

My sincere thanks to Dr. Karl-Heinz Linne von Berg and Hans-Peter Bollhagen for SEM image analysis, Dr. Barbara Surek for culturing techniques, Christopher Göttlinger for flow cytometry and Karin Komsic-Buchmann for TEM analysis for sharing their valuable time in this PhD work.

I express my gratitude to entire Melkonian group and my colleagues, in particular: Birger Marin, Björn Podola, Zehra Cebi, Sebastian Hess, Nicole Feja, Lenka Caisova, Nelli Vardanyan and Eva Nowack for accepting me as one of integral part of this work group, discussing scientific intellectual questions and cultural activities.

I thank to Deutsche Forschungsgemeinschaft and Universität zü Köln for funding this project. Also I would like to thank Prof Dr. Hartmut Arndt and Prof Dr. Jürgen Dohmen for coaching me as members of my thesis committee.

I am obliged to Burhard Becker, Stuart Sym, Kerstin Hoef-Emden, and my friends Veena and Vinod, who spend their time to proofread different parts of this thesis, for all their useful corrections and comments.

My hearty thanks to my close friends, Kicha, Venkatesh, Deepa, Saroja, Vinoy, Karthick and Mani for their constant encouragement and support during throughout my carrier. Also thanks to all friends from Cologne Cricket Club, for wonderful sporting activities in köln.

Last but not the least; I would like to thank my family members for their love and care throughout my life.

Erklärung

“Ich versichere, dass ich die von mir vorgelegte Dissertation selbständig angefertigt habe, die benutzten Quellen und Hilfsmittel vollständig angegeben und die Stellen der Arbeit - einschließlich Tabellen, Karten und Abbildungen -, die anderen Werken im Wortlaut oder dem Sinn nach entnommen sind, in jedem Einzelfall als Entlehnung kenntlich gemacht habe; dass diese Dissertation noch keiner anderen Fakultät oder Universität zur Prüfung vorgelegen hat; dass sie abgesehen von der unten angegebenen Teilpublikation noch nicht veröffentlicht worden ist sowie, dass ich eine solche Veröffentlichung vor Abschluss des Promotionsverfahrens nicht vornehmen werde. Die Bestimmungen dieser Promotionsordnung sind mir bekannt. Die von mir vorgelegte Dissertation ist von Prof. Dr. Michael Melkonian betreut worden“.

Köln, März 2013

Ramkumar Seenivasan

Lebenslauf

Ramkumar Seenivasan

Geboren am 13.05.1978 in Thirumangalam, Indien.

Staatsangehörigkeit: Indisch

Familienstand: Ledig

Schulausbildung

Juni 1986 – März 1995 P.K.N. High School, Thirumangalam, Indien.

Hochschulstudium

Juni 1995 – März 1998 Bachelor of Science (Microbiology)
Sourashtra College, Madurai Kamaraj University, Madurai, Indien.

Oktober 1998 – Oktober 1999 Post B.Sc Diploma in Biotechnology,
Madurai Kamaraj Univeristy, Madurai, Indien.

November 2001 – Mai 2003 Master of Science in Bioinformatics,
Annamalai University, Chidambaram, Tamil Nadu, Indien.
Thema: An innovative in-silico enzyme modelling for increasing the efficiency of conversion of vinblastine to vincristine.

Berufserfahrung

Dezemebr 1999 – Januar 2002 Junior Research Fellow, Genotypic technologies, Bangalore, Indien.

Februar 2002– Juli2004 Research Fellow, Avestha Gengraine Technologies Pvt. Ltd., Bangalore, Indien

Juli 2004 – March 2007 Project Leader, Microbial Biotherapeutics, Avestha Gengraine Technologies Pvt. Ltd., Bangalore, Indien.

Ab Mai 2007 Doctorand, AG Melkonian, Universität zu Köln.